AD-A090 143 ENGELHARD MINERALS AND CHEMICALS CORP EDISON N J ENG--ETC F/G 10/2
PHOSPHORIC ACID FUEL CELL DEVELOPMENT.(U)
SEP 80 A KAUFMAN, P L TERRY DAAK70-77-C-0206

UNCLASSIFIED NL

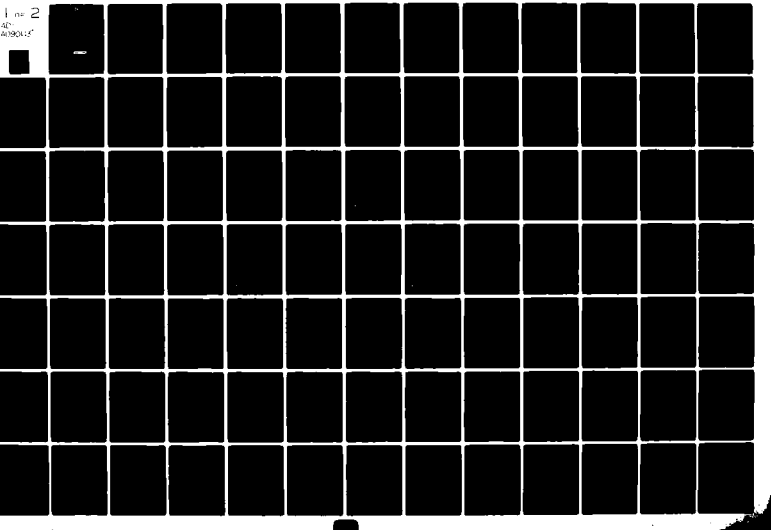

LEVEL II

12

PHOSPHORIC ACID FUEL CELL DEVELOPMENT

FINAL TECHNICAL REPORT

SEPTEMBER 1980

Prepared by

A. Kaufman, P. Terry

Prepared for

U. S. Army Mobility Equipment
Research and Development Command
Fort Belvoir, Va. 22060

Contract DAAK 70-77-C-0206

ENGELHARD

Engelhard Industries Division
Engelhard Minerals & Chemicals Corporation
Menlo Park, Edison, New Jersey 08817

NOTICE

This report was prepared as an account of work sponsored by an agency of the United States Government. Neither the United States nor any agency thereof, nor any of its employees, nor any of its contractors, subcontractors, or their employees, makes any warranty, expressed or implied, or assumes any legal liability or responsibility for any third party's use or the results of such use of any information, apparatus, product or process disclosed in this report or represents that its use by such third party would not infringe privately owned rights.

DISCLAIMERS

The citation of tradenames and names of manufacturers in this report is not to be construed as official Government endorsement or approval of commercial products or services referenced herein.

DISPOSITION

Destroy this report when it is no longer needed. Do not return it to originator.

UNCLASSIFIED

SECURITY CLASSIFICATION OF THIS PAGE (When Data Entered)

REPORT DOCUMENTATION PAGE	READ INSTRUCTIONS BEFORE COMPLETING FORM
1. REPORT NUMBER	2. GOVT ACCESSION NO. AD-A090 743	3. RECIPIENT'S CATALOG NUMBER
4. TITLE (and Subtitle) Phosphoric Acid Fuel Cell Development	5. TYPE OF REPORT & PERIOD COVERED Final Technical Report. Sep 77 – Nov 79
	6. PERFORMING ORG. REPORT NUMBER
7. AUTHOR(s) A. Kaufman, P. L. Terry	8. CONTRACT OR GRANT NUMBER(s) DAAK70-77-C-0206
9. PERFORMING ORGANIZATION NAME AND ADDRESS Engelhard Industries Division Engelhard Minerals & Chemicals Corporation Menlo Park, Edison, New Jersey 08817	10. PROGRAM ELEMENT, PROJECT, TASK AREA & WORK UNIT NUMBERS 63702B, 1L763702DG11, 03, 013EF
11. CONTROLLING OFFICE NAME AND ADDRESS US Army Mobility Equipment Research and Development Command, DRDME-ECS Fort Belvoir, VA 22060	12. REPORT DATE January 1980
	13. NUMBER OF PAGES
14. MONITORING AGENCY NAME & ADDRESS (if different from Controlling Office) Chief, DCASMA 240 Route 22 Springfield, N. J. 07081	15. SECURITY CLASS. (of this report) UNCLASSIFIED
	15a. DECLASSIFICATION/DOWNGRADING SCHEDULE

16. DISTRIBUTION STATEMENT (of this Report)

This document has been approved for public release and sale. Its distribution is unlimited.

17. DISTRIBUTION STATEMENT (of the abstract entered in Block 20, if different from Report)

18. SUPPLEMENTARY NOTES

19. KEY WORDS (Continue on reverse side if necessary and identify by block number)

Fuel Cells
Electrochemistry
Energy Conversion
Electrodes
Matrix

20. ABSTRACT (Continue on reverse side if necessary and identify by block number)

Phosphoric acid fuel cells and fuel cell stacks were evaluated operating on simulated product gases from a methanol reformer. Three-cell stack performance in a start-up/shut-down cycling mode was investigated. Improved matrix and electrode formulations were utilized later in the program, and these components accumulated a total of 8496 hours of testing and 268 shut-down cycles.

DD FORM 1 JAN 73 1473 EDITION OF 1 NOV 65 IS OBSOLETE

UNCLASSIFIED

SECURITY CLASSIFICATION OF THIS PAGE (When Data Entered)

ENGELHARD

TABLE OF CONTENTS

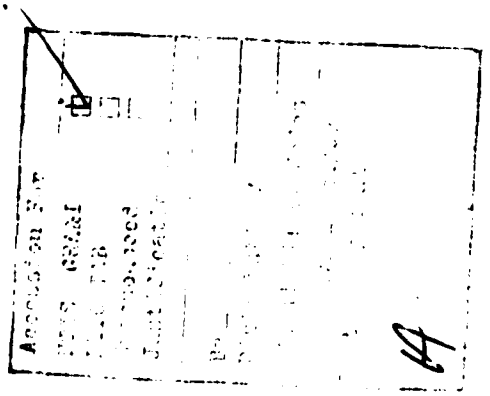

ENGELHARD

TABLE OF CONTENTS
(continued)

LIST OF FIGURES

ENGELHARD

LIST OF FIGURES
(continued)

LIST OF FIGURES
(continued)

ENGELHARD

LIST OF TABLES

ENGELHARD

SUMMARY

The objectives of this program were to design, construct and test phosphoric acid fuel cells and fuel cell stacks capable of operating on typical product gases of a methanol or hydrocarbon reformer. Electrode performance was initially screened in a series of parametric tests in which operating temperature, fuel composition and fuel utilization were varied. Results of the parametric testing were used to establish the operating conditions to be used in the multiple cell stack testing phase of this program.

Preliminary multiple cell stack testing was performed using three-cell stacks, each electrode having an active area of approximately 0.4 ft^2. During initial testing on intermittent load profiles, it was observed that the three-cell stacks exhibited a marked performance decline associated with start-up/shut-down cycling. Upon observing this effect in two three-cell stacks the project effort was directed towards determination of the causes of cycling related performance losses.

Additional three-cell stacks were constructed and tested strictly for start-up/shut-down investigation. Individual cells which exhibited degradation due to start-up/shut-down cycling showed a corresponding decline in open circuit voltage. This observation led to the conclusion that the performance losses were due to reactant cross leakage caused by local breaching of the matrix, probably caused by acid loss during the transient conditions of water production and removal experienced during start-up/shut-down cycling. This conclusion was further verified by the fact that tolerance to start-up/shut-down cycling could be improved through use of a thicker, higher acid content matrix.

A parallel development program being conducted by Engelhard Industries for the Department of Energy (Contract No. DE-AC01-78ET15366) was devoted to developing alternate matrix and electrolyte management concepts. It was, therefore, decided to postpone further start-up/shut-down tolerance testing until improved matrices were available from the matrix development program.

Upon availability of a matrix with improved acid transport properties, three additional three-cell stacks were constructed and committed to start-up/shut-down cycling. The three stacks accumulated a total of 8,496 hours of testing and 268 shut-down cycles. During the course of this testing, long-term performance declines were observed but no declines specifically related to start-up/shut-down cycling were noted.

ENGELHARD

This work was performed by the

Research and Development Department of
Engelhard Industries Division,
Engelhard Minerals & Chemicals Corporation.

E. Starkovich, W. Taschek, and R. Belt of
MERADCOM provided valuable assistance.

4.0 INTRODUCTION

This program was performed in support of the U. S. Army's efforts to develop a family of lightweight, high efficiency, silent power sources suitable for military, field operation.

The objective of this program was to proceed stepwise from parametric testing of small scale, single-cell, phosphoric acid fuel cells to construction of full size, 2-KW, liquid cooled fuel cell stacks. This program was to have proceeded in the following steps.

A. Parametric single cell testing (3 units)

B. Fuel composition choice

C. Three-cell stack construction and test (6 units)

D. Ten-cell stack construction and test (2 units)

E. Full size stack (2-KW net output at maximum rated load) construction and test (2 units)

The parametric single-cell testing was conducted utilizing a variety of fuel compositions typical of those which would be produced by a methanol or hydrocarbon reformer. As a result of the parametric testing and other inputs, a fuel composition of 65% H_2, 2% CO, 10% H_2O balance CO_2 was chosen for mixed gas testing of the multi-cell stacks.

Two of the three-cell stacks were tested using a continuous load profile. Two other stacks were tested using an intermittent load profile in which the stacks were periodically shut-down and allowed to cool to room temperature. The two stacks tested on the intermittent load profile showed substantial losses in performance which were not observed in the identical stacks operated on the continuous load profile.

As a result of this observation, the program was modified to investigate the causes of the observed performance losses associated with start-up/shut-down cycling. Four additional, identical three-cell stacks were constructed. One stack was operated on a constant load as a base-line. The other three stacks were operated on cycles which included shut-down periods of varying frequency and duration. During this testing, each individual cell's performance was monitored.

It was found that with all individual cells that showed a performance decline associated with start-up/shut-down cycling the performance decline was accompanied by a corresponding decrease in open circuit voltage. These results suggest that the observed performance declines could be due to breaching of the electrolyte matrix resulting from the transient operating conditions which occur during start-up/shut-down cycling.

Further testing was performed on stacks which utilized a newly developed matrix having high acid transport characteristics. During this test series of approximately 300 shut-down cycles, no matrix related performance declines were observed.

5.0 EXPERIMENTAL

5.1 Description of Test Samples - Parametric Single-Cell Testing

The parametric single-cell tests were conducted using 2 3/4 in. x 2 3/4 in. active-area cells. Carbonized graphite termination plates were used for current collection and reactant gas distribution. This was the same material that was used later in the stack tests. These 2 3/4 in. x 2 3/4 in. x 0.160 in. plates were inserted into gold-plated brass frames that had the same thickness and 2 3/4 in. x 2 7/8 in. openings. A 1/16 in. gap was left on both inlet and outlet ends for gas manifolding. 1 in. x 6 in. x 6 in. aluminum blocks were used on both sides as end-plates. These blocks were machined to allow the gases to be routed to and from the gas manifolds.

The electrodes utilized a 30% Pt/C catalyst (anode and cathode). The nominal loading for each electrode was 1.4 mg Pt/cm^2. Electrode substrates were Teflon-wetproofed Pfizer FD-33 carbon paper. The matrix was Engelhard's standard phosphoric acid membrane with a nominal thickness of 0.020 inches.

5.2 Description of Test Samples - Three-Cell Stack Testing

An isometric view of a three-cell fuel cell stack is shown in Figure 1. Figure 2 shows the end plate configuration of the first four stacks of this series. In an effort to eliminate the possibility of cell poisoning due to off-gasing from some non-metallic materials of construction minor changes were made in the construction of subsequent stacks. These construction changes are shown in Figure 3.

Tabular data on the fuel cell stacks are given below:

Cell active area	6" x 9-3/4" (0.406 ft^2)
Electrodes, anode & cathode	
Stacks 1a, 1b, 2a, 2b, 3a, 3b, 3c & 3d	
Substrate	Pfizer FD-33, 0.015" thick
Catalyst type	30% Platinum on carbon
Platinum loading	1.4 mg/cm^2 each
Stacks 1e, 2e & 3e	
Substrate	Stackpole PC-206, 0.015" thick
Catalyst type	10% Platinum on carbon
Platinum loading	0.46 mg/cm^2 each

ENGELHARD

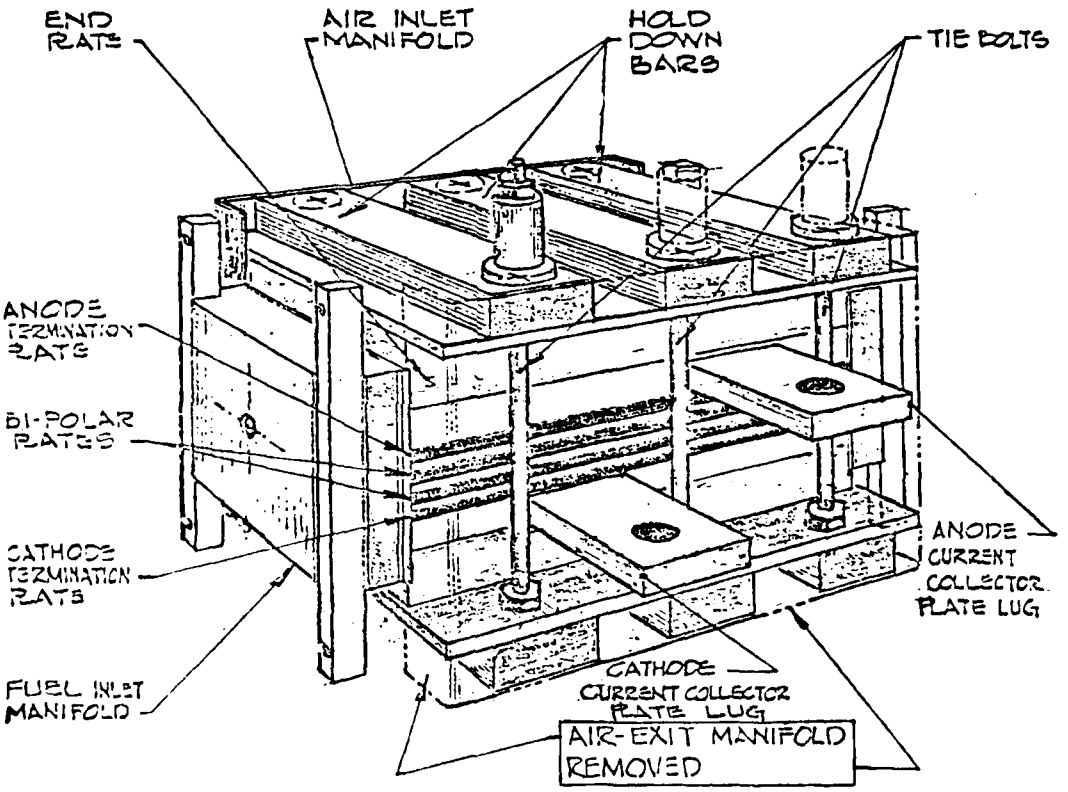

3 CELL FUEL-CELL STACK ASSEMBLY

Figure 1

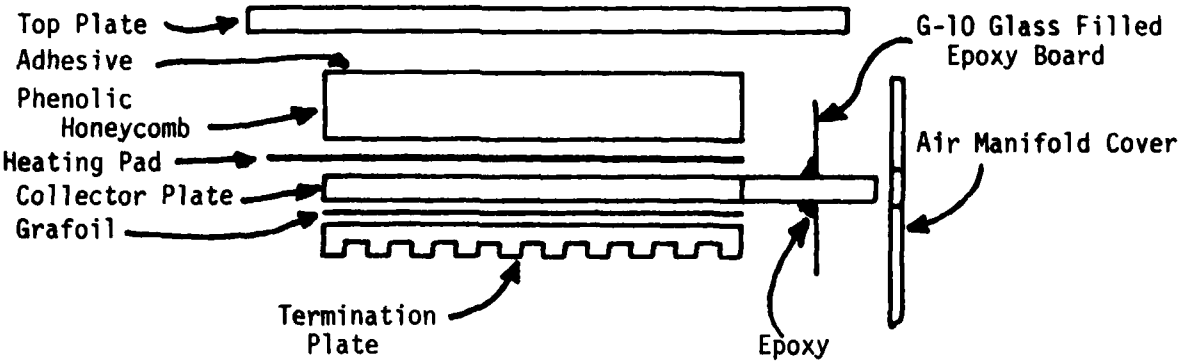

Figure 2

CONSTRUCTION STACKS

1a, 1b, 2a & 2b

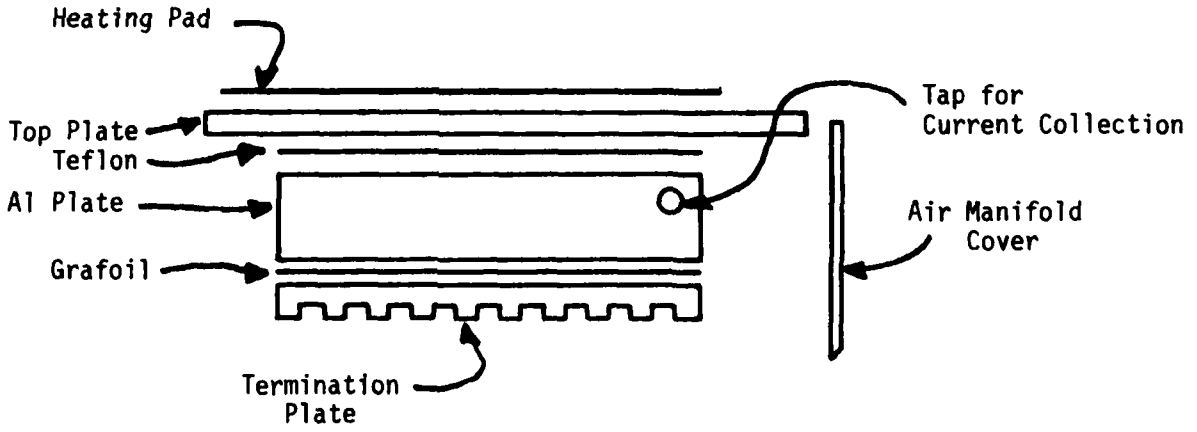

Figure 3

CONSTRUCTION STACKS

3a, 3b, 3c & 3d

1e, 2e, 3e

Matrix type

Stacks 1a, 1b, 2a, 2b, 3a, 3b, 3c & 3d

Standard Engelhard phosphoric acid membrane 0.020" thick (Stacks 3b, 3c & 3d employed 2 matrices per cell for extra acid inventory)

Stacks 1e, 2e & 3e

Laminated, SiC based, with provision for acid addition, 0.010" thick

Bipolar Plates

The bipolar plates were 7" x 10.688" overall and 0.140" thick. They were machined from Stackpole Grade 2020 graphite. Air and fuel gas flow grooves were machined in the corresponding surfaces of the plates.

The porosity of the plates was sealed off by coating the surfaces with Tylan Corporation's Vitrigraf process.

Fuel Cell Edge Seal

The edges of the individual fuel cell electrodes were sealed from exposure to the opposite reactant manifolds by sealing strips placed along the edges of the electrodes. These sealing strips were of a free-standing matrix material as described in U. S. patent 3,453,149.

5.3 Description of Test Facilities - Parametric Single-Cell Testing

All parametric single-cell tests utilized the same test apparatus. The gas flow diagram for this apparatus is shown in Figure 4. Figure 5 shows the wiring diagram for this test station.

5.4 Description of Test Facilities - Three-Cell Stack Testing

Three separate test stands were used in the course of fuel cell stack testing. Each of the three test stands was of identical flow configuration. Figure 6 shows the flow schematic of the test stands. Figure 7 shows the electrical schematic.

ENGELHARD

PARAMETRIC SINGLE-CELL TEST STATION

GAS FLOW DIAGRAM

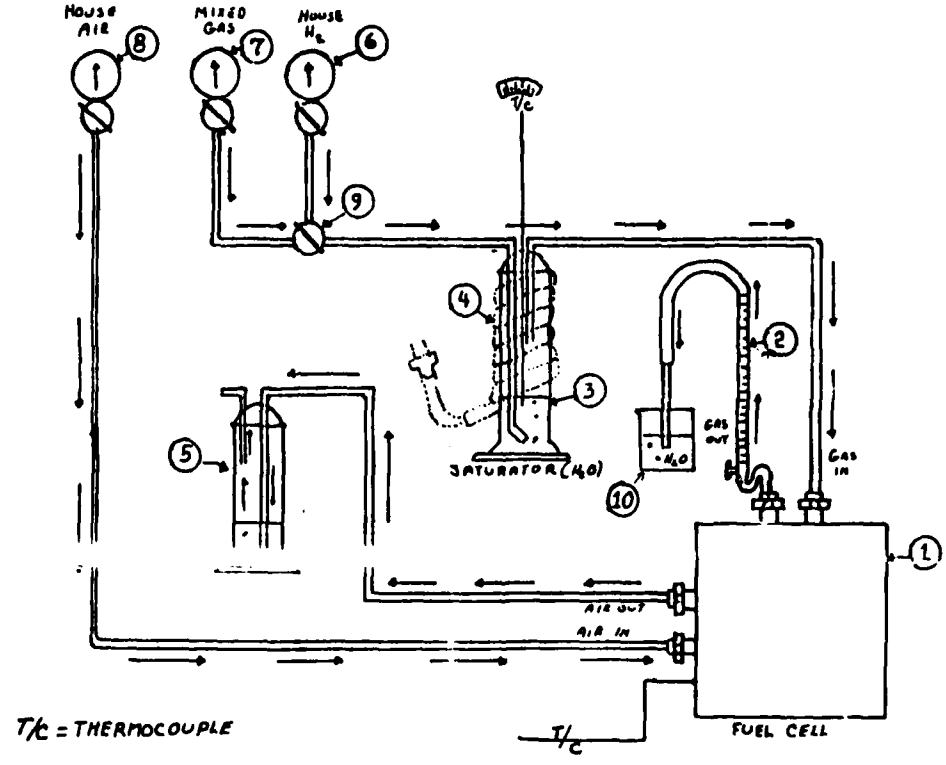

LEGEND

1. Fuel Cell
2. Gas Flow Meter
3. Saturator
4. Heating Tape
5. Gas Washing Bottle
6. Pressure Gauge & Regulator
7. " " "
8. " " "
9. 3 Way Ball Valve
10. Beaker

Figure 4

PARAMETRIC SINGLE-CELL TEST STATION

WIRING DIAGRAM

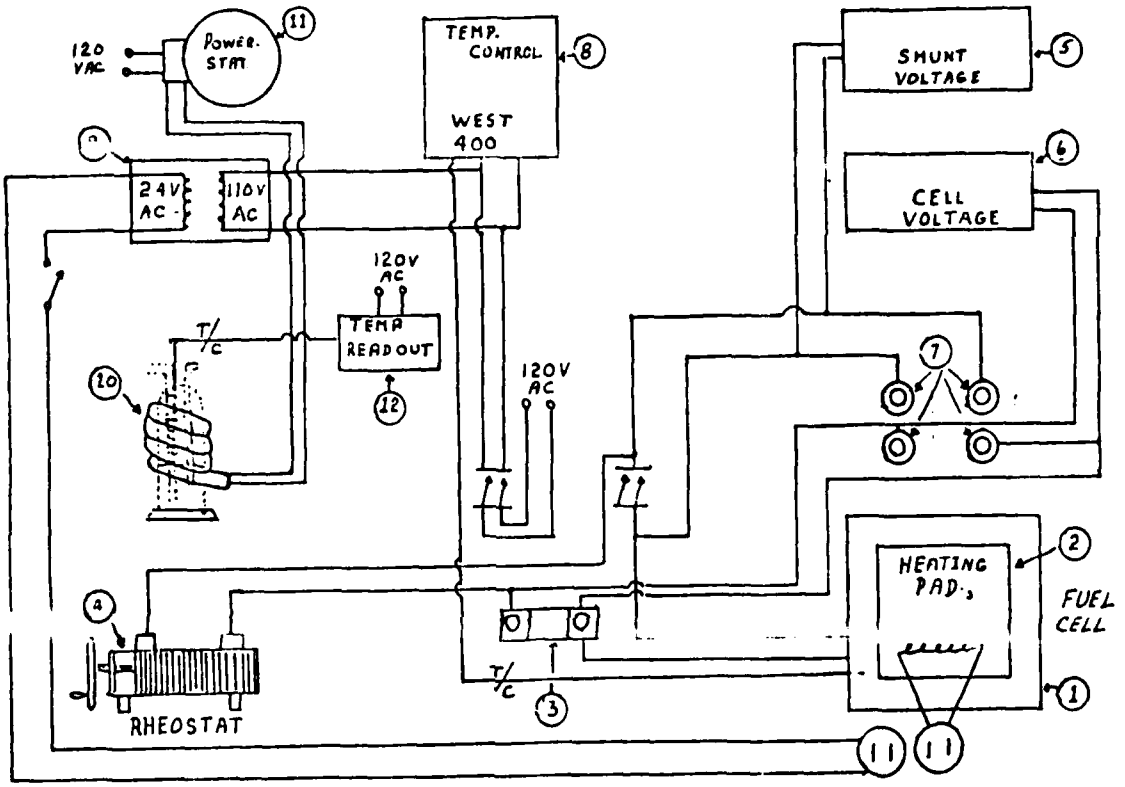

LEGEND

1. Fuel Cell
2. Heating Pads
3. Ammeter Shunt
4. Load Resistance
5. Millivoltmeter
6. Millivoltmeter
7. Binding Posts
8. Temperature Controller
9. Transformer
10. Saturator Heating Tape
11. Variable Transformer
12. Temperature Indicator

Figure 5

GAS FLOW DIAGRAM

FUEL CELL STACK TEST STAND

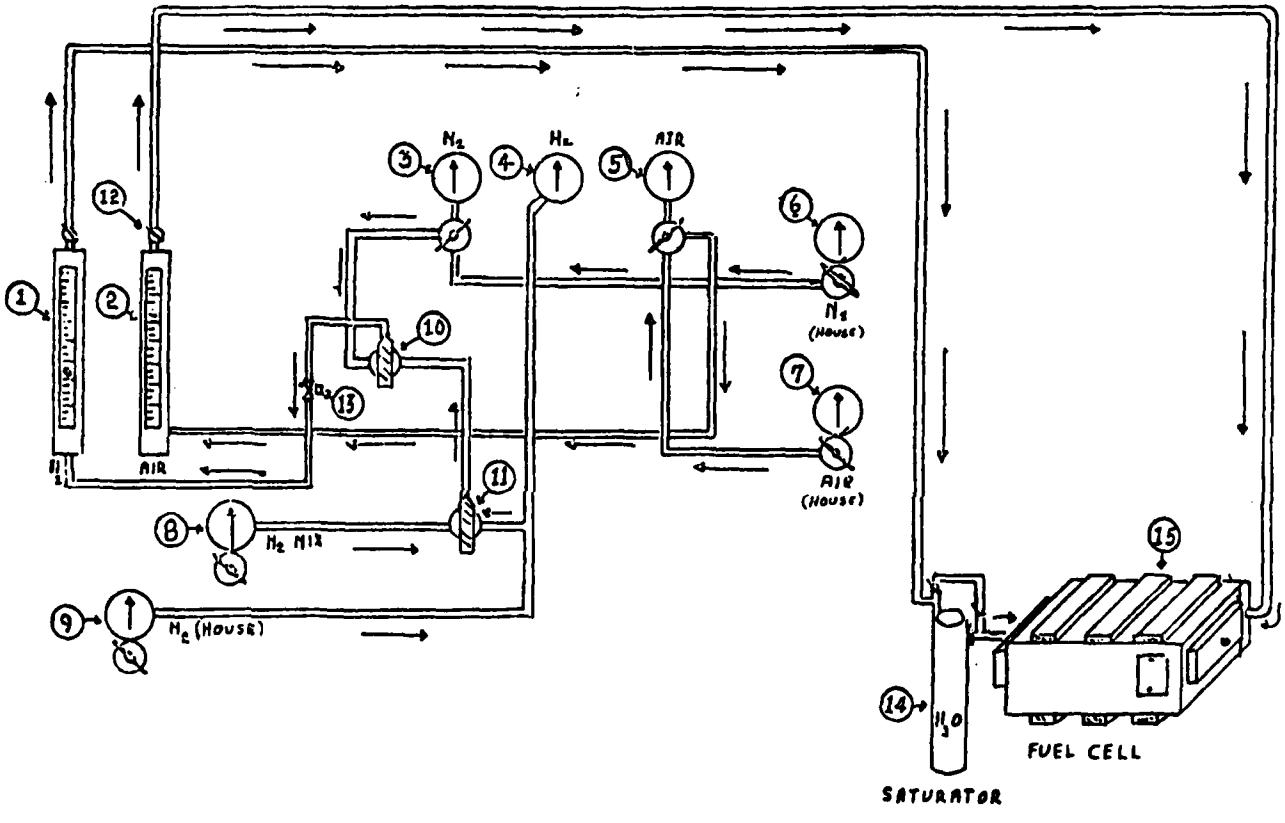

LEGEND

1. H_2 Flowmeter & Valve
2. Air Flowmeter
3. Pressure Regulator
4. " "
5. " "
6. " "
7. " "
8. " "
9. Pressure Regulator
10. 3 Way Ball Valve
11. " " " "
12. Air Metering Valve
13. Shut-down Solenoid Valve
14. Saturator
15. Fuel Cell Stack

Figure 6

WIRING DIAGRAM

FUEL CELL STACK TEST STAND

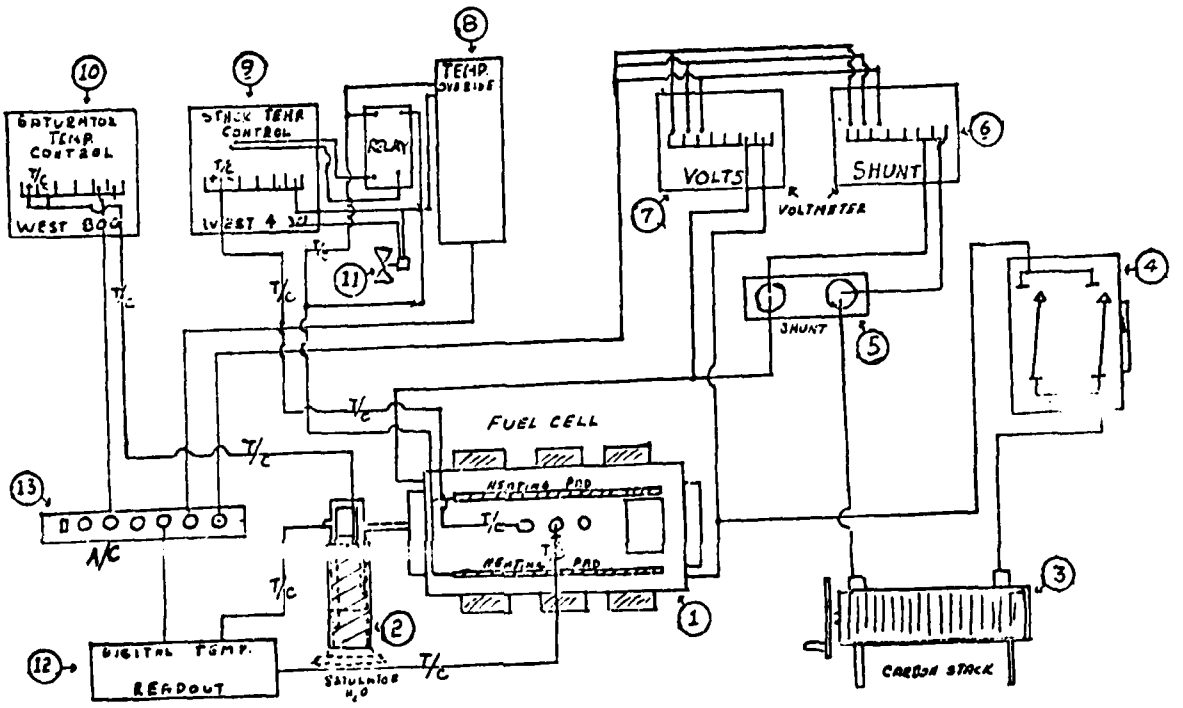

LEGEND

1. Fuel Cell Stack
2. Saturator
3. Carbon Pile Resistor
4. Load Switch
5. Ammeter Shunt
6. Millivoltmeter
7. Voltmeter
8. Over Temperature Protector
9. Stack Temperature Controller
10. Saturator Temperature Controller
11. Hydrogen Solenoid Valve
12. Temperature Indicator
13. AC Bus

Figure 7

5.5 Test Procedure - Parametric Single-Cell Testing

5.5.1 Cell No. 1

Data on pure hydrogen were acquired at 300°F in the current-density range 0-150 ASF in 25 ASF increments. At each stable current-density, voltage was recorded for a hydrogen utilization of 90%. At a current-density of 150 ASF, voltage was recorded for hydrogen utilizations of 70%, 80%, and 90%. Testing then continued using an anode feed gas of the following composition:

65% H_2

10% H_2O

0.5% CO

24.5% CO_2

The composition of 10% H_2O was obtained by saturating the appropriate dry gas mixture with water at a temperature of 115°F. Voltages were recorded at current-densities of 0, 25, 50, 75, and 100 ASF with hydrogen utilizations of 70%, 80%, and 90% at each current-density. Pure hydrogen was then rerun as described above. The following anode feed gas was then utilized:

65% H_2

10% H_2O

1% CO

24% CO_2

Voltages were again recorded at current-densities of 0, 25, 50, 75, and 100 ASF with hydrogen utilization of 70%, 80%, and 90% at each current-density. Baseline hydrogn was then run again as described initially. This was followed by a third 'reformate' gas:

65% H_2

10% H_2O

2% CO

23% CO_2

Voltages were recorded as before at current-densities of 0, 25, 50, 75, and 100 ASF with hydrogen utilizations of 70%, 80%, and 90% at each current-density. Baseline hydrogen was again repeated as described initially. The following anode feed gas was then run:

65% H_2

10% H_2O

3% CO

22% CO_2

Voltages were recorded at current-densities of 0, 25, 50, 75, and 100 ASF with hydrogen utilization of 70%, 80%, and 90% at each current-density. Finally, testing was concluded by rerunning pure hydrogen as described initially.

The temperature was then raised to 325°F, and the entire sequence of events described above was repeated for this temperature.

5.5.2 Cell No. 1A

Testing for this cell was identical to that for Cell No. 1 except that each time pure hydrogen was run voltages were recorded for hydrogen utilizations of 70%, 80%, and 90% at each current-density (not just at 150 ASF).

5.5.3 Cell No. 2

Data on pure hydrogen were acquired at 300°F in the current-density range 0-150 ASF in 25 ASF increments. At each stable current-density, voltage was recorded for hydrogen utilizations of 70%, 80%, and 90%. The following anode feed gas composition was then utilized:

65% H_2

8% H_2O

1.5% CO

25.5% CO_2

Voltages were recorded at current-densities of 0, 25, 50, 75, and 100 ASF with hydrogen utilizations of 70%, 80%, and 90% at

each current-density. Pure hydrogen was then rerun as described above. Testing then continued with an anode feed gas of the following composition:

65% H_2

10% H_2O

1.5% CO

23.5% CO_2

Voltages were again recorded at current-densities of 0, 25, 50, 75, and 100 ASF with hydrogen utilizations of 70%, 80%, and 90% at each current-density. Pure hydrogen was then run again as described above. The following anode feed gas was then run:

65% H_2

12% H_2O

1.5% CO

21.5% CO_2

Voltages were recorded at current-densities of 0, 25, 50, 75, and 100 ASF with hydrogen utilizations of 70%, 80%, and 90% at each current-density. Finally, pure hydrogen was run again as described above.

The temperature was then raised to 325°F, and the entire sequence of events described above was repeated for this temperature.

5.5.4 Cell No. 3

Data on pure hydrogen were acquired at 325°F in the current-density range 0-150 ASF in 25 ASF increments. At each stable current-density, voltage was recorded for hydrogen utilizations of 70%, 80%, and 90%. This was followed by an 85% H_2-15% CH_4 gas mixture. Voltages were recorded at current-densities of 0, 25, 50, 75, and 100 ASF with hydrogen utilizations of 70%, 80%, and 90% at each current-density.

This procedure was then repeated for an 85/15 H_2/CH_4 mixture containing 100 ppm H_2S. This was followed by 85/15 H_2/CH_4 mixtures with 200 ppm H_2S, 300 ppm H_2S, and 500 ppm H_2S, respectively.

In each case, voltages were recorded at current-densities of 0, 25, 50, 75, and 100 ASF with hydrogen utilizations of 70%, 80%, and 90% at each current-density.

5.6 Test Procedure

5.6.1 Stacks 1a & 2a

5.6.1.1 Fuel

Stack 1a was operated on a simulated reformer product gas of 65% hydrogen, 2% CO, 10% H_2O, balance CO_2. Stack 2a was operated on 90% H_2, 10% H_2O.

5.6.1.2 Load Profile

Both stacks were operated on the continuous load profile as shown in Figure 8. The stack operating temperature was varied a minimum of three times during the test. Each temperature change was maintained for 50 hours. At all hours marked X on Figure 8, a current density/voltage curve was obtained from 0-200 amperes per square foot in 25 ASF increments along with hydrogen utilizations of 70, 80 and 90% at each increment. All stack temperatures were recorded for each current density/voltage curve. Minor modifications were made to the load change and data collection sequence in order to accommodate the normal work day.

5.6.2 Stacks 1b & 2b

5.6.2.1 Fuel

Stack 1b was operated on the simulated reformer product gas as used in Stack 1a. Stack 2b was operated on 90% H_2, 10% H_2O.

5.6.2.2 Load Profile

Both stacks were operated on an intermittent load profile as shown in Figure 9. The stack operating temperature was varied in the continuous load profile test except when the stack was shut-down (see below). At all hours marked X on Figure 9, a current density/voltage curve and hydrogen utilizations were obtained as in the continuous load profile test.

5.6.2.3 Start-Up/Shut-Down Procedure

The following procedures were used when starting and stopping the fuel cell stacks. These procedures were designed to simulate the

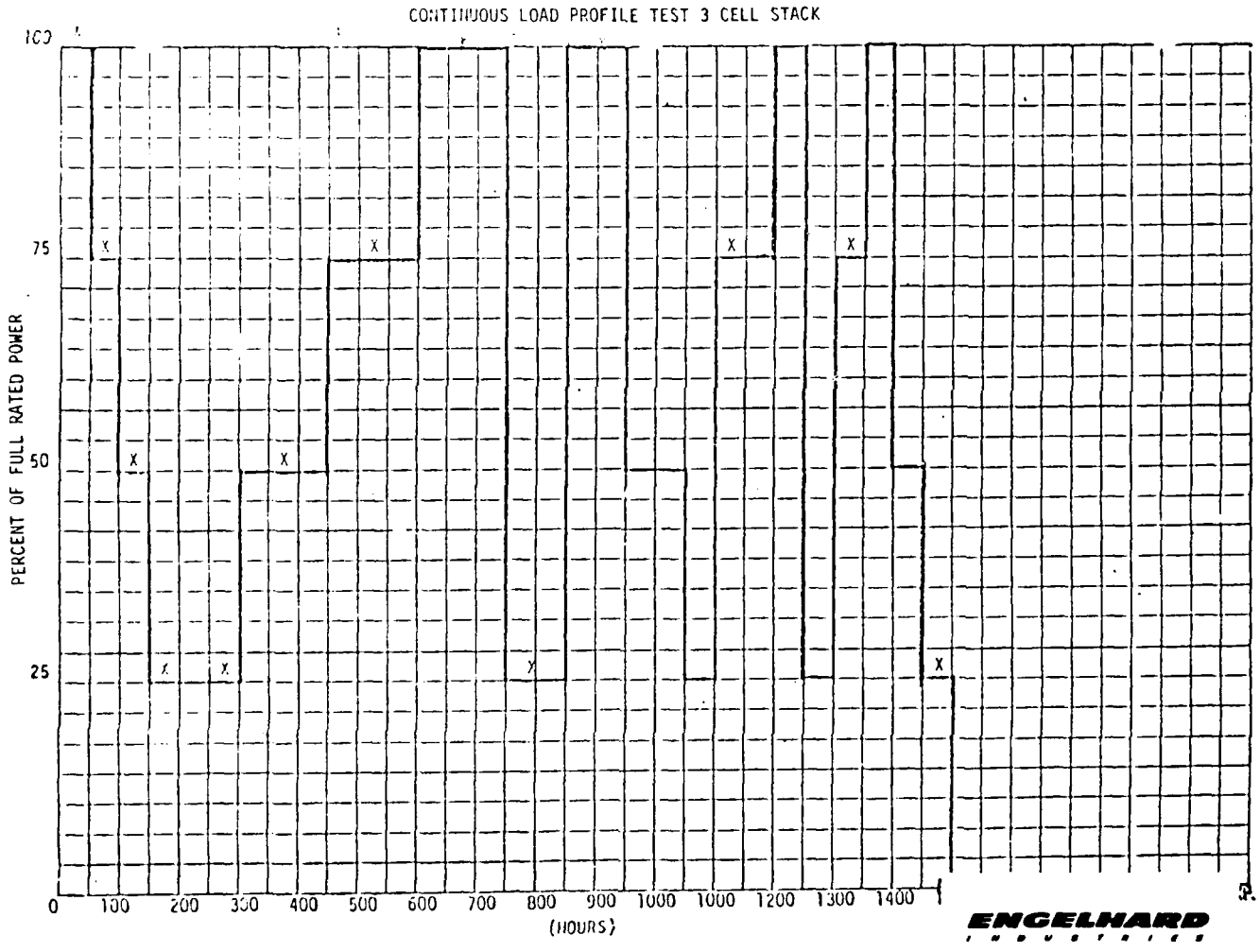
CONTINUOUS LOAD PROFILE TEST 3 CELL STACK
100
75
50
25
0
PERCENT OF FULL RATED POWER
100
200
300
400
500
600
700
800
900
1000
1000
1200
1300
1400
(HOURS)
ENGELHARD

Figure 8

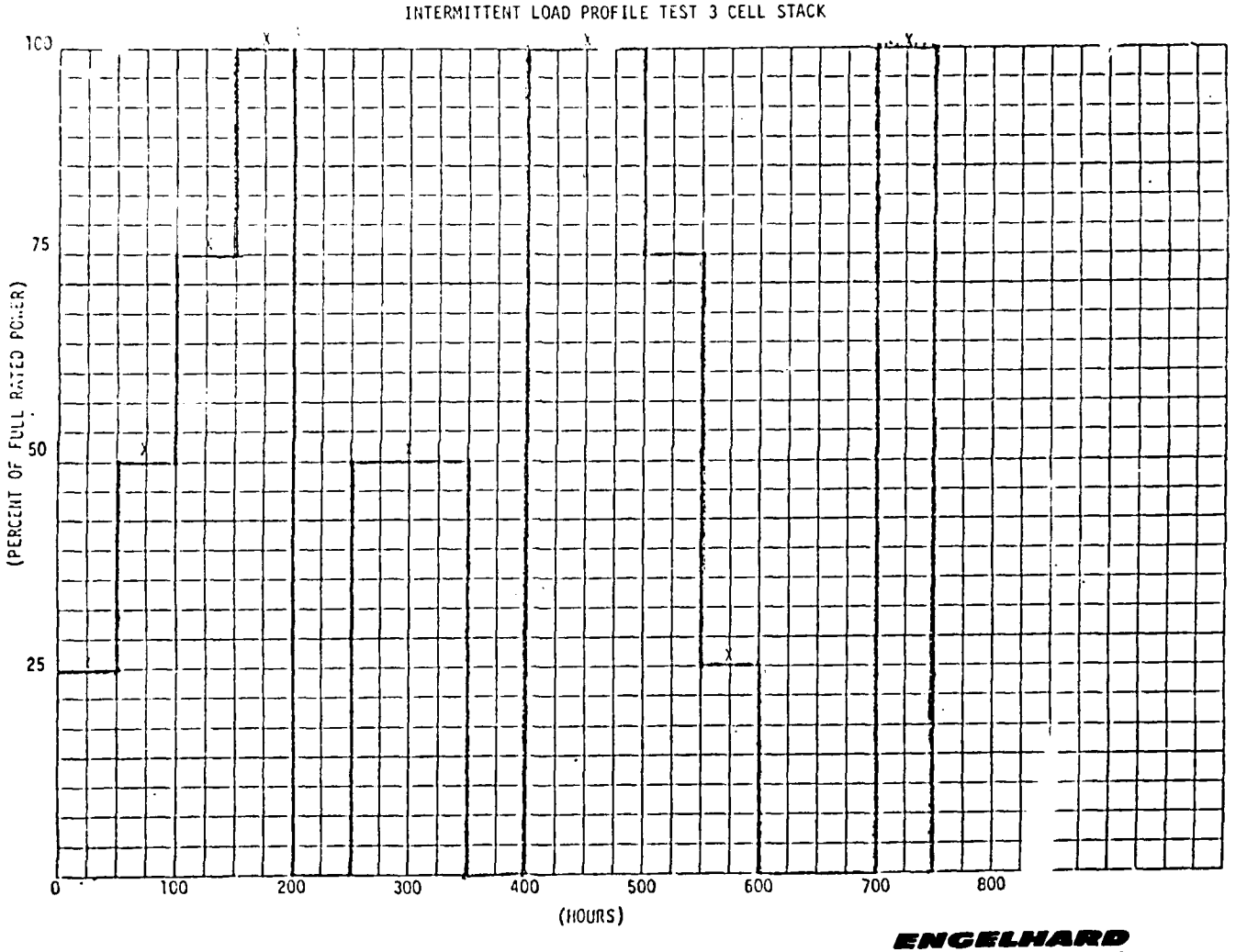
INTERMITTENT LOAD PROFILE TEST 3 CELL STACK
100
75
50
25
0
(PERCENT OF FULL RATED POWER)
100
200
300
400
500
600
700
800
(HOURS)
ENGELHARD

Figure 9

start and stop event sequence which would occur in a typical field model fuel cell system with an integrated reformer.

Start-Up Procedure:

A - Apply external electrical load (in a field model this load could be internal supplementary starting heaters).

B - Heat fuel cell stack from ambient temperature to approximately 240°F.

C - Open fuel and air exits.

D - Start air flow.

E - Start fuel flow.

F - Allow stack to heat to operating temperature.

G - Adjust load.

H - Control at operating temperature.

Shut-Down Procedure:

A - Leave external electrical load on.

B - Shut off air flow.

C - Turn off heating pads.

D - 1-1/2 minutes after shutting off air flow, shut off fuel flow.

E - Close fuel and air exits.

F - Allow stack to cool to ambient temperature.

5.6.3 Stacks 3a, b & c

5.6.3.1 Fuel

Stacks 3a, b & c were operated on 90% H_2, 10% H_2O.

5.6.3.2 Load Profile

To evaluate the effects of start/stop cycling only, Stacks 3a, b & c were operated on constant load interrupted by shut-down periods. The start-up/shut-down procedure of Section 5.6.2.3 was followed. Shut-downs were performed at random and were of varying duration.

5.6.4 Stack 3d

5.6.4.1 Fuel

Stack 3d was operated on 90% H_2, 10% H_2O.

5.6.4.2 Load Profile

In order to provide baseline data, fuel cell Stack 3d was operated on constant load with no intentional shut-down or temperature cycling.

5.6.5 Stacks 1e, 2e & 3e

5.6.5.1 Fuel

During the first 1400 hours of testing, each fuel cell stack was to be operated on a fuel mixture of 90% hydrogen, 10% water. At the completion of 1400 hours of testing, one fuel cell stack was to continue operating on the hydrogen/water mixture, one fuel cell stack was to be operated on 65% H_2, 23% CO_2, 10% H_2O, 2% CO and the third stack was to be operated on 88% H_2, 10% H_2O, 2% CO.

5.6.5.2 Load Profile

The stacks were operated at a continuous load of 150 Amps per square foot. The continuous load was interrupted with complete shut-down/start-up cycles. Cycling frequency was selected to yield a minimum of fifty shut-down cycles during the first 1400 hours of operation (approximately 6 shut-downs per week). The shut-down/start-up procedure of section 5.6.2.3 was followed.

6.0 RESULTS AND DISCUSSION

6.1 Parametric Single-Cell Testing

6.1.1 Cell No. 1

The parametric single-cell test results for Cell No. 1 are shown in Tables 1 and 2 for temperatures of 300°F and 325°F, respectively. These are also shown in Figures 10 through 17.

It should be noted that the performance on "reformate" gas at 300°F was only slightly inferior to that at 325°F. In two cases at 325°F and hydrogen utilizations of 90% substantial penalties were incurred on reformate gas. These occurred at a current-density of 100 Amp/ft^2 using the 1% and 3% CO gases.

In a few instances running on hydrogen at 90% utilization, stable performance could not be obtained. This occurred only at low current-densities, and the cause is thought to be hydrogen maldistribution as a result of extremely low exit flows under these conditions.

6.1.2 Cell No. 1A

The results for Cell No. 1A are shown in Tables 3 and 4 for temperatures of 300°F and 325°F, respectively. This cell was a repeat of Cell No. 1 except that additional data were acquired during running on baseline hydrogen.

The performance of Cell No. 1A was similar to that of Cell No. 1, but the tolerance of high hydrogen utilizations was more consistent.

The Cell No. 1 and Cell No. 1A test results on "reformate" fuel indicate that the combined effects of CO (to concentrations up to 3%) and hydrogen dilution could be tolerated for hydrogen utilization rates to at least 80%. In fact, it appears that a 90% hydrogen utilization rate can be accommodated - with moderate performance penalties - at least for temporary periods.

It is seen that the effect of CO concentration in the range of 1-3% was not severe. Also, reasonable tolerance of CO was maintained to a temperature as low as 300°F.

6.1.3 Cell No. 2

The results for Cell No. 2 are shown in Tables 5 and 6 for temperatures of 300°F and 325°F, respectively. These are also shown in Figures 18 through 23.

ENGELHARD

PARAMETRIC SINGLE-CELL TESTING

CELL NO. 1

T=300°F

ANODE GAS	CELL VOLTAGE (MV)							% H_2 UTILIZATION
	0	25	50	75	100	125	150 AMP/FT^2	
H_2							607	70
H_2							606	80
H_2	959	761	715	680	652	626	603	90
0.5% CO 10% H_2O 65% H_2 24.5% CO_2		750	698	657	631			70
	964	750	697	664	635			80
	970	629	691	651	623			90
H_2							616	70
H_2							616	80
H_2	961	754	711	679	657	635	614	90
1.0% CO 10% H_2O 65% H_2 24% CO_2	971	763	708	670	640			70
	971	749	698	658	630			80
	971	740	683	642	620			90
H_2							607	70
H_2							606	80
H_2	960	757	712	679	653	625	604	90
2.0% CO 10% H_2O 65% H_2 23% CO_2	970	752	701	661	631			70
		750	695	656	628			80
		746	690	640	616			90
H_2							607	70
H_2							606	80
H_2	952	761	710	679	651	625	604	90
3.0% CO 10% H_2O 65% H_2 22% CO_2	971	755	702	662	629			70
		749	687	656	624			80
		742	685	634	613			90
H_2							606	70
H_2							605	80
H_2	978	735	681	678	651	628	604	90

Table 1

ENGELHARD

PARAMETRIC SINGLE-CELL TESTING

CELL NO. 1

T = 325°F

ANODE GAS	CELL VOLTAGE (MV)							% H_2 UTILIZATION
	0	25	50	75	100	125	150 AMP/FT^2	
H_2		774	728	693	665	638	620	70
H_2	976	772	726	692	664	637	618	80
H_2		770	725	689	663	637	614	90
0.5% CO	910	760	710	673	643			70
10% H_2O								
65% H_2		747	707	669	642			80
24.5% CO_2	933	743	681	653	633			90
H_2							618	70
H_2							616	80
H_2	925	768	721	686	662	637	614	90
1.0% CO	894	756	708	672	643			70
10% H_2O								
65% H_2		752	704	669	641			80
24% CO_2	934	734	690	643	586			90
H_2							615	70
H_2							613	80
H_2	908	-	-	668	659	638	609	90
2.0% CO	904	751	702	664	634			70
10% H_2O								
65% H_2		747	697	660	628			80
23% CO_2		730	681	636	621			90
H_2							616	70
H_2							613	80
H_2	884	-	700	660	653	630	609	90
3.0% CO	941	754	707	666	633			70
10% H_2O								
65% H_2		723	697	656	625			80
22% CO_2	934	703	672	630	576			90
H_2		773	724	689	660	634	611	70
H_2		772	723	688	659	633	609	80
H_2	915	-	693	679	657	635	611	90

Table 2

ENGELHARD INDUSTRIES

PARAMETRIC SINGLE-CELL TESTING - CELL No. 1

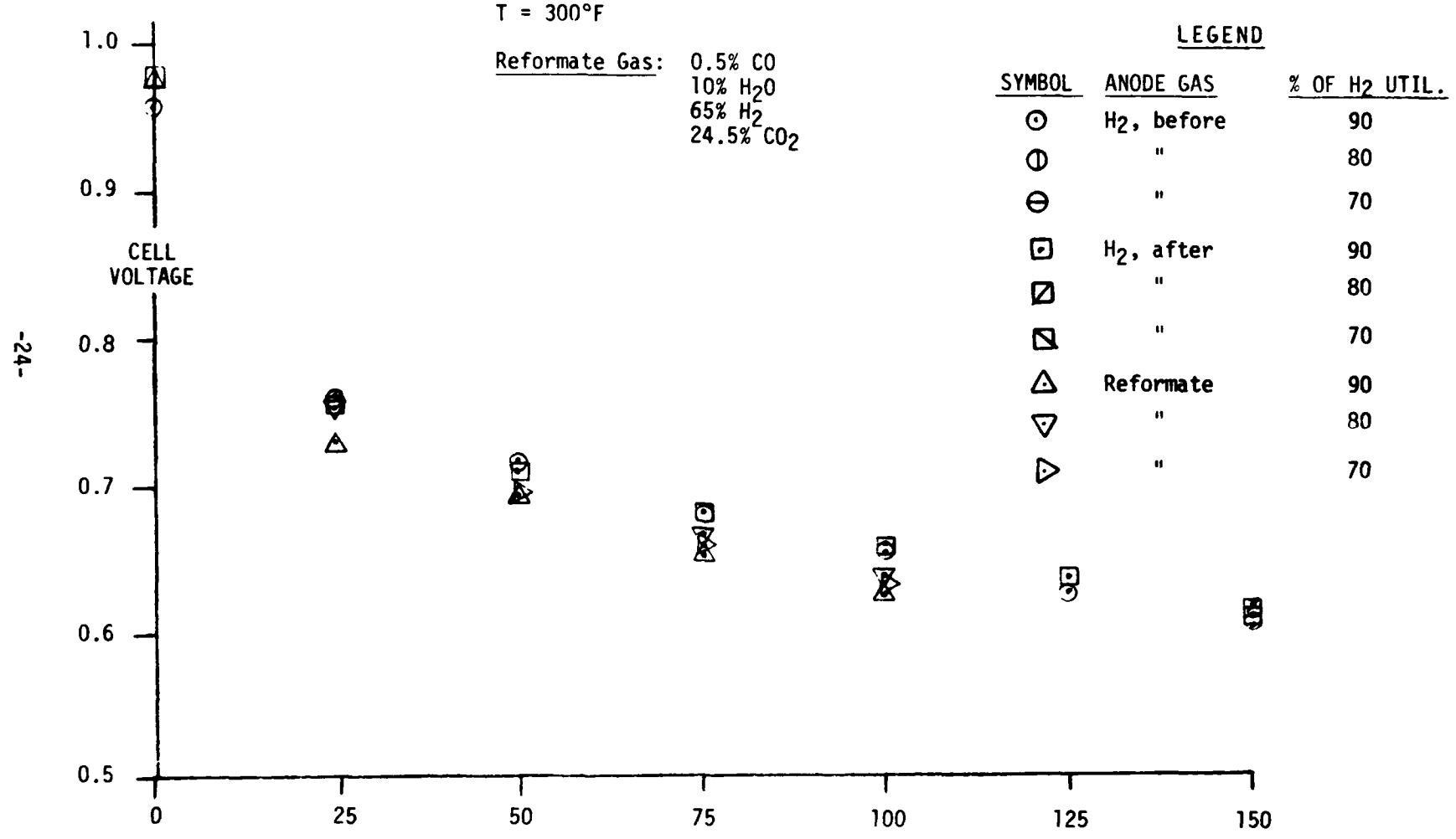

Figure 10

ENGELHARD INDUSTRIES

PARAMETRIC SINGLE-CELL TESTING - CELL No. 1

T = 300°F

Reformate Gas: 1.0% CO
10% H_2O
65% H_2
24% CO_2

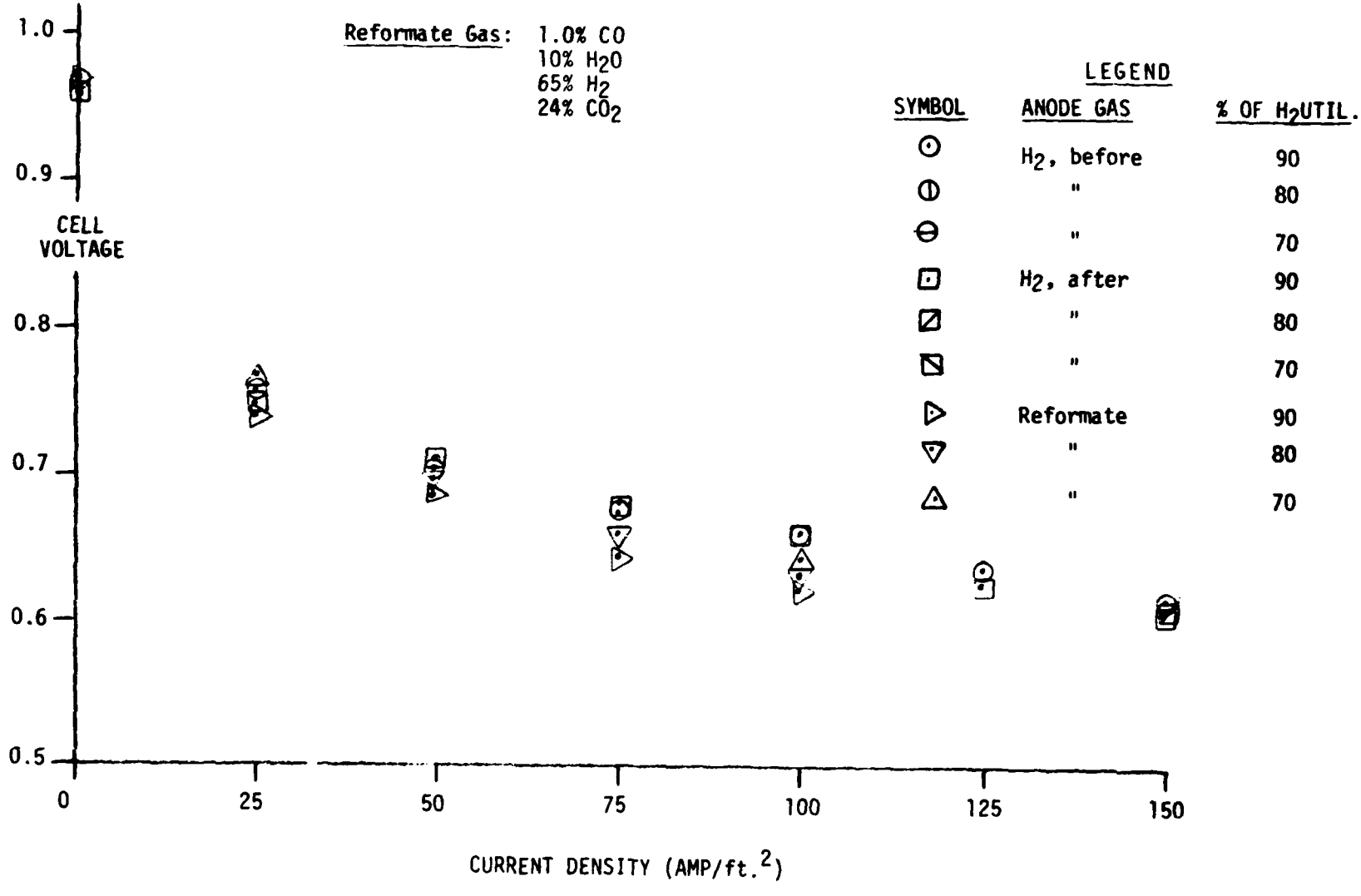

Figure 11

ENGELHARD INDUSTRIES

PARAMETRIC SINGLE-CELL TESTING - CELL No. 1

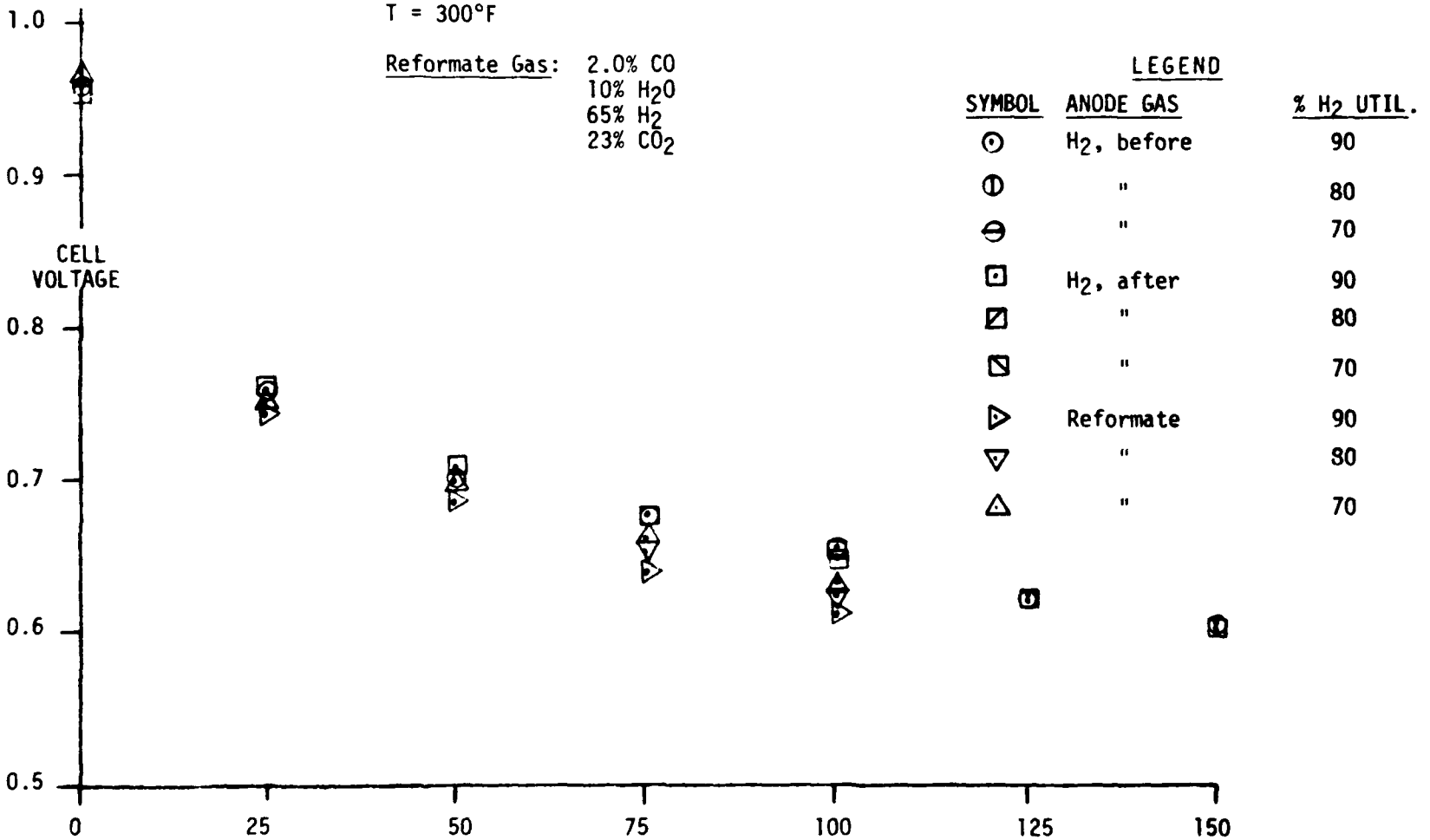

Figure 12

ENGELHARD INDUSTRIES

PARAMETRIC SINGLE-CELL TESTING - CELL No. 1

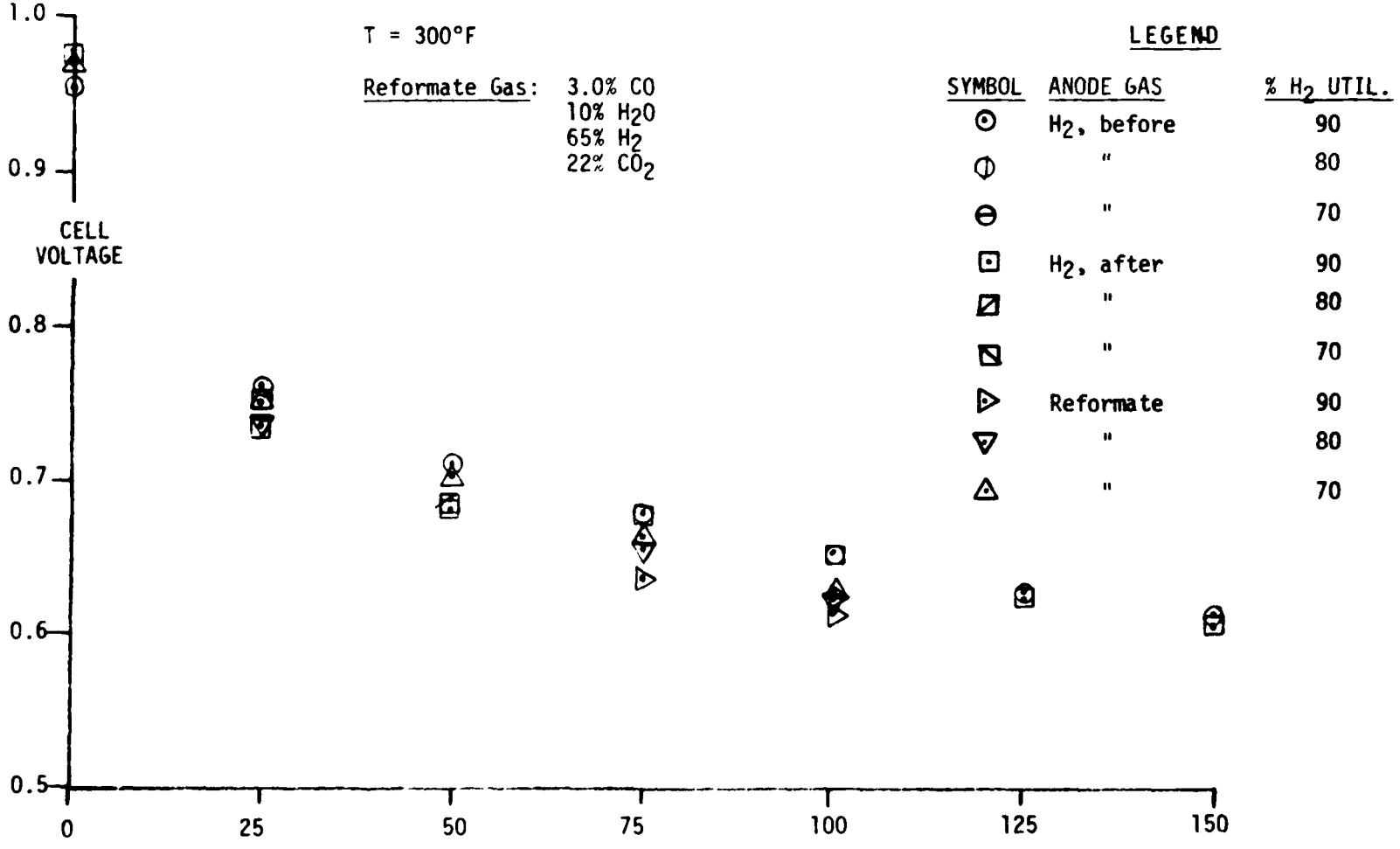

Figure 13

ENGELHARD INDUSTRIES

PARAMETRIC SINGLE-CELL TESTING - CELL No. 1

T = 325°F

Reformate Gas: 0.5% CO
10% H_2O
65% H_2
24.5% CO_2

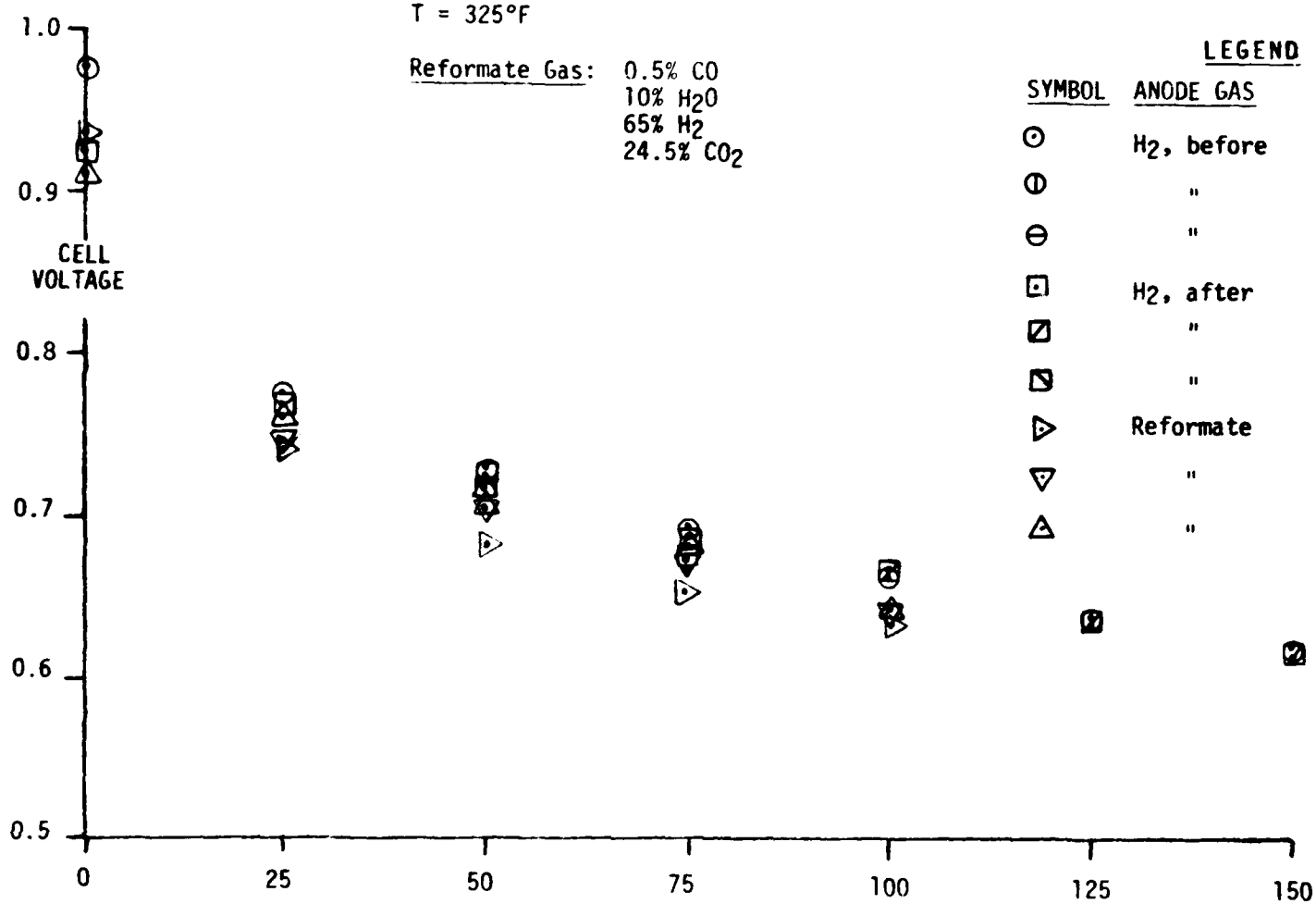

Figure 14

ENGELHARD INDUSTRIES

PARAMETRIC SINGLE-CELL TESTING - CELL No. 1

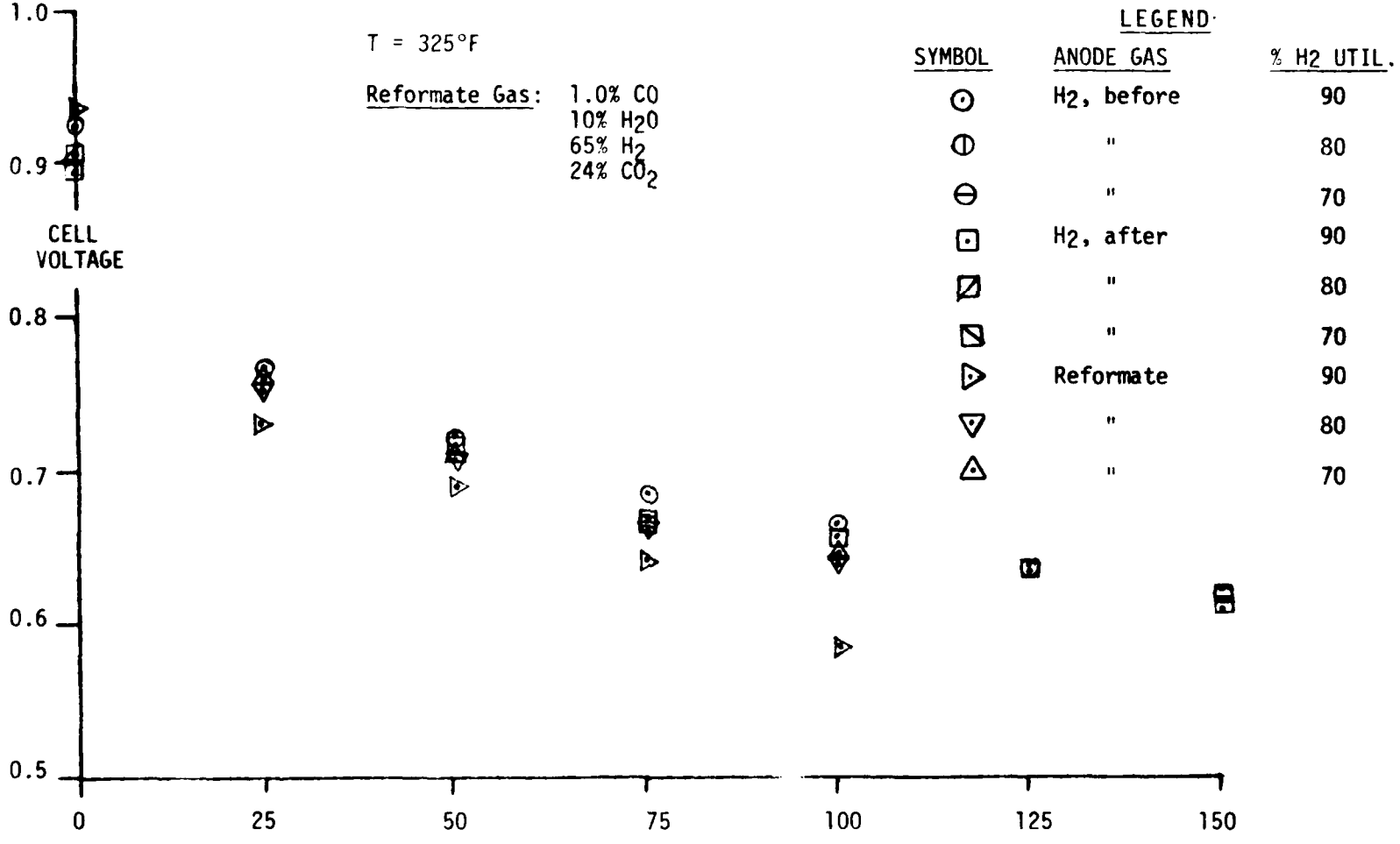

Figure 15

ENGELHARD INDUSTRIES

PARAMETRIC SINGLE-CELL TESTING - CELL No. 1

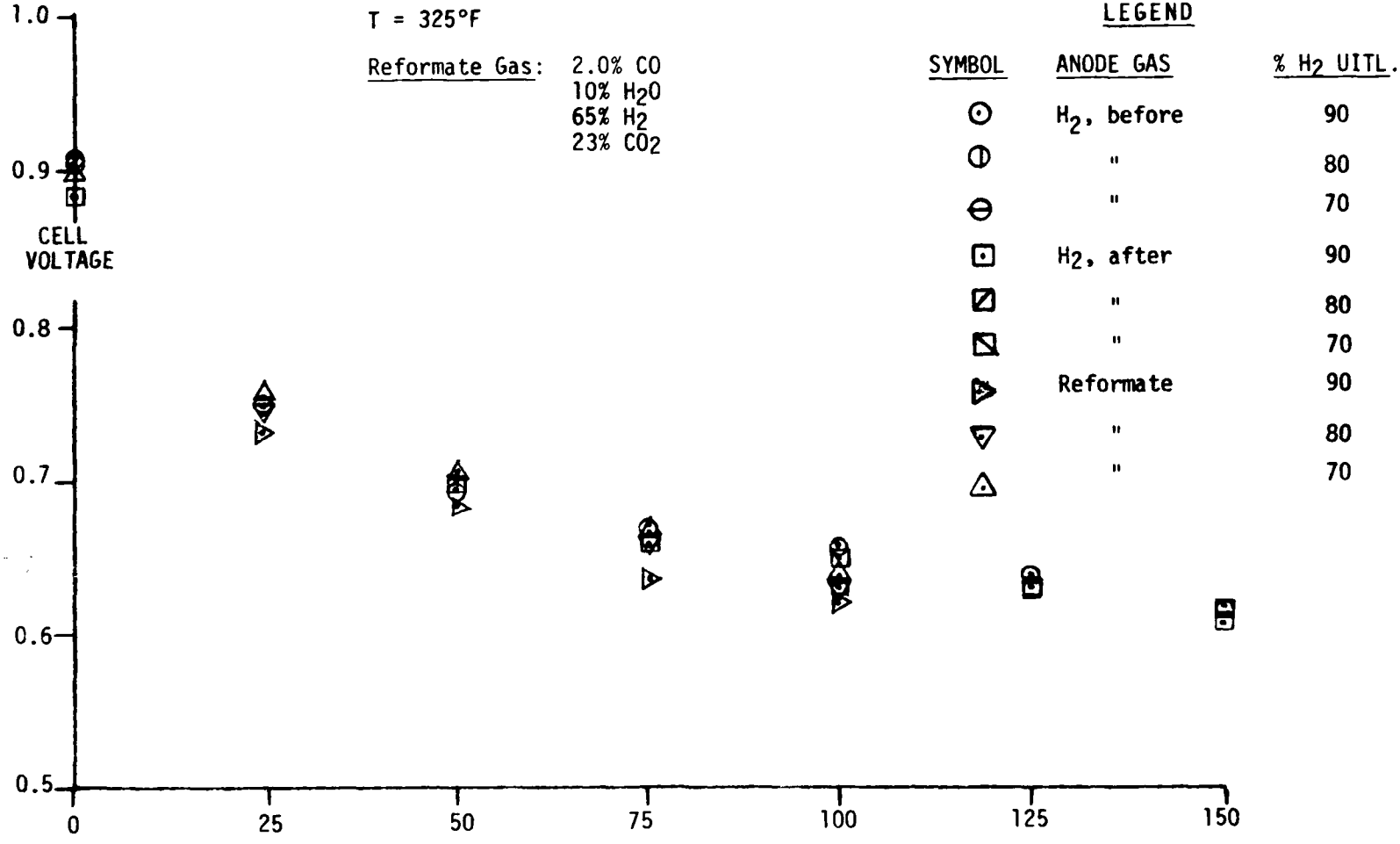

Figure 16

ENGELHARD INDUSTRIES

PARAMETRIC SINGLE-CELL TESTING - CELL No. 1

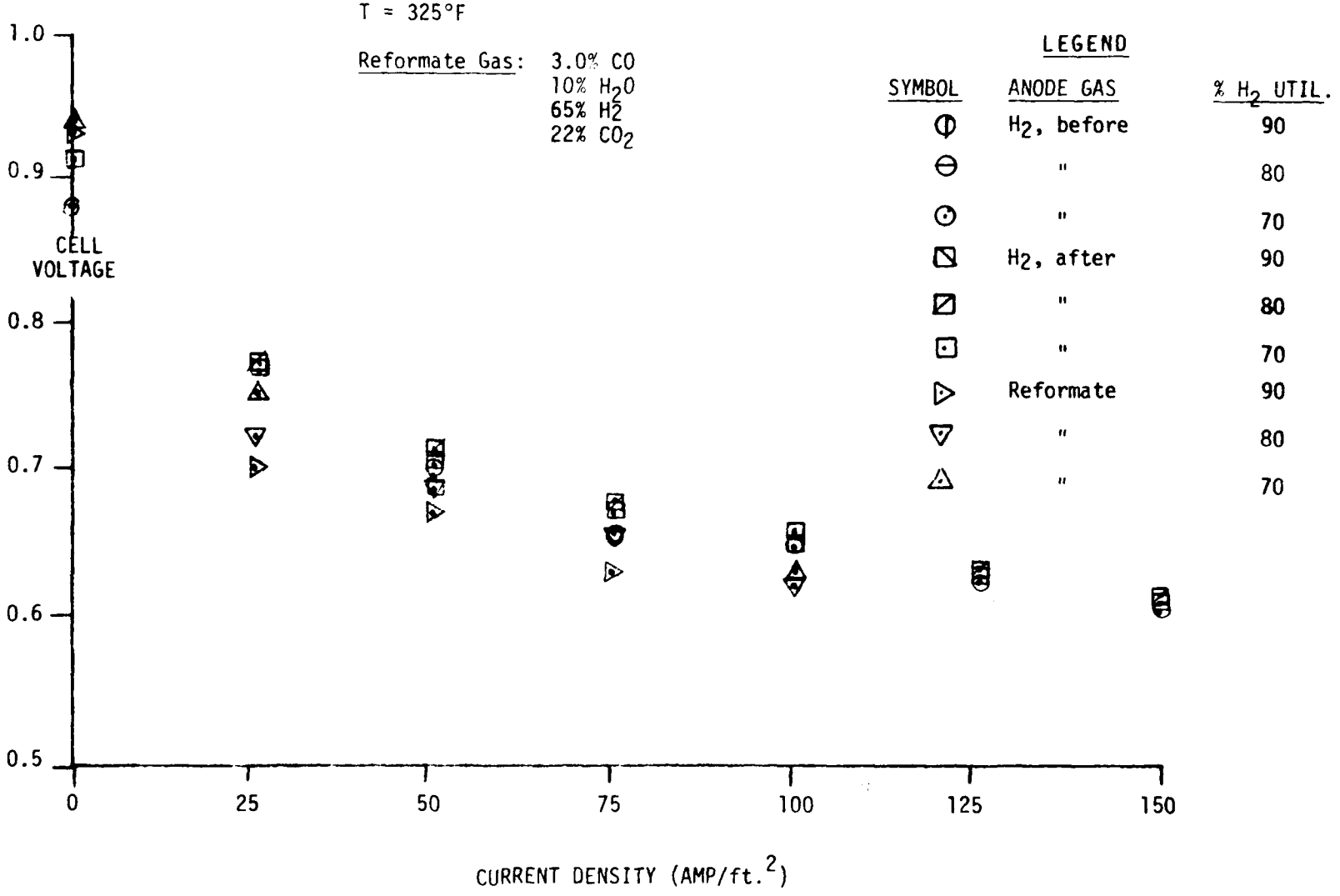

Figure 17

ENGELHARD

PARAMETRIC SINGLE-CELL TESTING

CELL NO. 1A

T = 300°F

ANODE GAS	CELL VOLTAGE (MV)							% H_2 UTILIZATION
	0	25	50	75	100	125	150 AMP/FT^2	
H_2	921	763	718	685	655	629	604	70
H_2	927	763	717	684	655	628	604	80
H_2	928	762	717	684	655	629	605	90
0.5% CO, 10% H_2O, 65% H_2, 24.5% CO_2	930	756	705	670	642			70
	928	750	699	668	641			80
	926	743	691	659	632			90
H_2	926	760	715	683	655	631	605	70
H_2	926	765	718	686	657	632	607	80
H_2	926	763	718	685	658	632	607	90
1.0% CO, 10% H_2O, 65% H_2, 24% CO_2	924	748	699	663	635			70
	923	744	695	664	63			80
	924	749	687	654	626			90
H_2	932	761	716	683	656	631	608	70
H_2	932	764	717	685	657	633	609	80
H_2	932	762	715	680	654	630	607	90
2.0% CO, 10% H_2O, 65% H_2, 23% CO_2	928	749	699	663	634			70
	928	749	695	659	630			80
	928	744	694	649	622			90
H_2	931	760	715	682	654	631	608	70
H_2	931	765	718	686	657	633	610	80
H_2	931	763	718	683	655	632	608	90
3.0% CO, 10% H_2O, 65% H_2, 22% CO_2	926	747	696	660	631			70
	925	743	693	656	628			80
	928	735	687	647	615			90
H_2	935	762	715	683	655	629	607	70
H_2	935	762	715	682	655	630	607	80
H_2	937	762	716	683	656	630	608	90

Table 3

ENGELHARD

PARAMETRIC SINGLE-CELL TESTING

CELL NO 1A

T = 325°F

ANODE GAS	CELL VOLTAGE (MV)							% H_2 UTILIZATION
	0	25	50	75	100	125	150 AMP/FT^2	
H_2	934	771	725	693	666	640	618	70
H_2	910	761	718	687	660	635	614	80
H_2	929	766	722	690	665	640	617	90
0.5% CO 10% H_2O 65% H_2 24.5% CO_2	930 923 921	766 751 745	712 703 698	677 664 664	650 643 642			70 80 90
H_2	920	761	717	686	660	641	619	70
H_2	932	768	723	691	666	641	620	80
H_2	933	769	724	692	665	642	623	90
1.0% CO 10% H_2O 65% H_2 24% CO_2	931 928 928	755 748 753	708 704 701	676 669 661	649 643 637			70 80 90
H_2	924	769	722	691	665	641	618	70
H_2	930	765	722	689	665	640	620	80
H_2	934	768	722	691	666	642	620	90
2.0% CO 10% H_2O 65% H_2 23% CO_2	928 928 927	752 749 737	706 702 686	672 670 656	645 641 628			70 80 90
H_2	926	768	723	692	667	642	620	70
H_2	936	767	724	692	666	642	620	80
H_2	935	768	722	692	665	642	620	90
3.0% CO 10% H_2O 65% H_2 22% CO_2	928 928 924	753 748 732	705 697 690	672 664 654	642 638 621			70 80 90
H_2	925	770	723	691	664	640	618	70
H_2	933	771	724	692	665	641	618	80
H_2	933	768	722	690	664	640	618	90

Table 4

ENGELHARD

PARAMETRIC SINGLE-CELL TESTING

CELL NO. 2

$T = 300^{o}F$

ANODE GAS	CELL VOLTAGE (MV)							% H_2 UTILIZATION
	0	25	50	75	100	125	150 AMP/FT^2	
H_2	938	753	709	676	651	628	607	70
H_2	943	759	714	682	656	633	612	80
H_2	942	758	714	683	657	634	612	90
1.5% CO	935	748	700	666	639			70
8% H_2O	935	743	697	660	629			80
66.5% H_2	935	736	688	642	616			90
24% CO_2								
H_2	943	760	716	684	658	636	614	70
H_2	941	763	717	685	659	636	614	80
H_2	943	760	715	683	658	636	614	90
1.5% CO	942	748	699	664	634			70
10% H_2O	936	742	692	660	628			80
65% H_2	936	741	685	651	617			90
23.5% CO_2								
H_2	943	762	716	684	656	636	614	70
H_2	942	763	718	686	660	636	614	80
H_2	942	760	716	684	658	634	614	90
1.5% CO	940	747	696	660	630			70
12% H_2O	937	739	696	660	633			80
63.5% H_2	937	735	680	649	616			90
23% CO_2								
H_2	942	760	715	683	656	633	612	70
H_2	940	759	714	682	657	632	612	80
H_2	940	758	713	682	655	632	612	90

Table 5

ENGELHARD

PARAMETRIC SINGLE-CELL TESTING

CELL NO. 2

T = 325°F

ANODE GAS	CELL VOLTAGE (MV)							% H_2 UTILIZATION
	0	25	50	75	100	125	150 AMP/FT^2	
H_2	937	769	725	696	670	648	626	70
H_2	937	771	728	698	671	649	627	80
H_2	937	767	726	695	670	648	627	90
1.5% CO, 8% H_2O, 66.5% H_2, 24% CO_2	934	754	709	674	646			70
	934	749	704	668	641			80
	934	736	694	657	627			90
H_2	942	768	724	693	668	647	625	70
H_2	939	767	725	694	668	647	627	80
H_2	940	766	724	693	667	646	626	90
1.5% CO, 10% H_2O, 65% H_2, 23.5% CO_2	935	752	708	676	647			70
	935	750	705	672	643			80
	935	742	694	662	630			90
H_2	942	768	725	695	672	647	625	70
H_2	944	768	725	694	669	646	626	80
H_2	945	767	724	695	670	648	628	90
1.5% CO, 12% H_2O, 63.5% H_2, 23% CO_2	930	748	702	672	648			70
	935	747	704	672	640			80
	935	746	700	658	629			90
H_2	940	762	719	688	665	643	624	70
H_2	942	765	722	690	667	643	622	80
H_2	943	766	721	692	665	641	622	90

Table 6

ENGELHARD INDUSTRIES

PARAMETRIC SINGLE-CELL TESTING - CELL No. 2

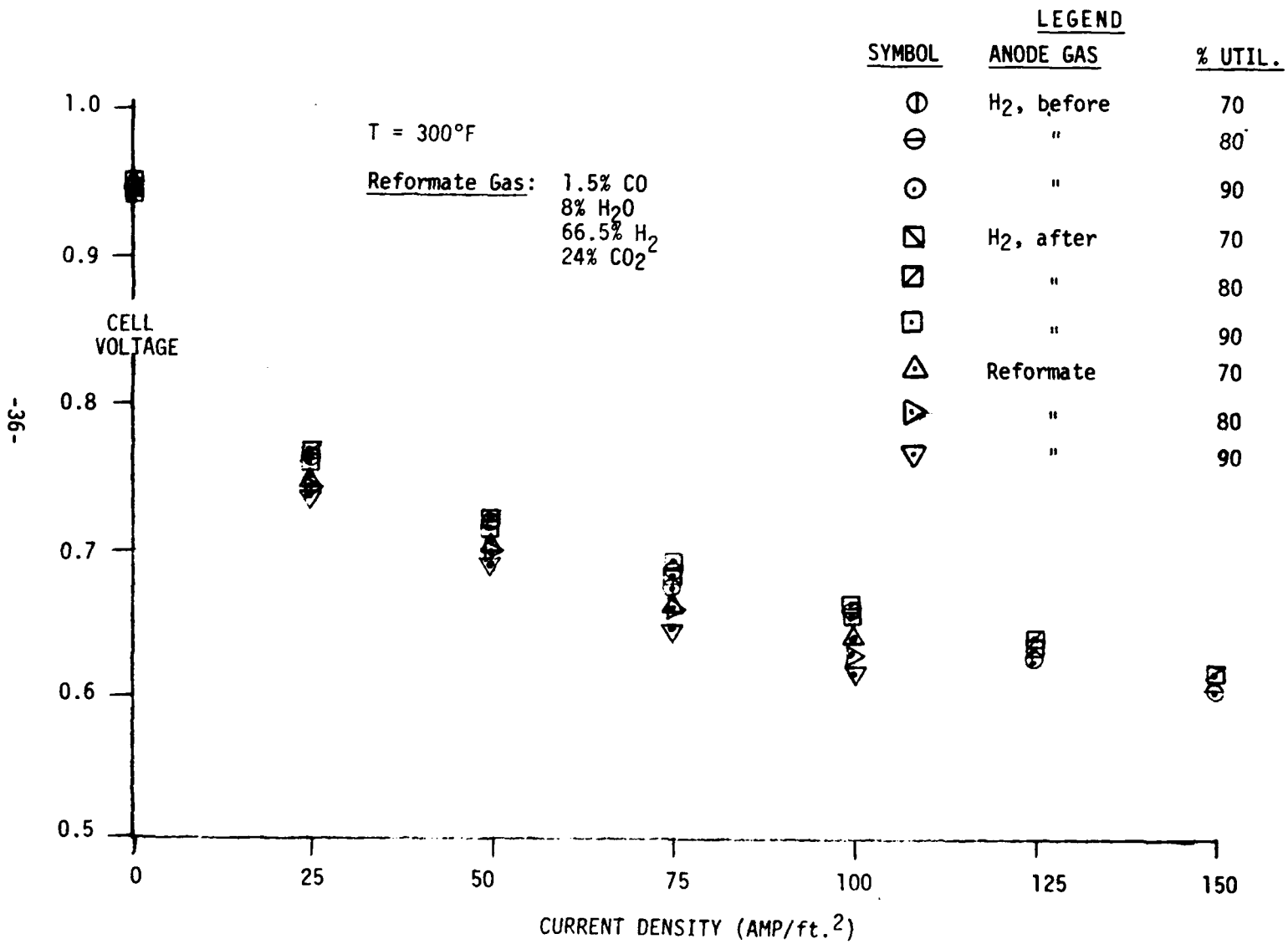

Figure 18

ENGELHARD INDUSTRIES

PARAMETRIC SINGLE-CELL TESTING - CELL No. 2

T = 300°F

Reformate Gas: 1.5% CO
10% H_2O
65% H_2
23.5% CO_2

LEGEND

SYMBOL	ANODE GAS	% UTIL.
◐	H_2, before	70
⊖	"	80
⊙	"	90
▨	H_2, after	70
▨	"	80
⊡	"	90
△	Reformate	70
▷	"	80
▽	"	90

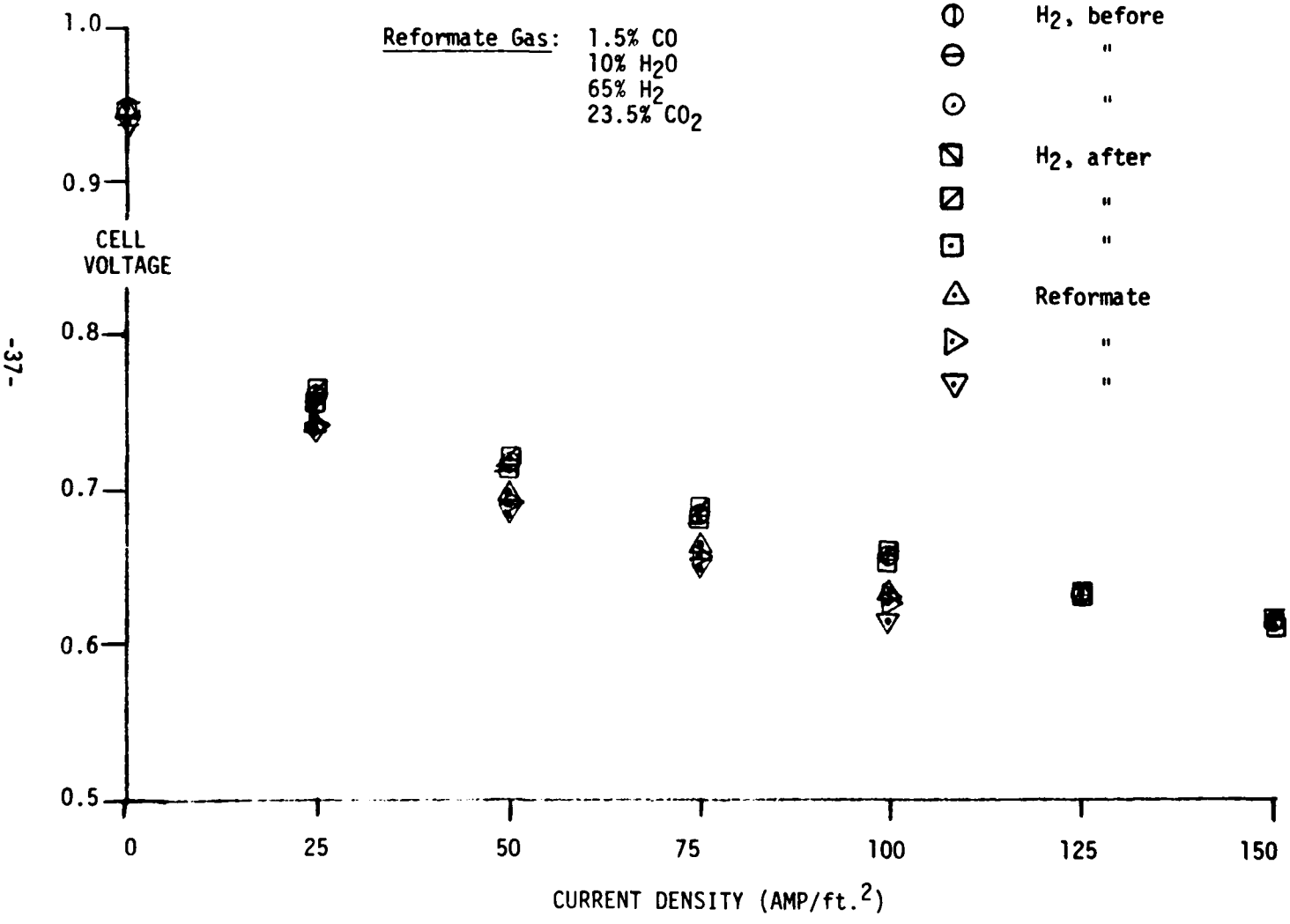

Figure 19

ENGELHARD INDUSTRIES

PARAMETRIC SINGLE-CELL TESTING - CELL No. 2

T = 300°F

Reformate Gas: 1.5% CO
12% H_2O
63.5% H_2
23% CO_2

LEGEND

SYMBOL	ANODE GAS	% UTIL.
⊙	H_2, before	70
⊖	"	80
⊙	"	90
⊠	H_2, after	70
⊠	"	80
⊡	"	90
△	Reformate	70
▷	"	80
▽	"	90

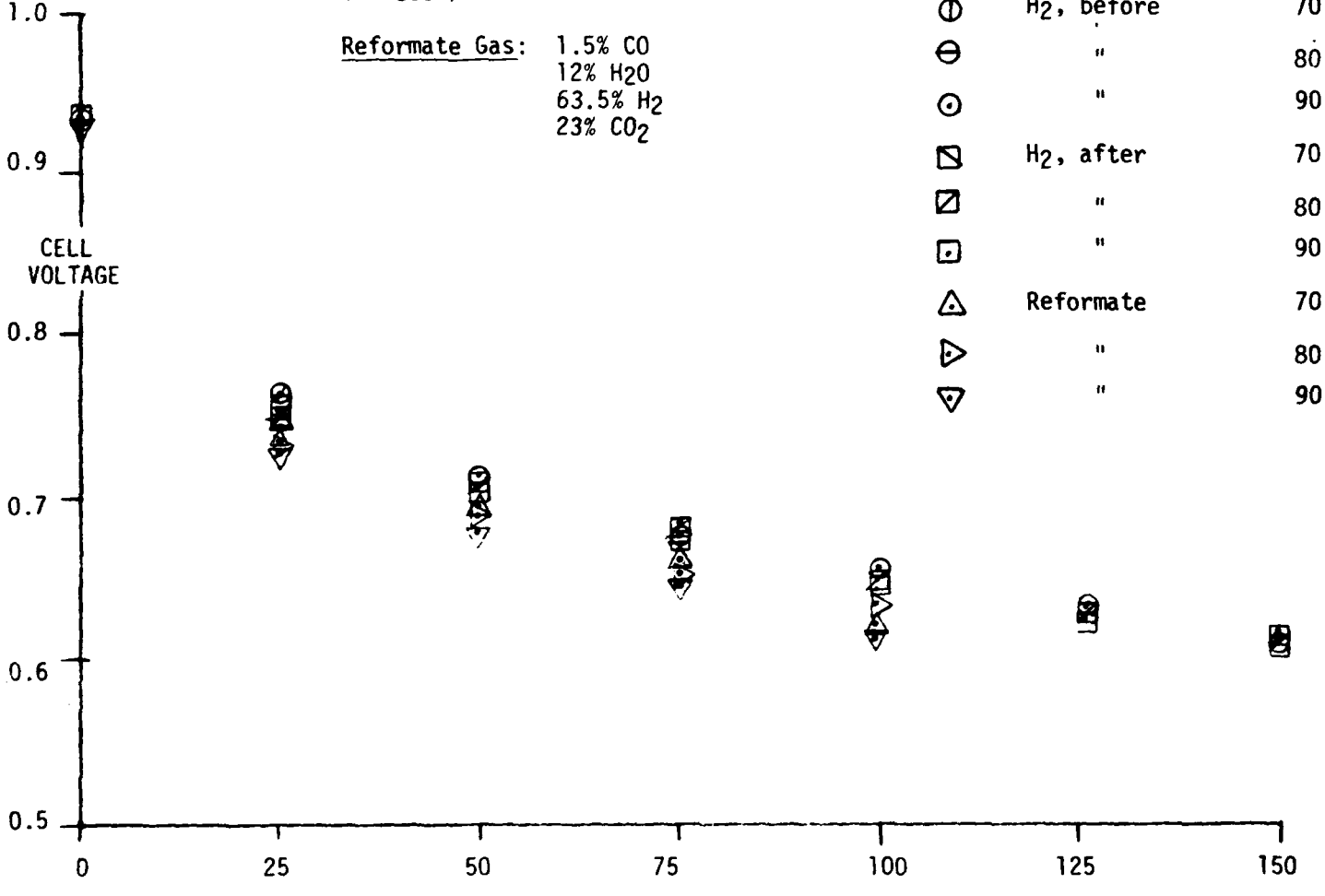

Figure 20

ENGELHARD INDUSTRIES

PARAMETRIC SINGLE-CELL TESTING - CELL No. 2

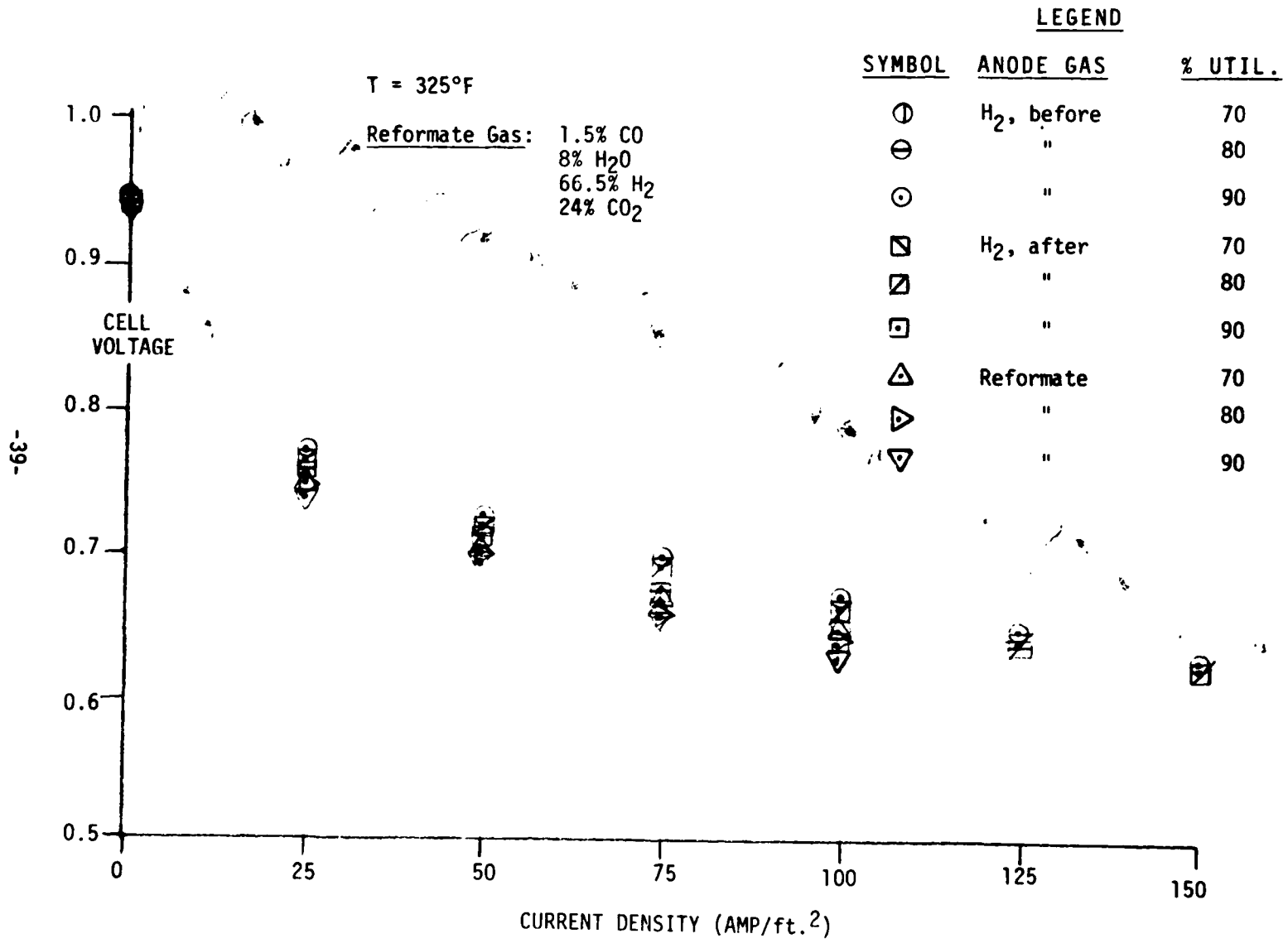

Figure 21

ENGELHARD INDUSTRIES

PARAMETRIC SINGLE-CELL TESTING - CELL No. 2

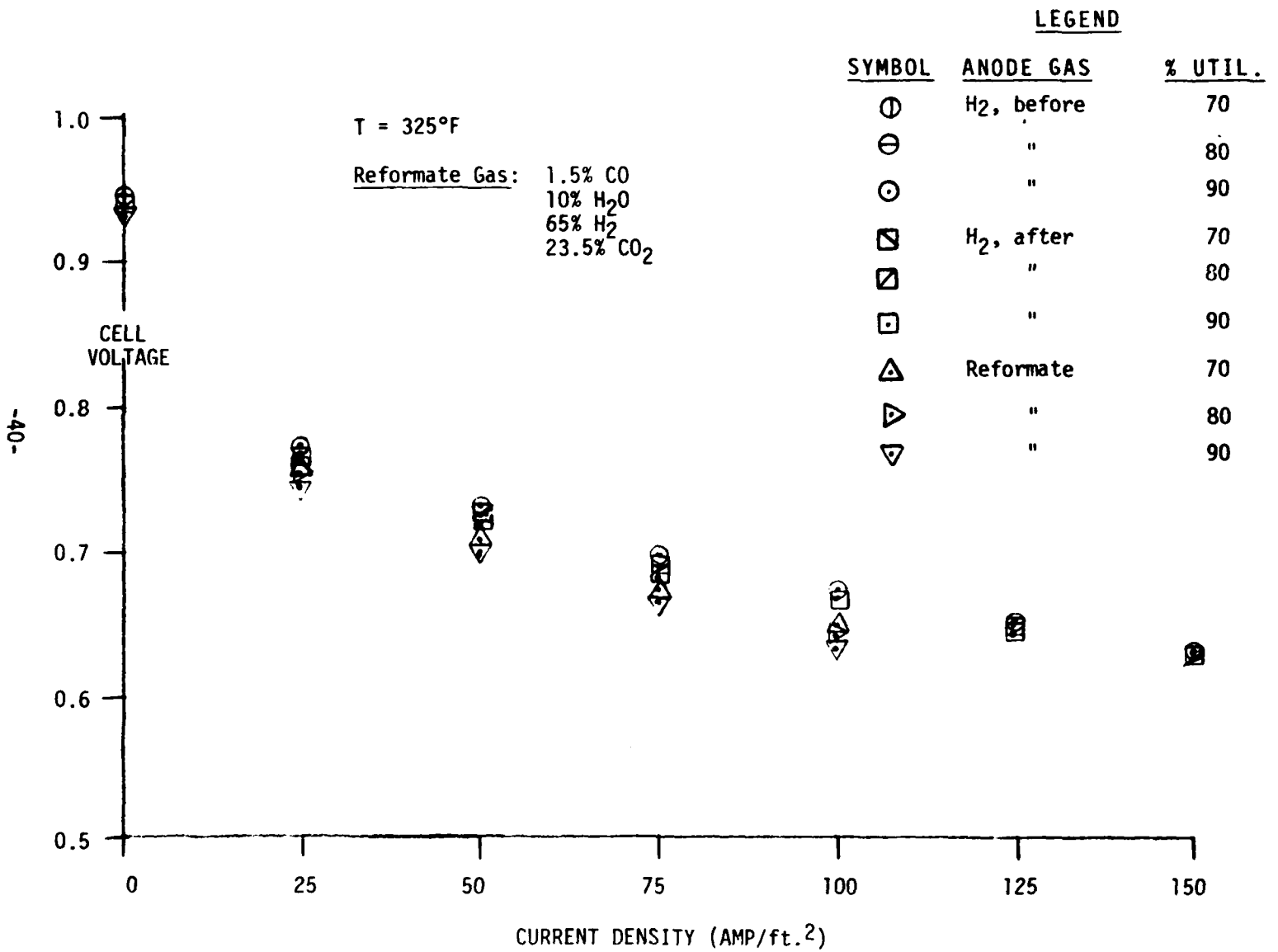

Figure 22

ENGELHARD INDUSTRIES

PARAMETRIC SINGLE-CELL TESTING - CELL No. 2

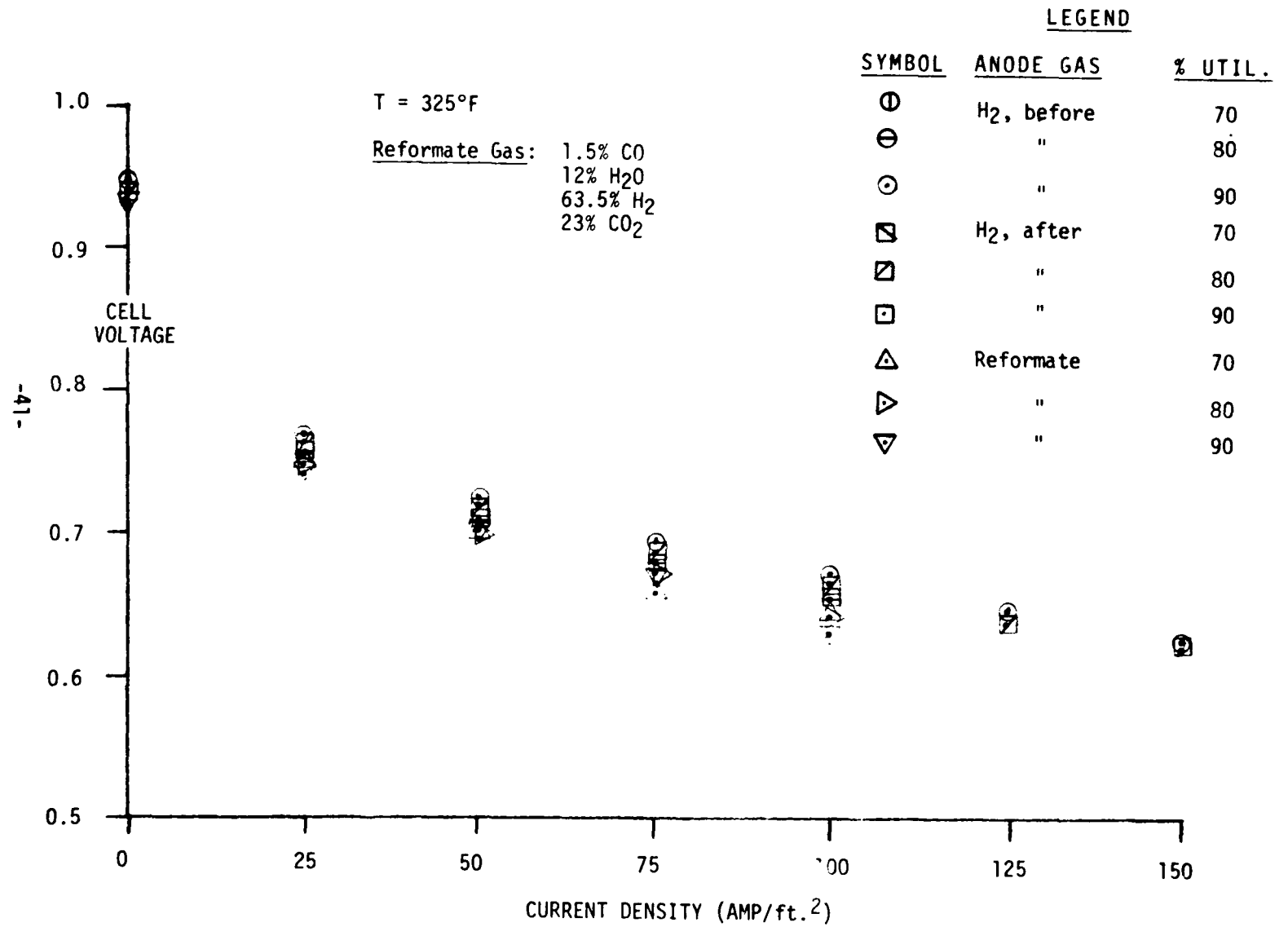

Figure 23

Performance was not strongly influenced by H_2O content in the range of 8-12%. The performance at 325°F was generally 10-15 mV higher than that at 300°F.

6.1.4 Cell No. 3

The results for Cell No. 3 are shown in Table 7. The data indicate no clear effect of H_2S in the 0-500 ppm range. At high hydrogen-utilizations the dilution effect of CH_4 in 85/15 H_2/CH_4 mixtures far outweighs any possible effect from added H_2S.

6.2 Three-Cell Stack Testing

6.2.1 Stack 1a

Figure 24 (see note below) shows the performance history of Stack 1a. The initial performance decline of Stack 1a was primarily attributable to the decline of the top and bottom cells.

At approximately 42 days into the test, the top cell was observed to decline more rapdily than the lower two cells. Open circuit readings taken at the 50 day point showed a depression in the top cell's open circuit, 0.788 volts versus 0.838 and 0.825 for the middle and bottom cells respectively.

6.2.2 Stack 2a

Figure 25 shows the performance history of Stack 2a.

Testing of Stack 2a was terminated after 696 hours of load profile testing (744 hours total load time) due to an over-temperature failure. The over temperature condition was caused by mixing of fuel and air within the inlet manifolds. Causes for the mixing were creep of the hydrogen manifold gasket and improper original positioning of this gasket.

- -

Note: Termination plate/current collector plate interface

To provide electrical contact between the carbon termination plates and the aluminum current collector plates an expanded copper mesh was employed in the preliminary stacks. Dissimilar metal corrosion between the copper and aluminum caused excessively high resistive losses at these interfaces. Examples of these losses are shown in Figures 24 and 25. The high resistive losses were reduced by copper plating the current collector plates and using a sheet of Grafoil between the collector and termination plate. Stacks 1a and 2a were rebuilt in this manner. All subsequent stacks employed this construction.

ENGELHARD

PARAMETRIC SINGLE-CELL TESTING

CELL NO. 3

T = 325°F

ANODE GAS	CELL VOLTAGE (MV)							% H_2 UTILIZATION
	0	25	50	75	100	125	150 AMP/FT^2	
H_2	926	763	715	685	658	634	610	70
H_2	926	754	711	684	658	634	612	80
H_2	928	744	704	681	651	632	610	90
85% H_2	927	753	707	677	647			70
15% CH_4	927	746	702	760	651			80
	928	732	671	658	628			90
85% H_2	927	752	701	676	648			70
100 PPM H_2S	928	739	697	668	642			80
BAL. CH_4	928	737	693	654	632			90
85% H_2	928	756	707	674	648			70
200 PPM H_2S	929	733	698	670	643			80
BAL. CH_4	930	722	689	665	629			90
85% H_2	929	753	705	674	648			70
300 PPM H_2S	931	715	696	669	644			80
BAL. CH_4	930	693	667	643	639			90
85% H_2	929	746	706	673	645			70
400 PPM H_2S	931	719	694	667	641			80
BAL. CH_4	931	714	647	652	617			90
85% H_2	929	752	704	674	649			70
500 PPM H_2S	931	748	647	669	643			80
BAL. CH_4	931	729	640	645	633			90

Table 7

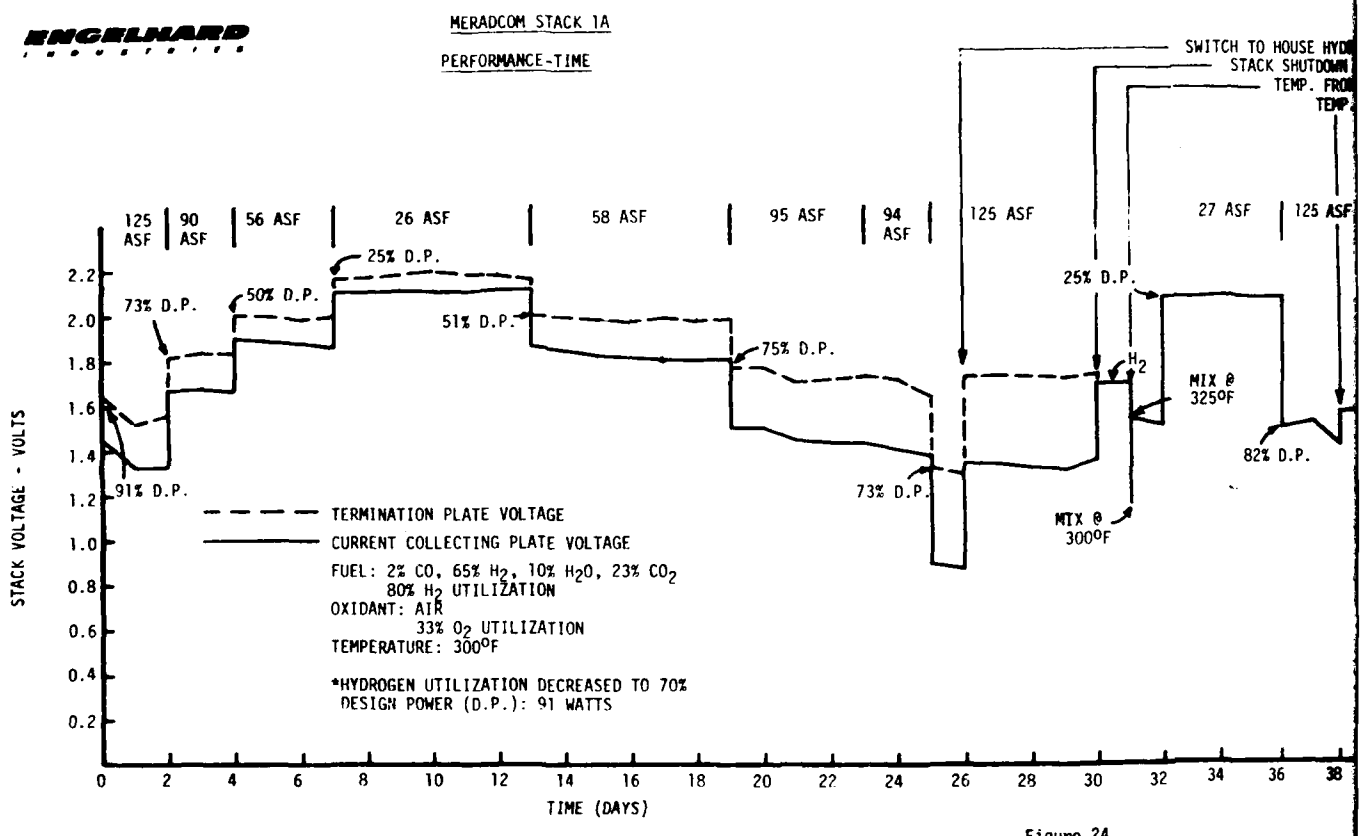
ENGELHARD
MERADCOM STACK 1A
PERFORMANCE-TIME
SWITCH TO HOUSE HYD
STACK SHUTDOWN
TEMP. FRO
TEMP.
125 ASF
90 ASF
56 ASF
26 ASF
58 ASF
95 ASF
94 ASF
125 ASF
27 ASF
125 ASF
25% D.P.
73% D.P.
50% D.P.
51% D.P.
75% D.P.
25% D.P.
H2
MIX @ 325°F
82% D.P.
91% D.P.
73% D.P.
MIX @ 300°F
TERMINATION PLATE VOLTAGE
CURRENT COLLECTING PLATE VOLTAGE
FUEL: 2% CO, 65% H2, 10% H2O, 23% CO2
80% H2 UTILIZATION
OXIDANT: AIR
33% O2 UTILIZATION
TEMPERATURE: 300°F
*HYDROGEN UTILIZATION DECREASED TO 70%
DESIGN POWER (D.P.): 91 WATTS
STACK VOLTAGE - VOLTS
TIME (DAYS)

Figure 24

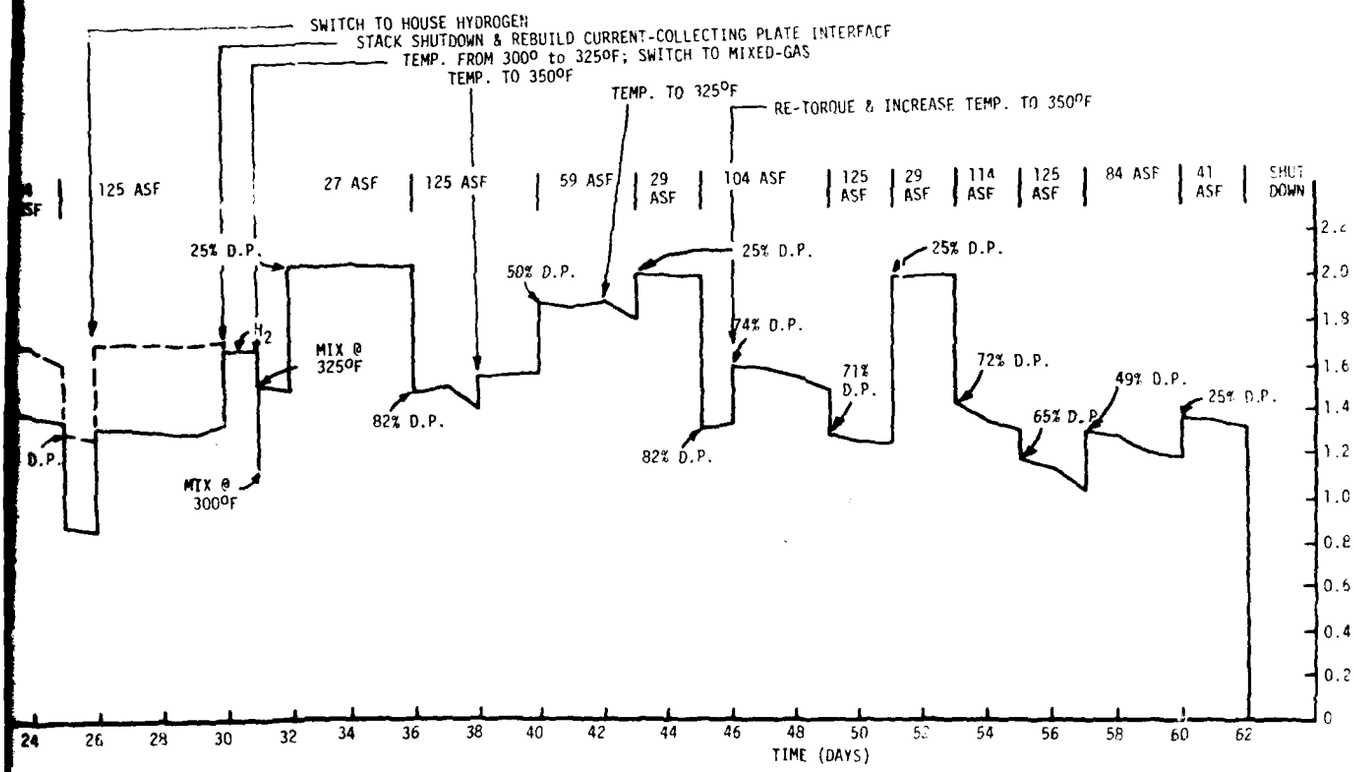
SWITCH TO HOUSE HYDROGEN
STACK SHUTDOWN & REBUILD CURRENT-COLLECTING PLATE INTERFACE
TEMP. FROM 300° to 325°F; SWITCH TO MIXED-GAS
TEMP. TO 350°F
TEMP. TO 325°F
RE-TORQUE & INCREASE TEMP. TO 350°F
125 ASF
27 ASF
125 ASF
59 ASF
29 ASF
104 ASF
125 ASF
29 ASF
114 ASF
125 ASF
84 ASF
41 ASF
SHUT DOWN
25% D.P.
50% D.P.
25% D.P.
74% D.P.
25% D.P.
H_2
MIX @ 325°F
MIX @ 300°F
82% D.P.
82% D.P.
71% D.P.
72% D.P.
65% D.P.
49% D.P.
25% D.P.
D.P.
2.0
1.8
1.6
1.4
1.2
1.0
0.8
0.6
0.4
0.2
0
24
26
28
30
32
34
36
38
40
42
44
46
48
50
52
54
56
58
60
62
TIME (DAYS)

Figure 24

ENGELHARD
INDUSTRIES

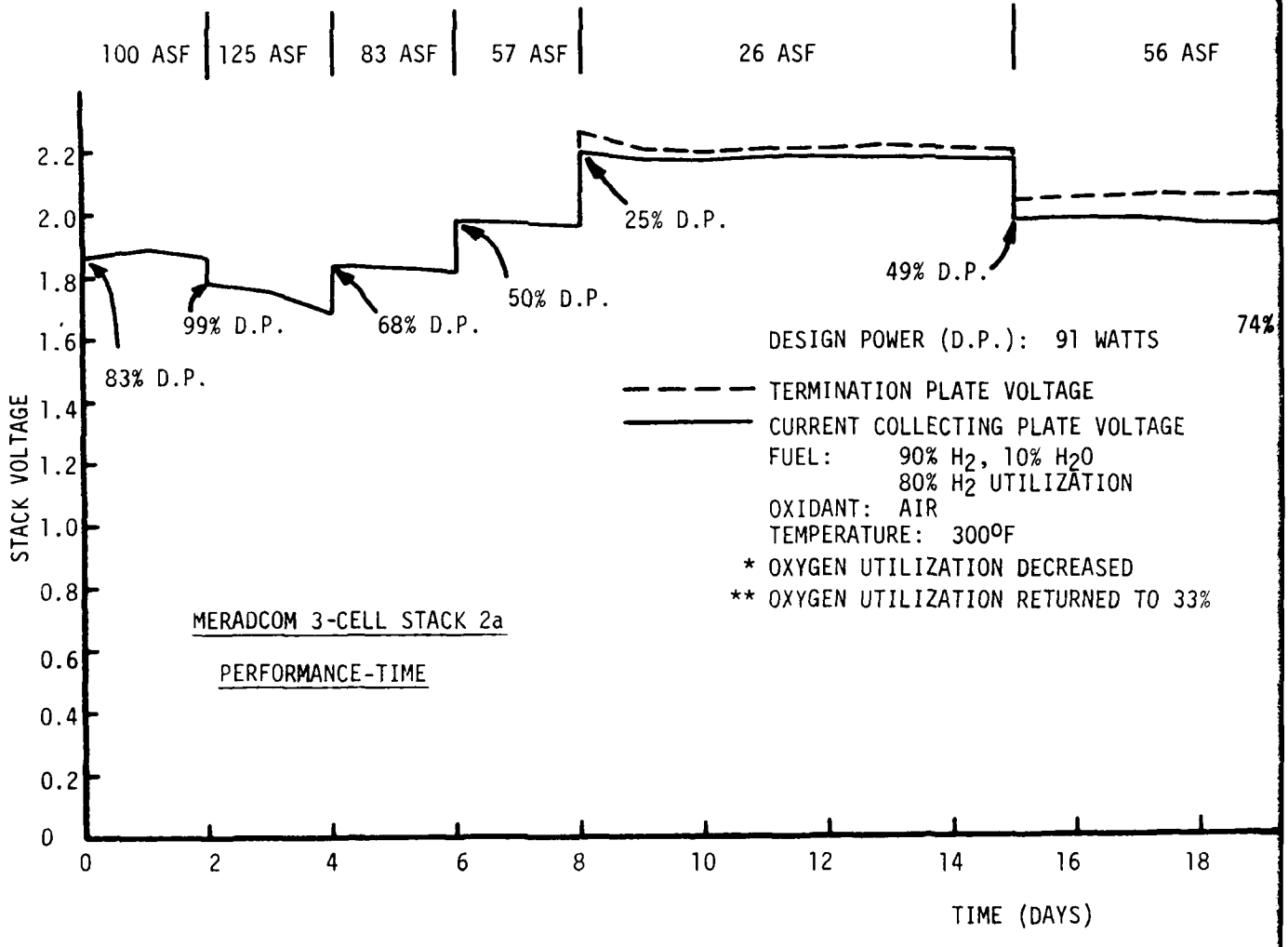

Figure 25

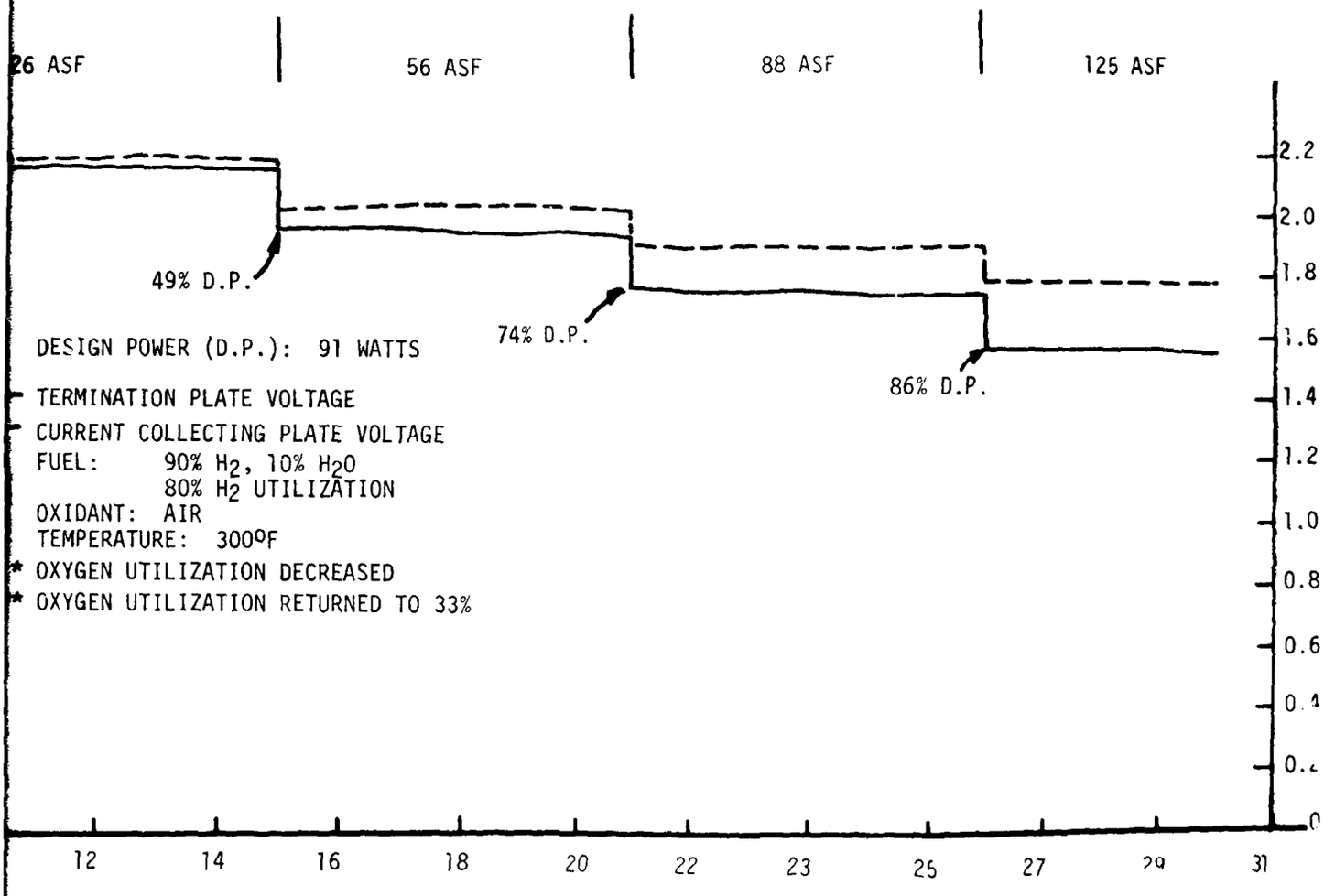
26 ASF
56 ASF
88 ASF
125 ASF
49% D.P.
74% D.P.
86% D.P.
DESIGN POWER (D.P.): 91 WATTS
TERMINATION PLATE VOLTAGE
CURRENT COLLECTING PLATE VOLTAGE
FUEL: 90% H_2, 10% H_2O
80% H_2 UTILIZATION
OXIDANT: AIR
TEMPERATURE: 300°F
* OXYGEN UTILIZATION DECREASED
* OXYGEN UTILIZATION RETURNED TO 33%
2.2
2.0
1.8
1.6
1.4
1.2
1.0
0.8
0.6
0
12
14
16
18
20
22
23
25
27
29
31
TIME (DAYS)

Figure 25

Prior to failure Stack 2a operated nominally. One day before failure, stack open circuit voltage was 2.672 volts. Individual cell voltages at 125 ASF, 300°F were 0.591, 0.590 and 0.600 for the top, middle and bottom cells respectively.

6.2.3 Stack 2b

Figure 26 shows the performance history of Stack 2b. Figure 27 shows the open circuit voltage history of Stack 2b.

The performance decline in Stack 2b was characterized by an accompanying decline in open circuit voltage, see Figure 27 Stack 2b - Open Circuit vs Time.

The extreme decline observed during the final two days of testing was primarily caused by the bottom cell. On day thirty, the bottom cell had declined to 0.263 volts at 125 ASF, 350°F as opposed to 0.601 and 0.565 respectively for the top and middle cells. Open circuit voltages of all cells were unacceptably low at the thirty day point with the bottom cell having the lowest voltage. Open circuit voltages at this point were: top cell 0.768, middle cell 0.726, bottom cell 0.583.

6.2.4 Stack 1b

Figure 28 shows the performance history of Stack 1b. Figure 29 shows the open circuit voltage history of Stack 1b.

As in Stack 2b, performance declines were accompanied by declines in open circuit voltage. See Figure 29, Stack 1b. Open Circuit Voltage vs. Time. Decline was uniform across the three cells. Final open circuit voltages (24 days) were: top cell 0.729 volts, middle cell 0.722 volts, bottom cell 0.738 volts.

At 24 days into the test, the temperature controller for Stack 1b failed in the on position causing gross overheating of the stack. As a result, no further testing was possible.

6.2.5 Stack 3a

Figure 30 shows the performance history of Stack 2a.

Stack 3a was the first stack specifically devoted to investigation of start-up/shut-down effects. It can be seen in Figure 30 that overall stack performance declines were accompanied by

ENGELHARD INDUSTRIES

MERADCOM 3-CELL STACK 2b

PERFORMANCE-TIME

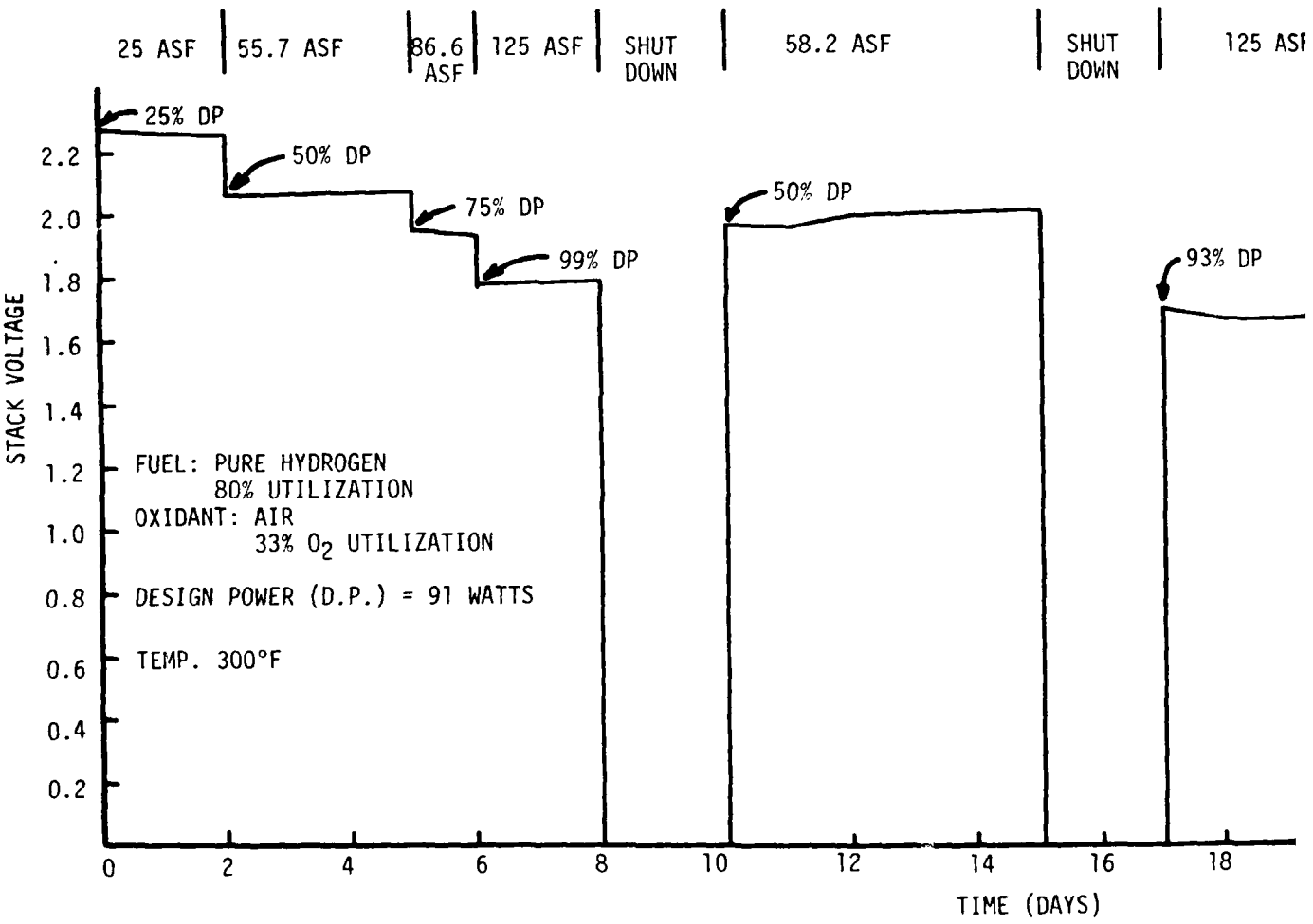

Figure 26

MERADCOM 3-CELL STACK 2b

PERFORMANCE-TIME

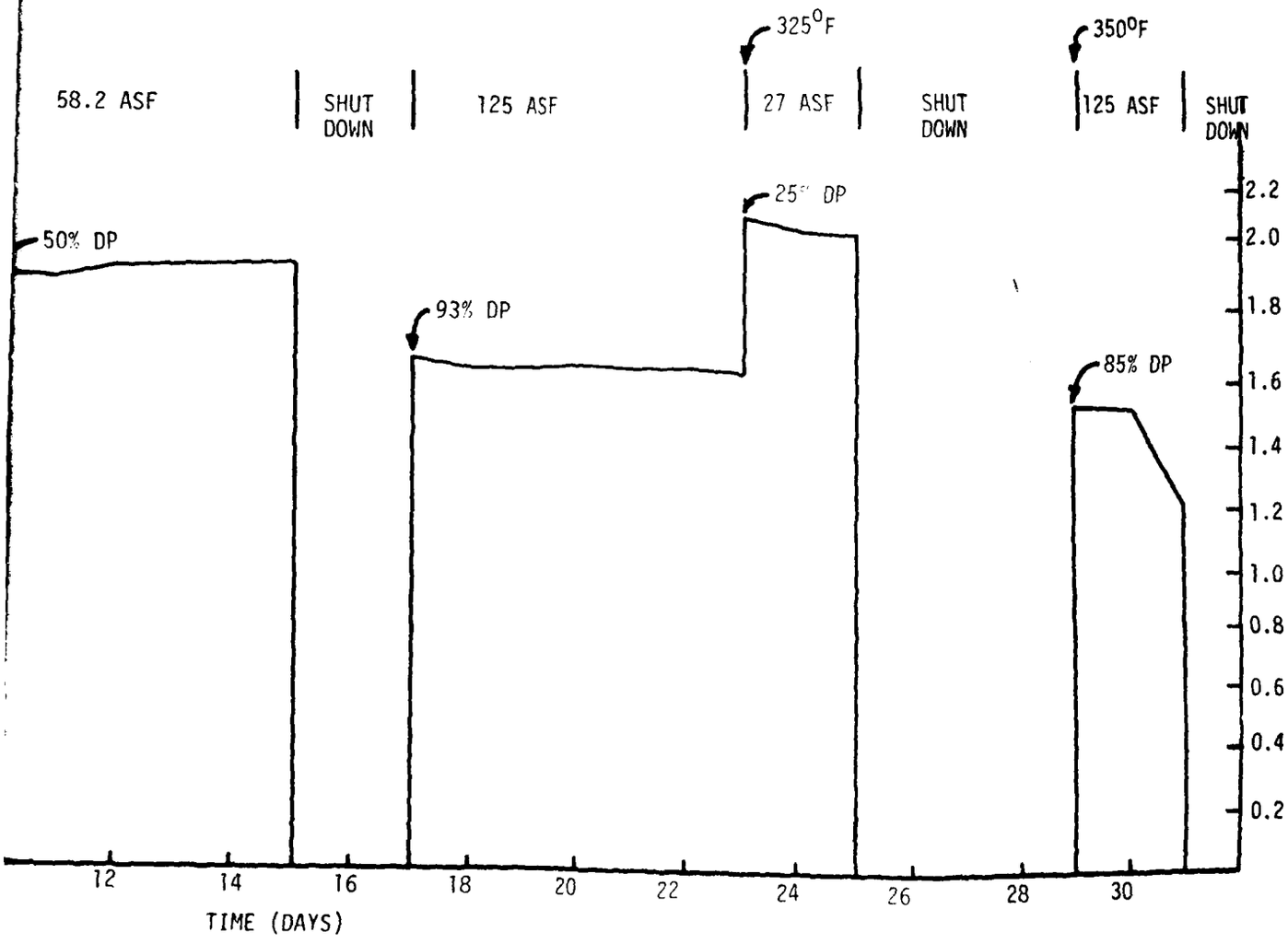

Figure 26

ENGELHARD
INDUSTRIES

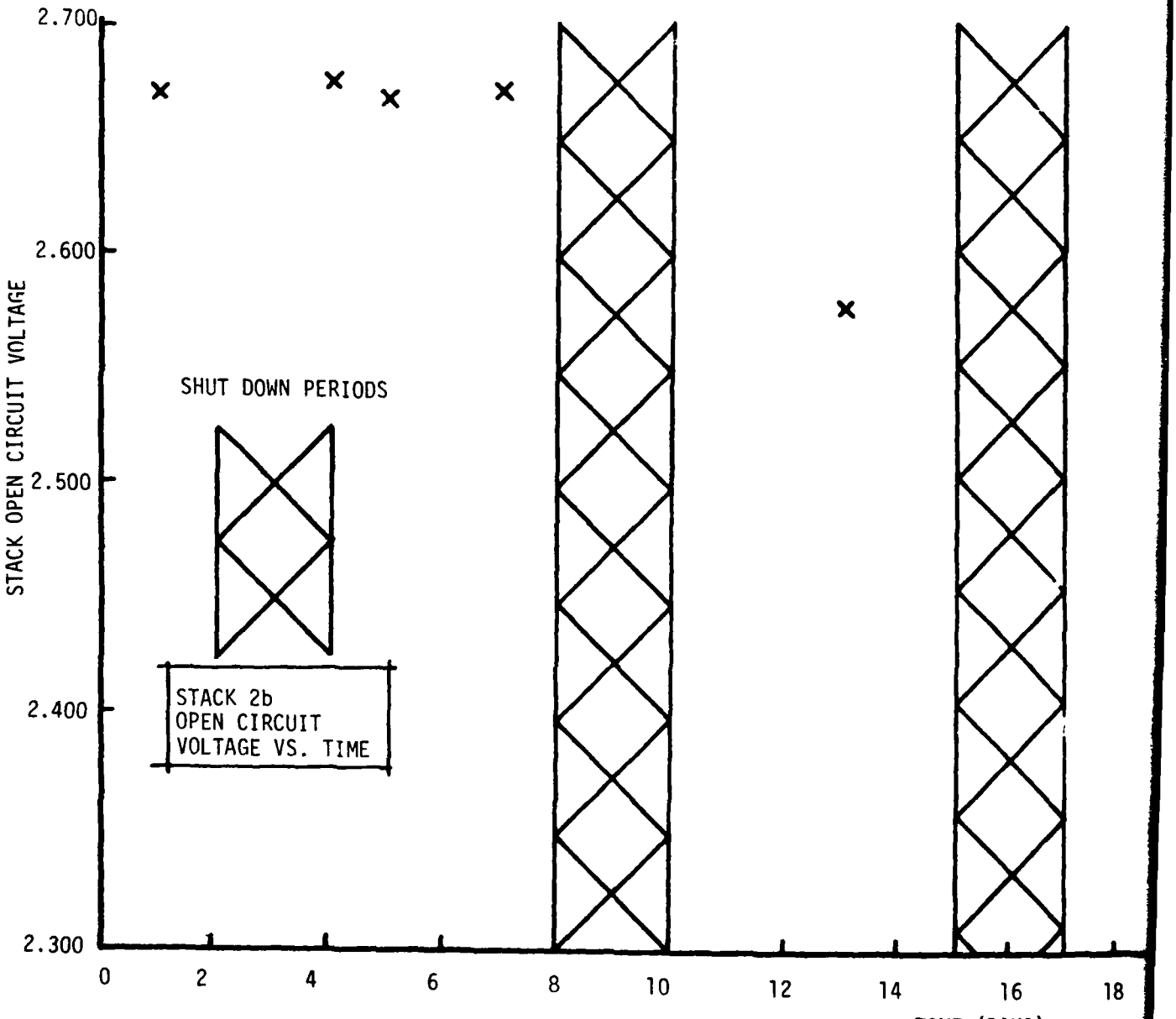

Figu

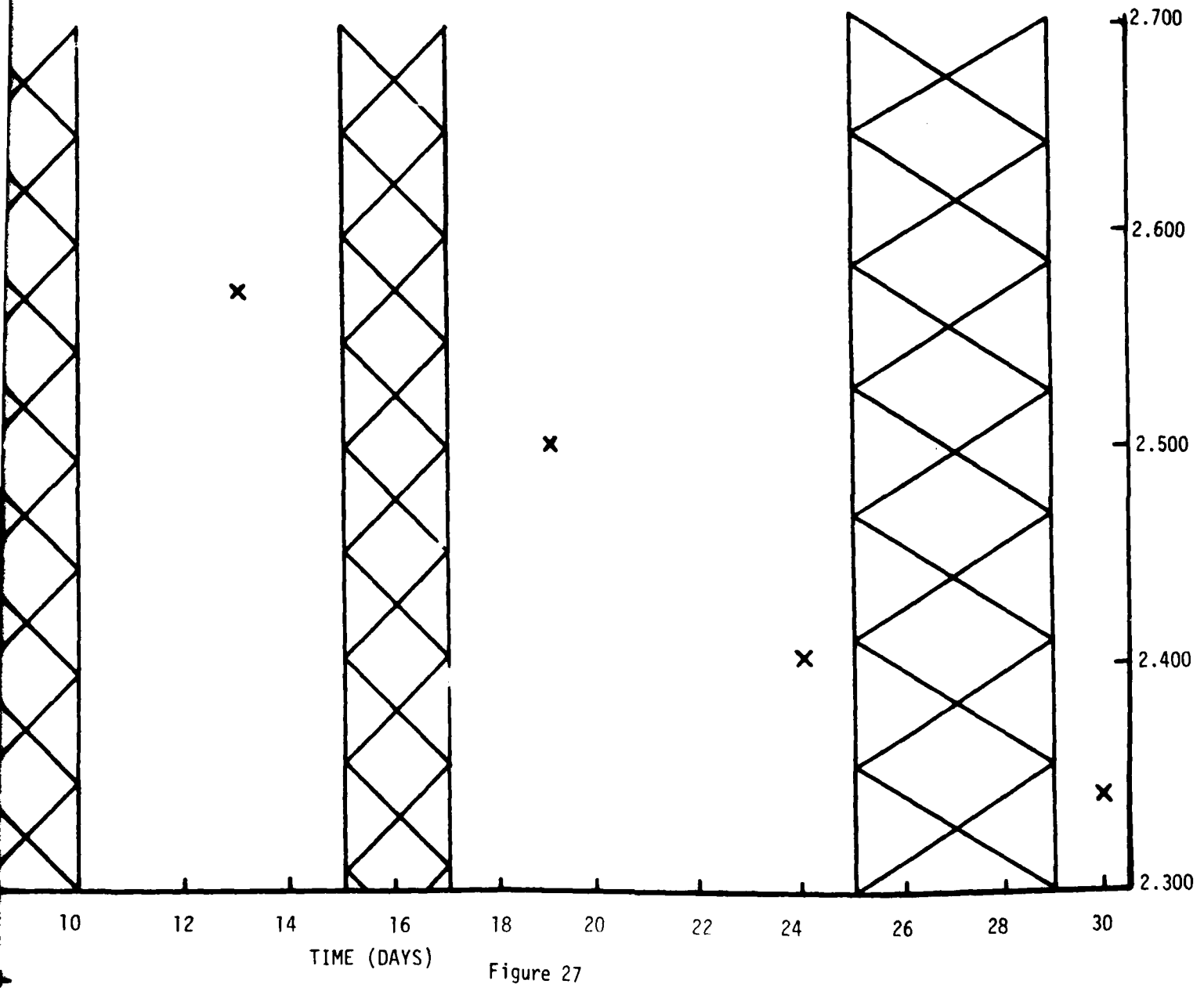
2.700
2.600
2.500
2.400
2.300
10
12
14
16
18
20
22
24
26
28
30
TIME (DAYS)

Figure 27

MERADCOM 3-CELL STACK 1b

PERFORMANCE - TIME

ENGELHARD INDUSTRIES

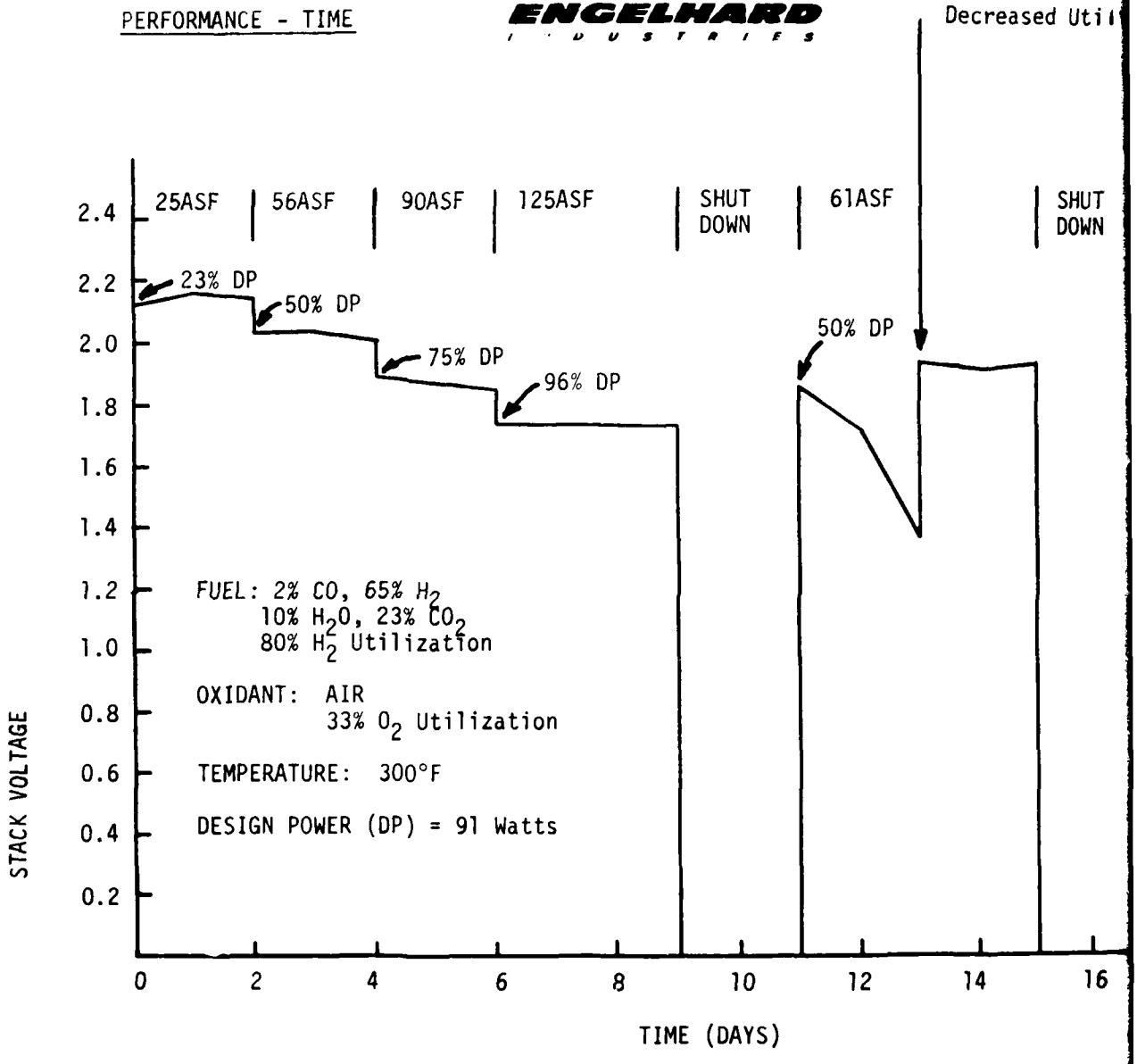

Figure 28

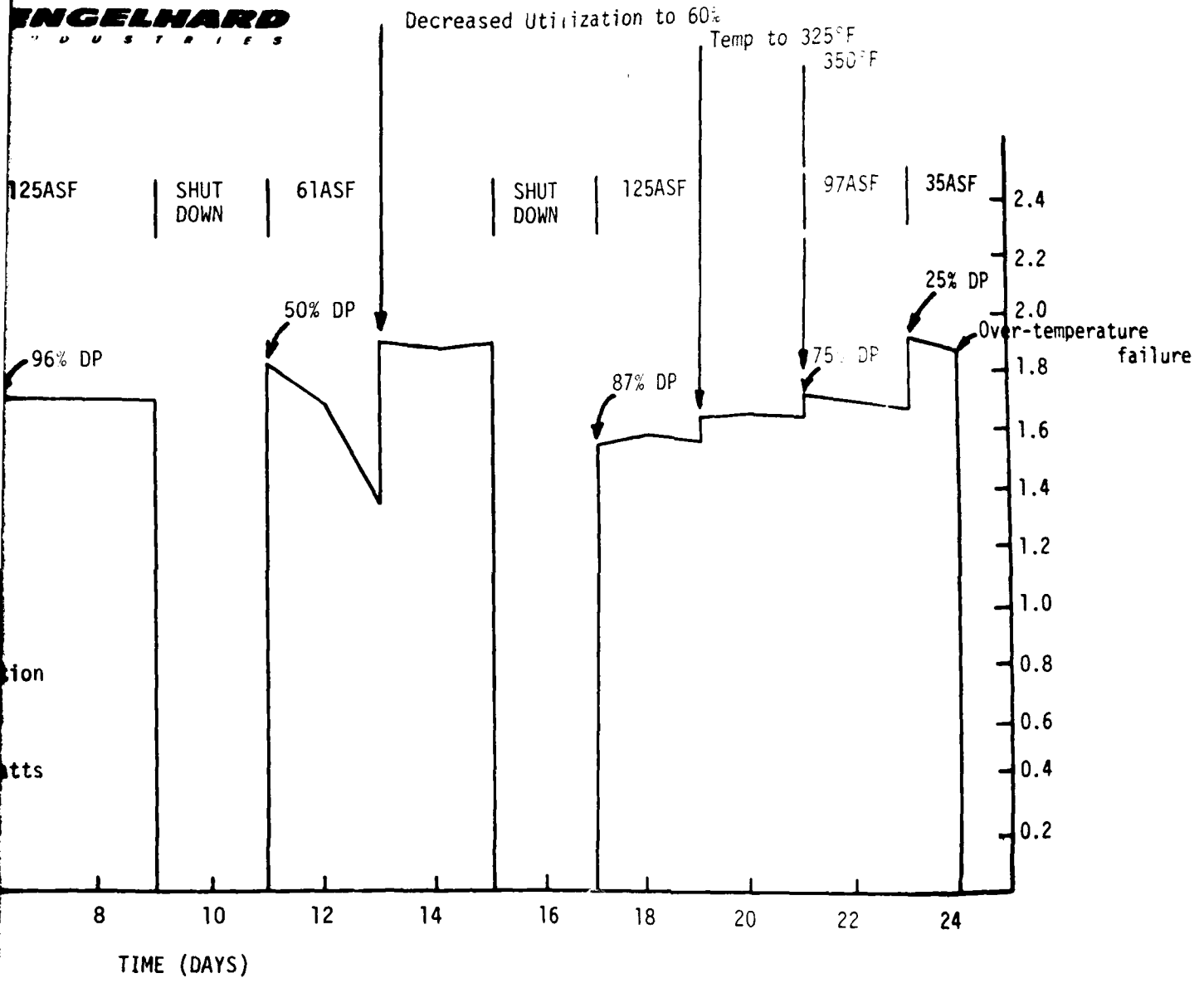
Decreased Utilization to 60%
Temp to 325°F
350°F
125ASF
SHUT DOWN
61ASF
SHUT DOWN
125ASF
97ASF
35ASF
96% DP
50% DP
87% DP
75% DP
25% DP
Over-temperature failure
2.4
2.2
2.0
1.8
1.6
1.4
1.2
1.0
0.8
0.6
0.4
0.2
8
10
12
14
16
18
20
22
24
TIME (DAYS)

Figure 28

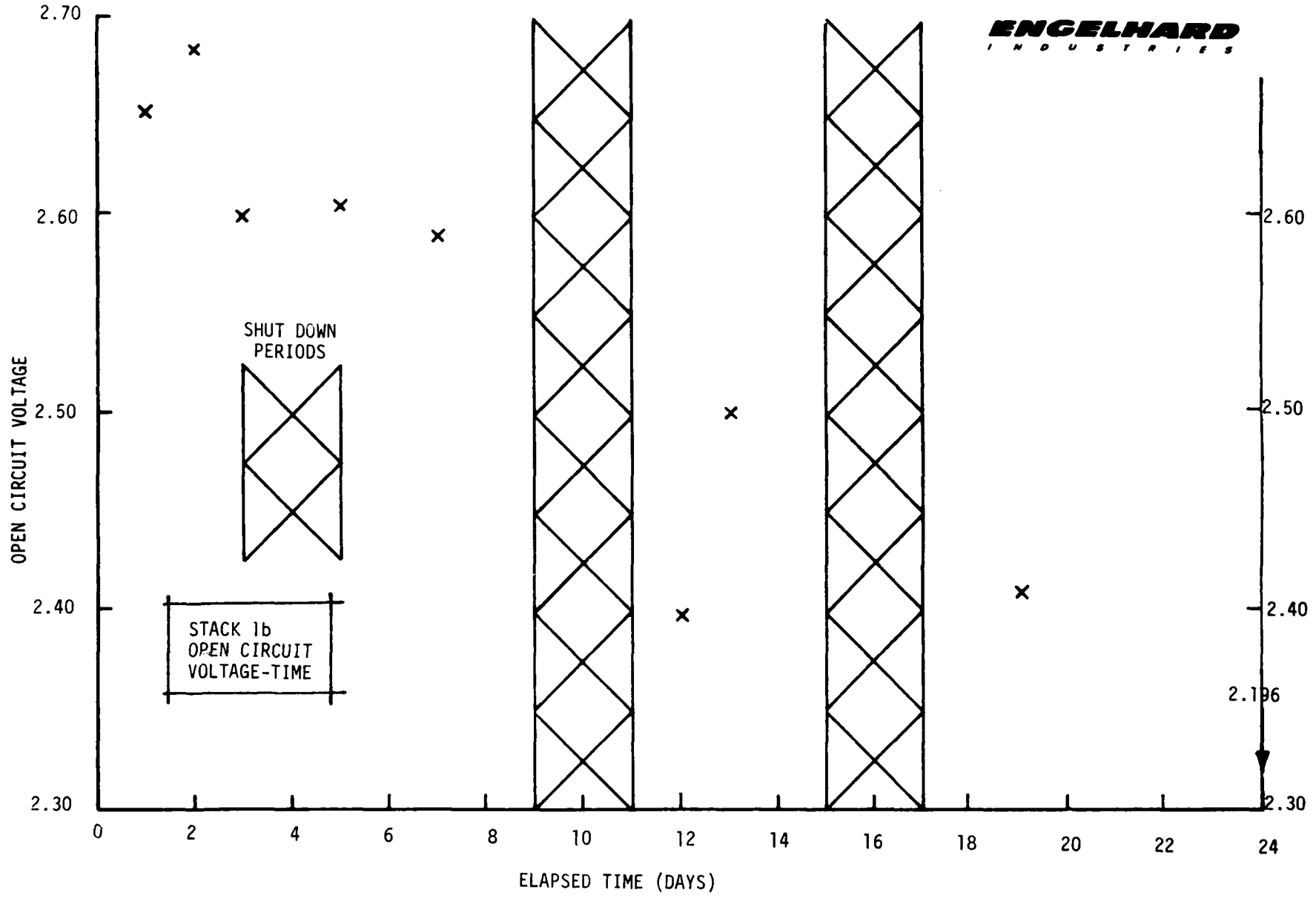
ENGELHARD
INDUSTRIES
OPEN CIRCUIT VOLTAGE
2.70
2.60
2.50
2.40
2.30
2.196
SHUT DOWN
PERIODS
STACK 1b
OPEN CIRCUIT
VOLTAGE-TIME
0
2
4
6
8
10
12
14
16
18
20
22
24
ELAPSED TIME (DAYS)

Figure 29

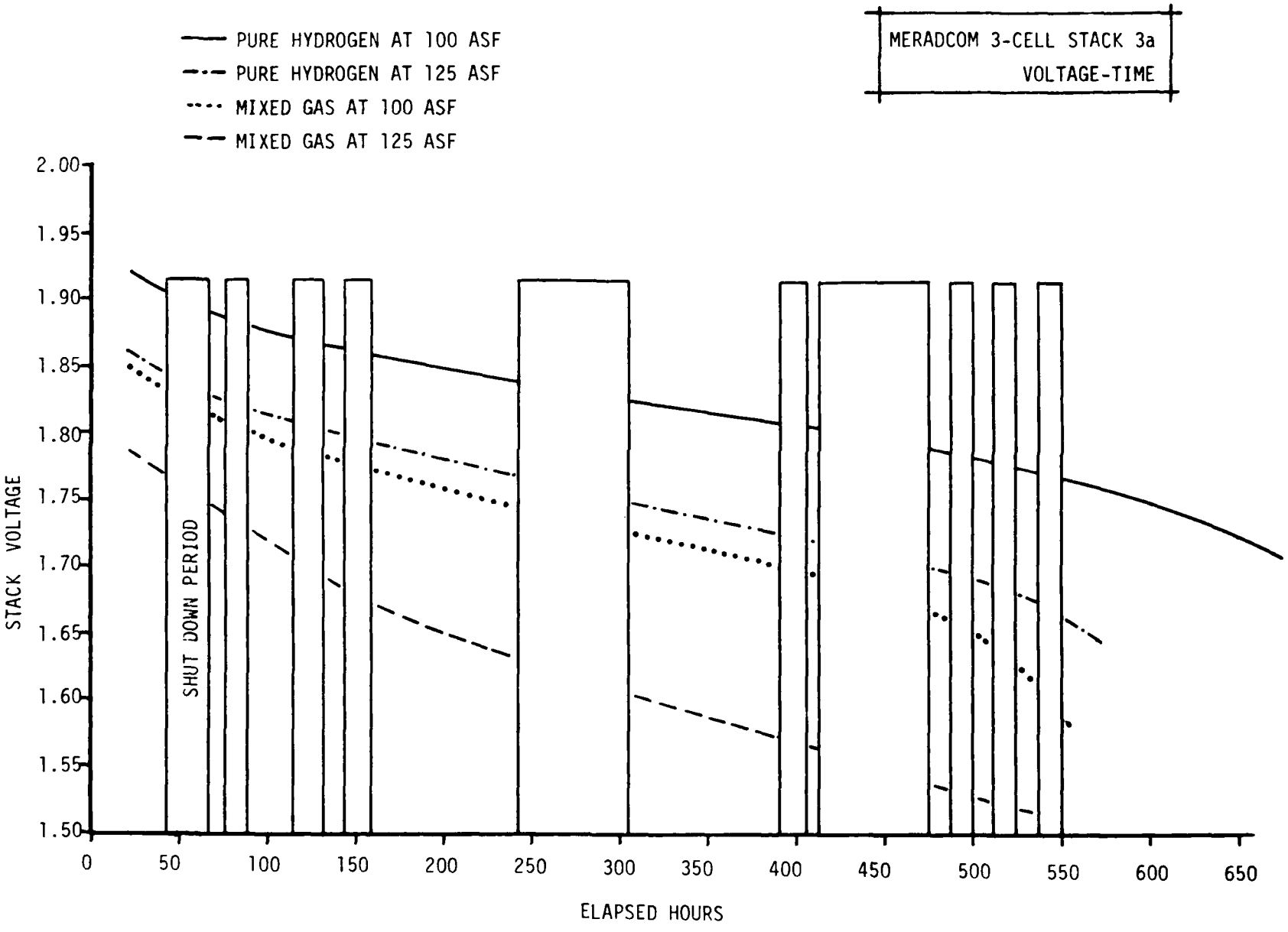
PURE HYDROGEN AT 100 ASF
PURE HYDROGEN AT 125 ASF
MIXED GAS AT 100 ASF
MIXED GAS AT 125 ASF
MERADCOM 3-CELL STACK 3a
VOLTAGE-TIME
STACK VOLTAGE
2.00
1.95
1.90
1.85
1.80
1.75
1.70
1.65
1.60
1.55
1.50
SHUT DOWN PERIOD
0
50
100
150
200
250
300
350
400
450
500
550
600
650
ELAPSED HOURS

Figure 30

losses in individual cell open circuit voltages. Two shut-downs (Nos. 9 and 10) were conducted by keeping the stack at operating temperature under an inert gas blanket. No change in the stack decline trends was observed as a result of this shut-down procedure.

Because it was felt that the loss of open circuit voltage might be related to reactant cross leakage caused by breaching of the electrolyte matrix due to acid loss, samples of the electrodes and matrix were titrated for acid content after termination of the run. Results of the titrations are given in Table 8.

Each of the three cells shows a total acid inventory approximately equal to that of a fresh matrix, suggesting that acid loss from the overall cell laminate package was not severe although a nominal amount of acid was transferred from the matrix to the electrodes. Acid loss from localized areas of the matrices which would not be detected by these titrations might have caused the open circuit voltage losses.

6.2.6 Stack 3b

Figure 31 shows the performance history of the individual cells of Stack 3b.

Because the previous stack testing indicated that poor shut-down tolerance was caused by breaching of the matrix through acid loss, Stack 3b was constructed to incorporate a higher acid inventory. The top cell of Stack 3b employed a standard matrix; however, the electrodes were prefilled with acid to a level typical of that observed in cells which had operated for one thousand hours. The lower two cells each employed matrices of almost twice the normal thickness containing twice the acid volume of a standard matrix.

Initially, the performance of all three cells declined at a rate similar to that observed in previous stacks which were subjected to shut-down cycling. At approximately the 225 hour point, the decline in performance of the center cell stopped and this cell ran stably for the final 400 hours of the test. The fact that the open circuit voltage of the middle cell remained high throughout the test indicates that no substantial breaching of the matrix occurred.

Testing of Stack 3b was terminated at 625 hours due to the inability of the top and bottom cells to support a load.

6.2.7 Stack 3c

Figure 32 shows the performance history of the individual cells of Stack 3c.

ENGELHARD
INDUSTRIES

PHOSPHORIC ACID CONTENT OF FUEL CELL STACK

COMPONENTS AFTER RUN NO. 3a

		mg. Phos. Acid/ cm^2 of Matrix*	% Volume **
	Matrix & Electrodes	35.5	37.4%
TOP CELL	Matrix	23.2	24.5%
	Electrodes	12.3	-
	Matrix & Electrodes	37.1	39.1%
MIDDLE CELL	Matrix	28.1	29.5%
	Electrodes	9.0	-
	Matrix & Electrodes	40.2	42.1%
BOTTOM CELL	Matrix	23.4	24.6%
	Electrodes	16.8	-

* Std. Matrix, 0.05 cm thick

** Assuming Phos. Acid density of 1.9 mg/l ; based on matrix volume.

Table 8

ENGELHARD
INDUSTRIES

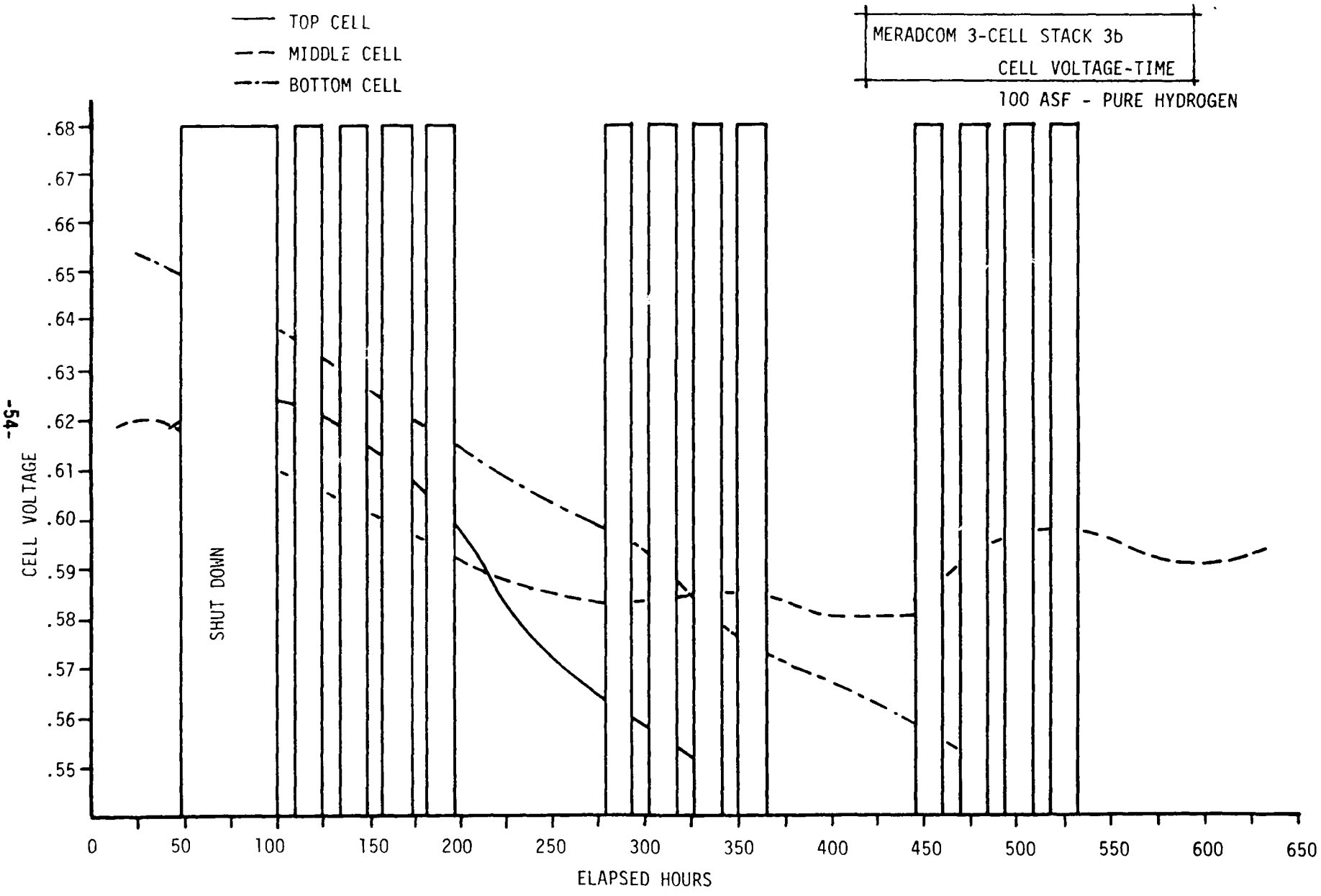

Figure 31

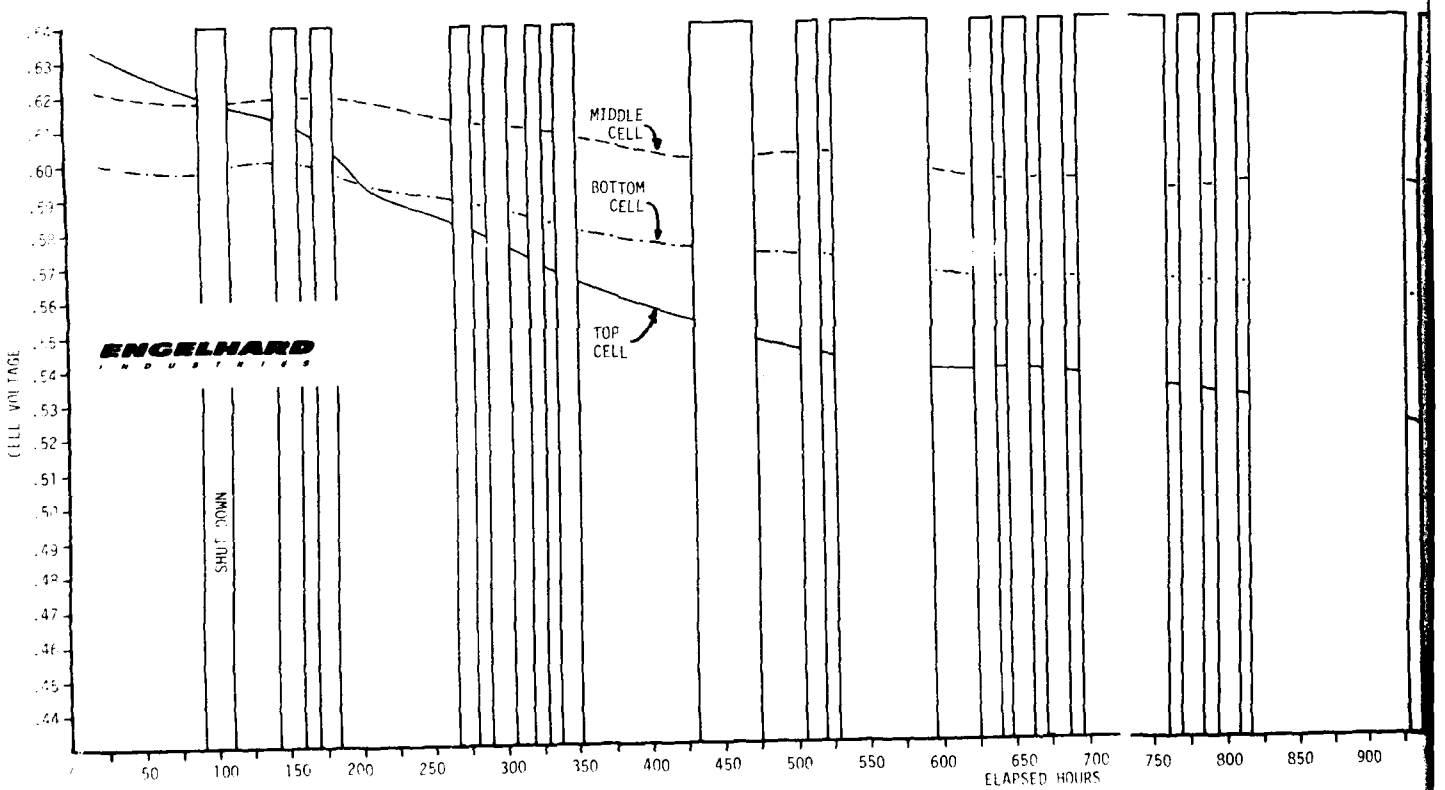

MERADCOM 3-CELL STACK 3c

TIME-VOLTAGE, HYDROGEN-AIR, 100 ASF (Amp/ft^2)

Figure 32

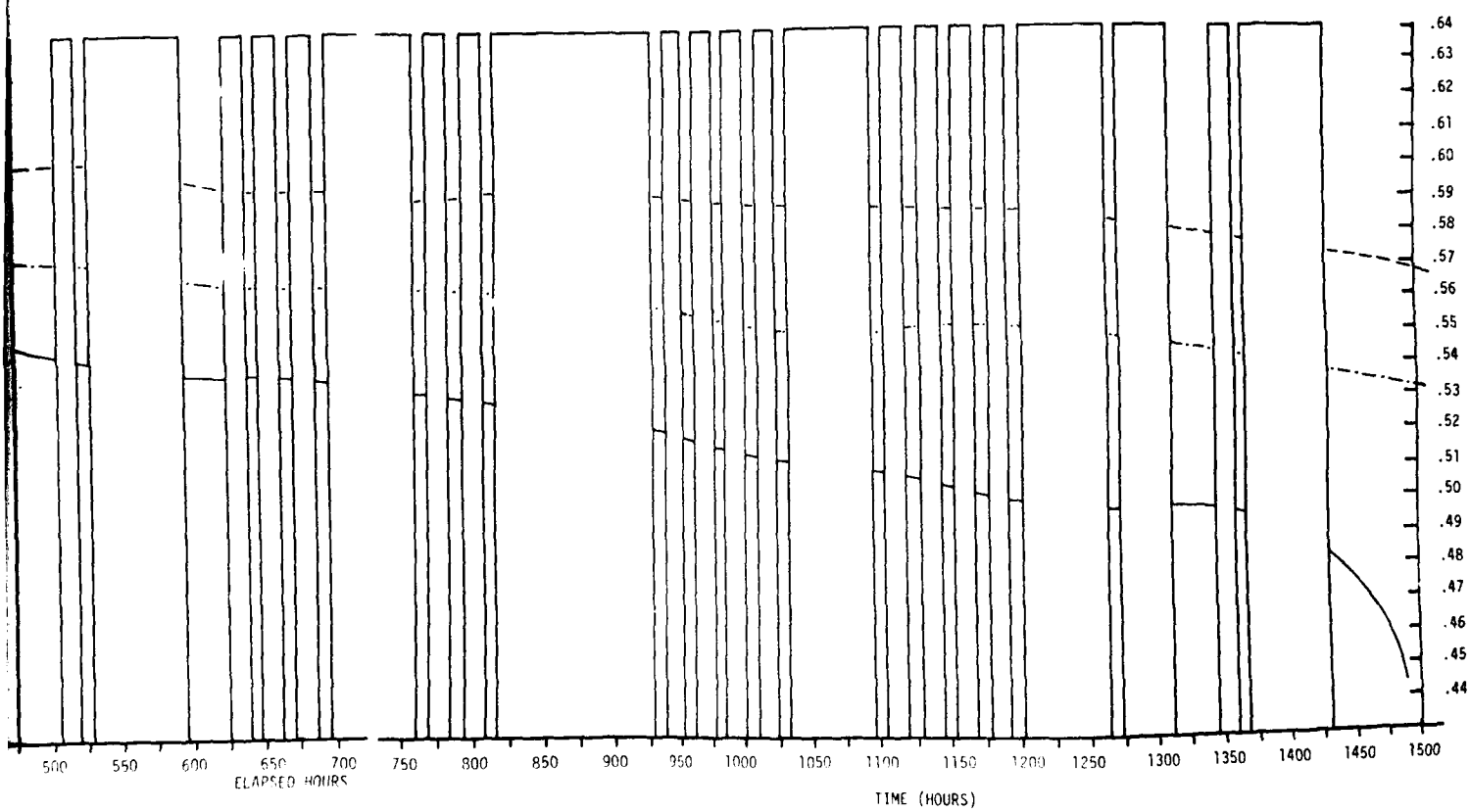
.64
.63
.62
.61
.60
.59
.58
.57
.56
.55
.54
.53
.52
.51
.50
.49
.48
.47
.46
.45
.44
500
550
600
650
700
750
800
850
900
950
1000
1050
1100
1150
1200
1250
1300
1350
1400
1450
1500
ELAPSED HOURS
TIME (HOURS)

Figure 32

In Stack 3c, all three cells were duplicates of the middle cell of Stack 3b (see Results and Discussion, Stack 3b).

It can be noted from Figure 32 that the performance of the top cell initially declined at a greater rate than did the performance of the lower two cells. As in previous tests, the performance decline of the top cell was accompanied with a corresponding decline in open circuit voltage.

There was a more gradual depression of open circuit voltages of the lower two cells, and their performance was not significantly affected by the shut-down cycling.

Upon disassembly, a small burn mark indicative of breaching of the matrix was observed on the top cell.

6.2.8 Stack 3d

Stack 3d was constructed to be identical with Stack 3c. Stack 3d was operated under constant load to provide a comparison with stacks undergoing start-up/shut-down cycling.

Stack 3d experienced three thermal upsets during the test. During the first day of operation a temperature control failure caused the stack temperature to decline to approximately 200°F.

At 210 hours, the temperature controller cycled the stack from operating temperature to lower temperatures for a period of about 8 hours. The lowest temperature observed by automatic recording equipment during this period was 172°F.

At 830 hours, the stack temperature controller failed in the off position permitting the stack to cool for a period of approximately 6 hours. When this fault was discovered, the stack operating temperature was observed to be 118°F (approximately the temperature of the hydrogen saturator).

The results of testing of Stack 3d are shown in Figure 33. All cells performed with minor degradation until the temperature controller malfunction occurred at the 830 hour point. After this malfunction, the middle cell continued to perform stably; however, the top and bottom cells suffered permanent performance losses. These performance losses were probably due to acid loss from the matrix caused by the build-up of product water within the cells at the low operating temperature. Upon disassembly, a burn mark, indicating breaching of the matrix, was found on the lower cell.

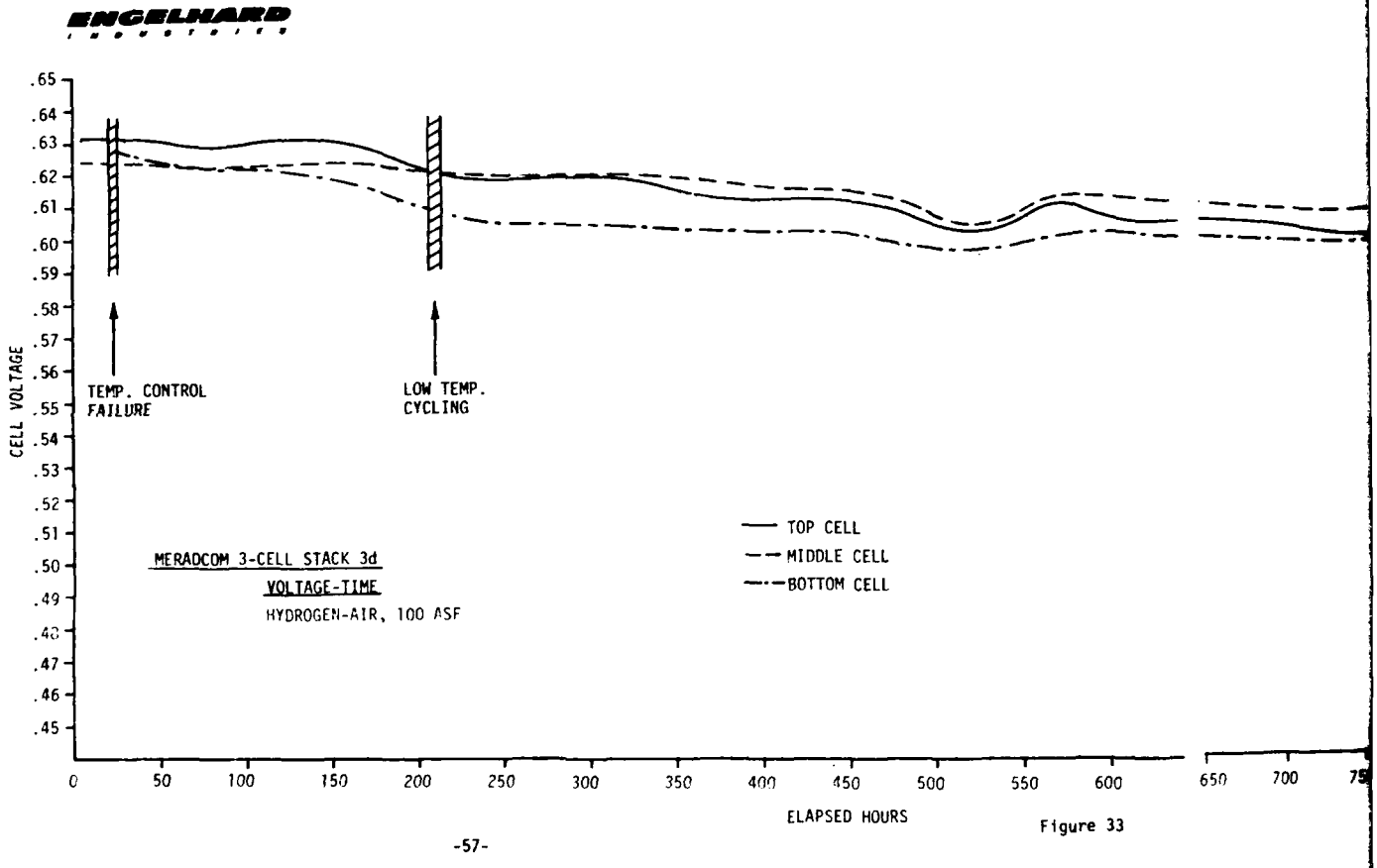
ENGELHARD
CELL VOLTAGE
.65
.64
.63
.62
.61
.60
.59
.58
.57
.56
.55
.54
.53
.52
.51
.50
.49
.48
.47
.46
.45
TEMP. CONTROL FAILURE
LOW TEMP. CYCLING
MERADCOM 3-CELL STACK 3d
VOLTAGE-TIME
HYDROGEN-AIR, 100 ASF
TOP CELL
MIDDLE CELL
BOTTOM CELL
0
50
100
150
200
250
300
350
400
450
500
550
600
650
700
ELAPSED HOURS

Figure 33

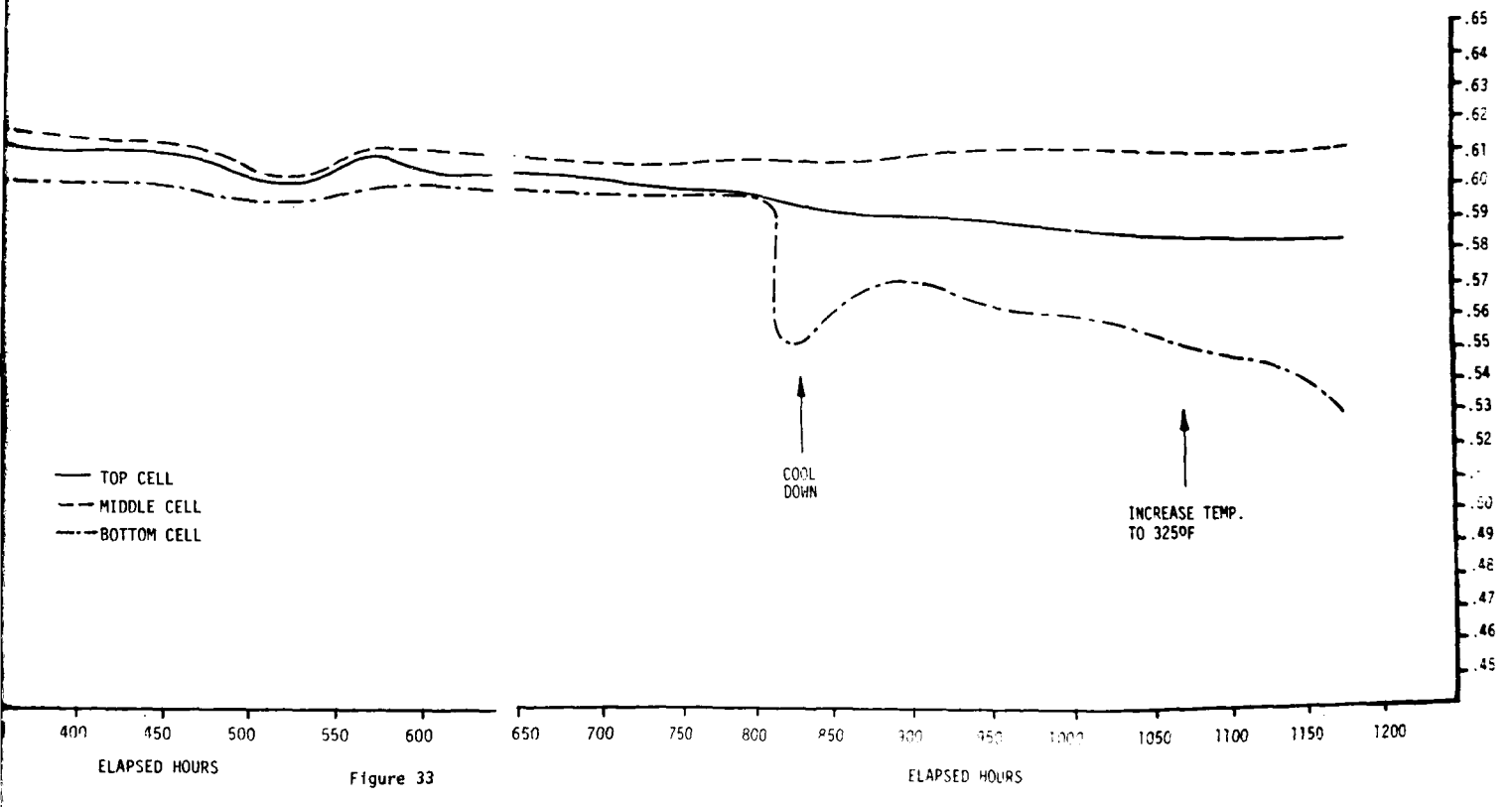
.65
.64
.63
.62
.61
.60
.59
.58
.57
.56
.55
.54
.53
.52
.49
.48
.47
.46
.45
TOP CELL
MIDDLE CELL
BOTTOM CELL
COOL DOWN
INCREASE TEMP. TO 325°F
400
450
500
550
600
650
700
750
800
1050
1100
1150
1200
ELAPSED HOURS
ELAPSED HOURS

Figure 33

6.2.9 Stack 1e

The performance history of Stack 1e is shown in Figure 34. The individual cell performance history, starting with the twenty-fifth day of operation is shown in Figure 35. Individual cell volt-ampere curves taken at 10 days, 50 days, and 100 days of operation are shown in Figure 36.

On approximately the twenty-fifth day of operation, the voltage under load of Stack 1e was observed to decline. This performance decline was caused solely by a decrease in voltage of the upper cell (see Figure 35).

It was observed that the phosphoric acid on the acid addition "shelf" of the top cell had turned blue, indicating that this acid was in communication with the copper plating of the termination plate/current collector plate interface. To reduce the possibility of similar contamination of the lower cells, acid addition to the upper cell was stopped.

On the 118th day of operation, the fuel of Stack 1e was changed from 90% H_2, 10% H_2O to 88% H_2, 10% H_2O, 2% CO. Operation was not continued on this fuel mixture due to the low performance of the upper cell.

The temperature control thermocouple failed open on the 130th day of operation permitting the stack to cool to approximately 110°F with the reactants flowing. Upon restoring the stack to operating temperature, a definite loss of performance of all three cells was observed (see Figure 35).

6.2.10 Stack 2e

The performance history of Stack 2e is shown in Figure 37. Individual cell volt-ampere curves taken at 10 days, 50 days, and 100 days of operation are shown in Figure 38.

Stack 2e was operated on the 90% H_2, 10% H_2O fuel mix. Between the 45th and 65th days of operation, the stack exhibited erratic performance accompanied by an increased sensitivity to air flow. Because air sensitivity can be caused by manifold leakage, the air inlet manifold was replaced on the 66th day. After replacement of the manifold, performance of the stack stabilized; however, some air sensitivity remained.

ENGELHARD
INDUSTRIES

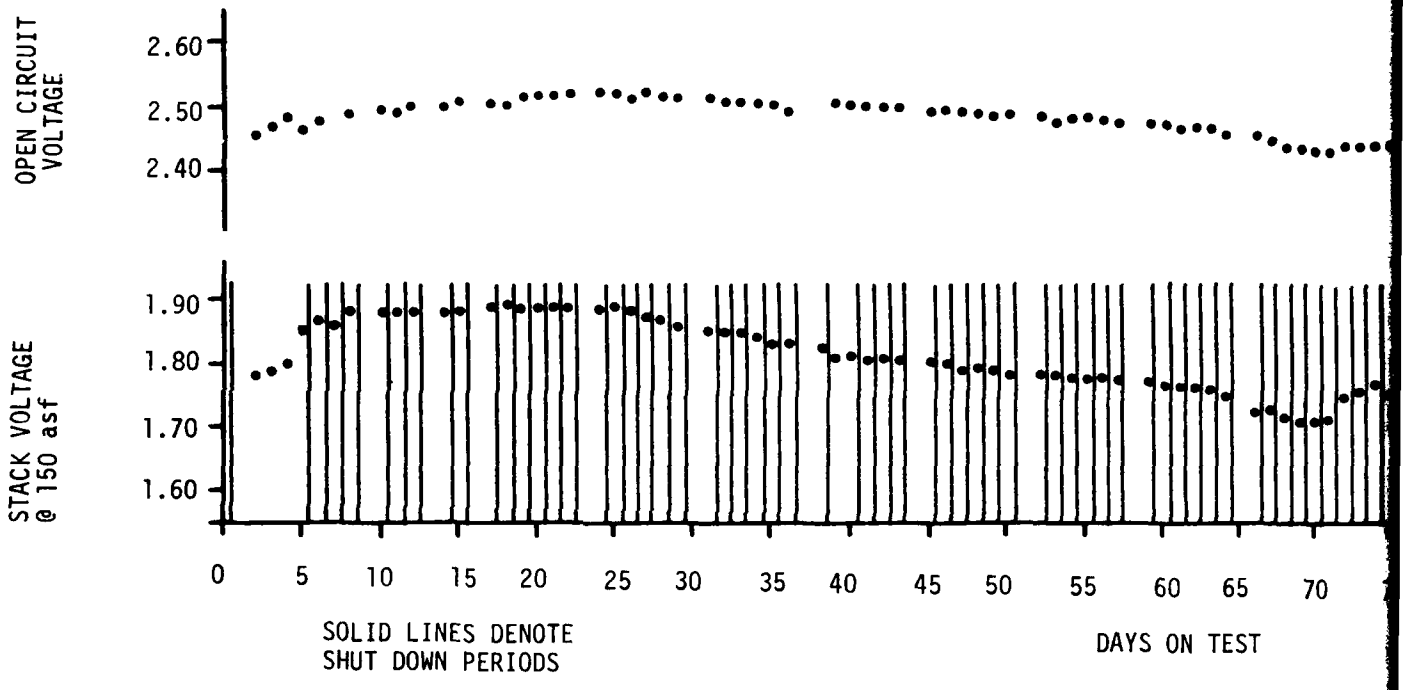

MERADCOM 3-Cell Stack 1e

H_2 - AIR, 350°F

Figure 34

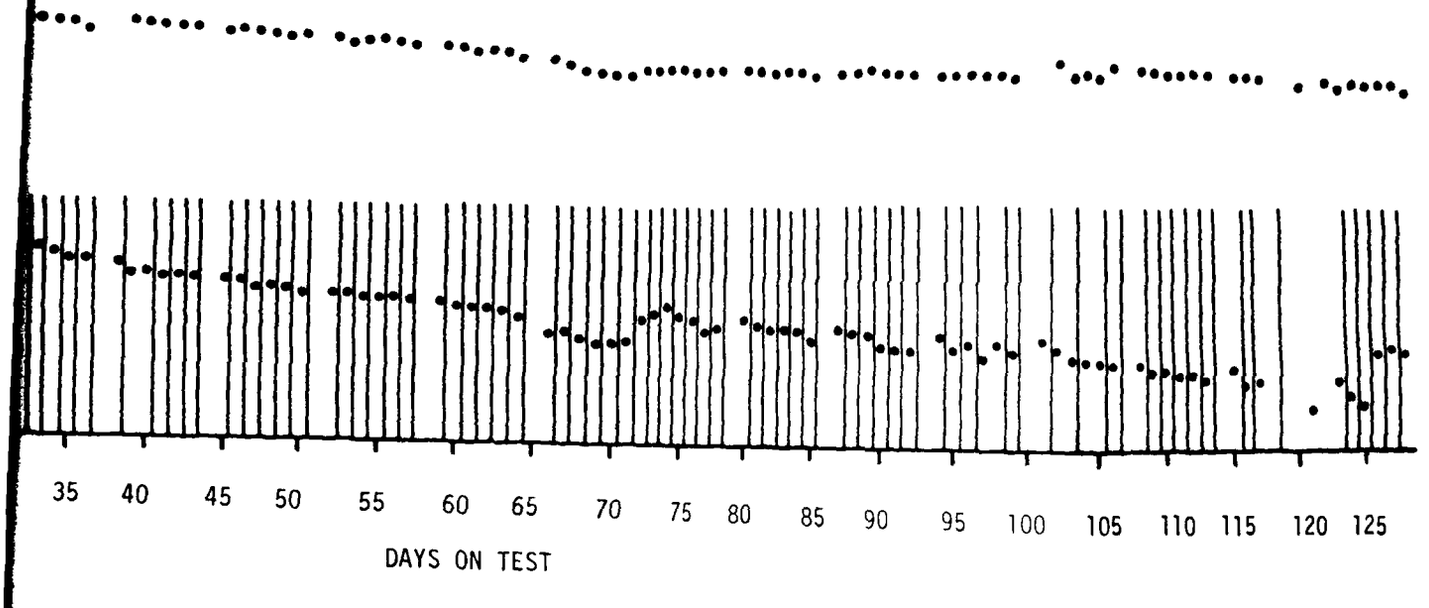
35 40 45 50 55 60 65 70 75 80 85 90 95 100 105 110 115 120 125
DAYS ON TEST

Figure 34

ENGELHARD
INDUSTRIES

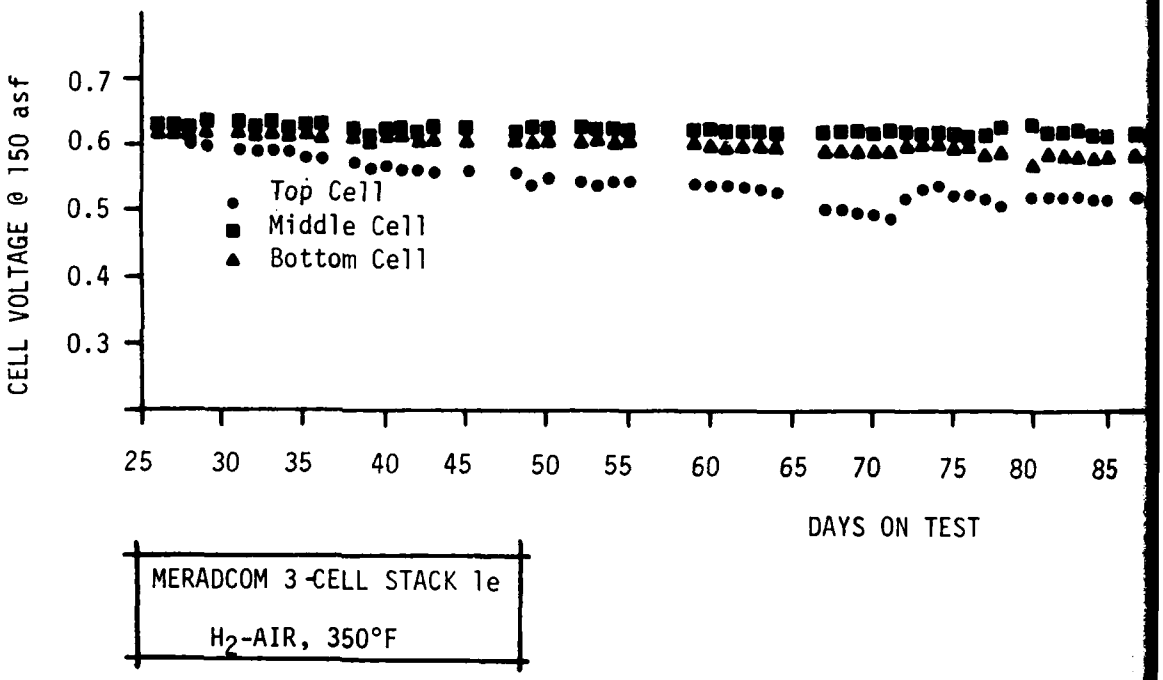

Figure 35

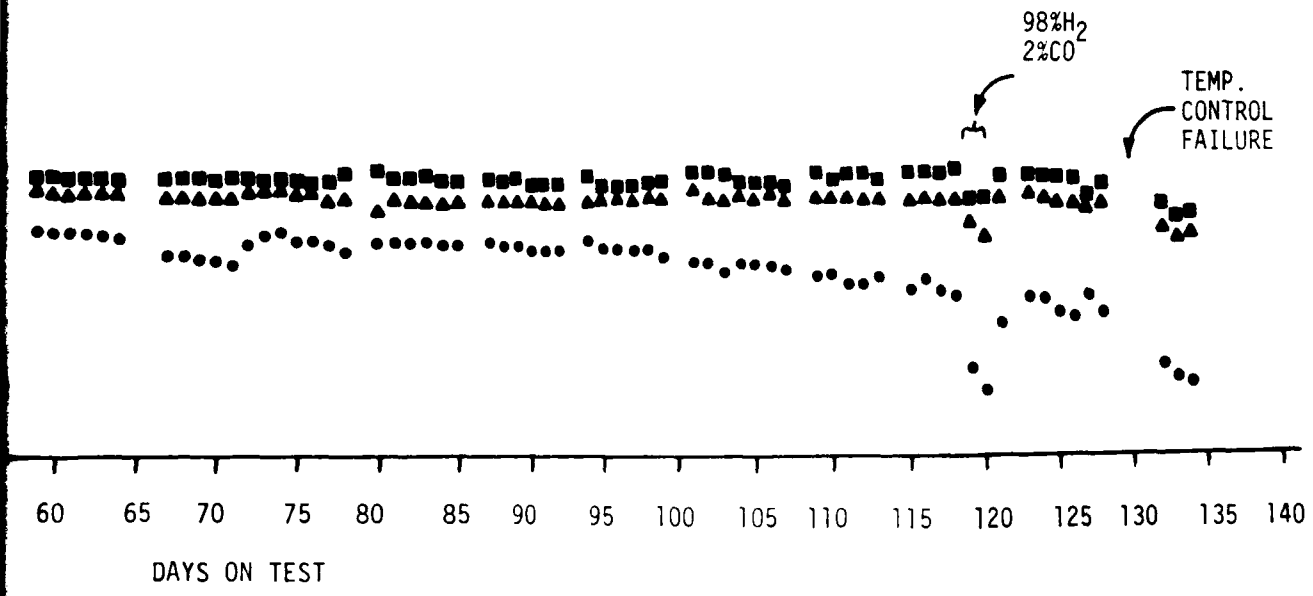
98%H2
2%CO
TEMP.
CONTROL
FAILURE
60
65
70
75
80
85
90
95
100
105
110
115
120
125
130
135
140
DAYS ON TEST

Figure 35

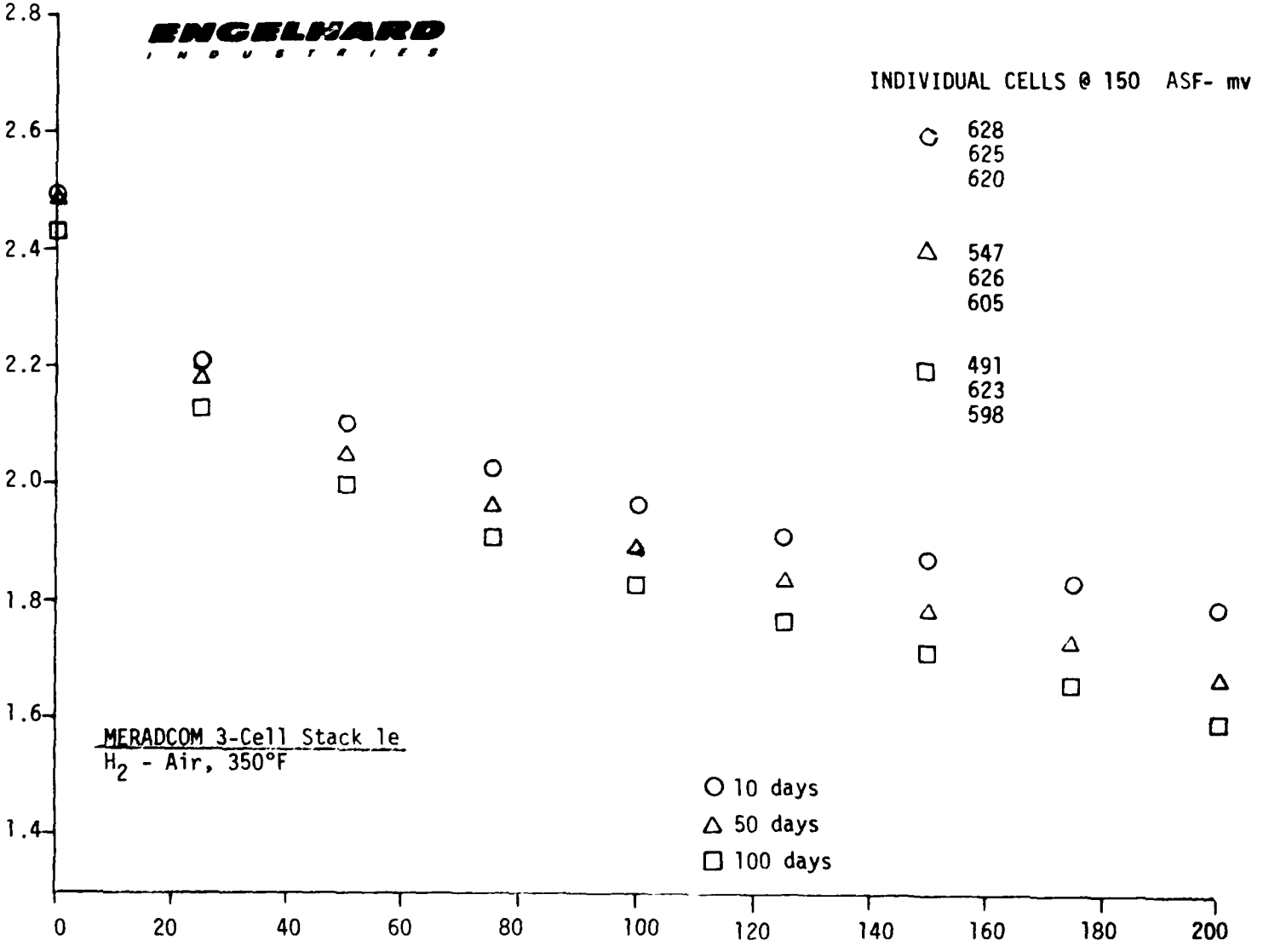
ENGELHARD
INDUSTRIES
INDIVIDUAL CELLS @ 150 ASF- mv
628
625
620
547
626
605
491
623
598
MERADCOM 3-Cell Stack 1e
H2 - Air, 350°F
10 days
50 days
100 days
STACK VOLTAGE - VOLTS
2.8
2.6
2.4
2.2
2.0
1.8
1.6
1.4
0
20
40
60
80
100
120
140
160
180
200
CURRENT DENSITY - ASF (Amps/ft2)

Figure 36

ENGELHARD
INDUSTRIES

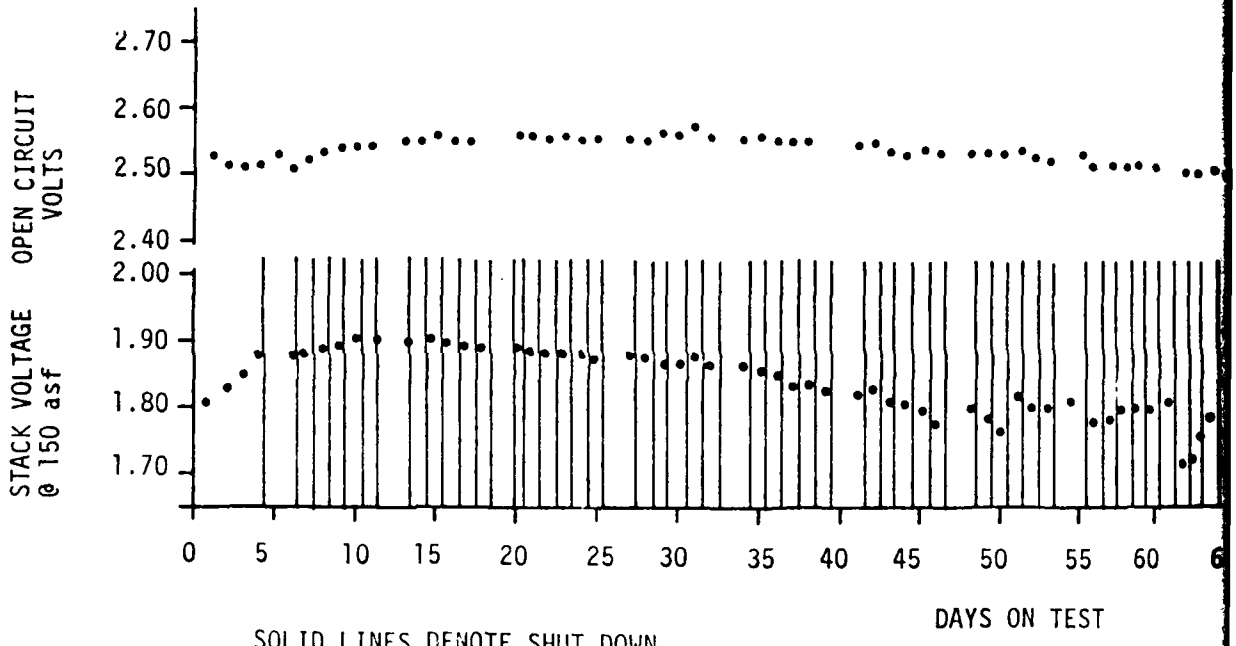

SOLID LINES DENOTE SHUT DOWN PERIODS

MERADCOM 3-CELL STACK 2e

H_2-AIR, 350°F

Figure 37

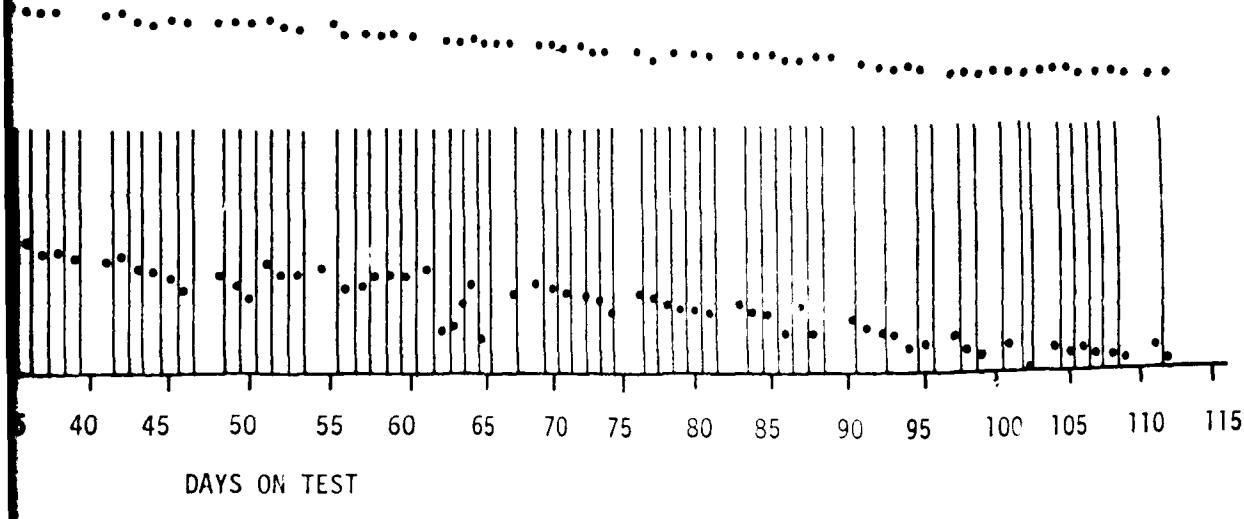

Figure 37

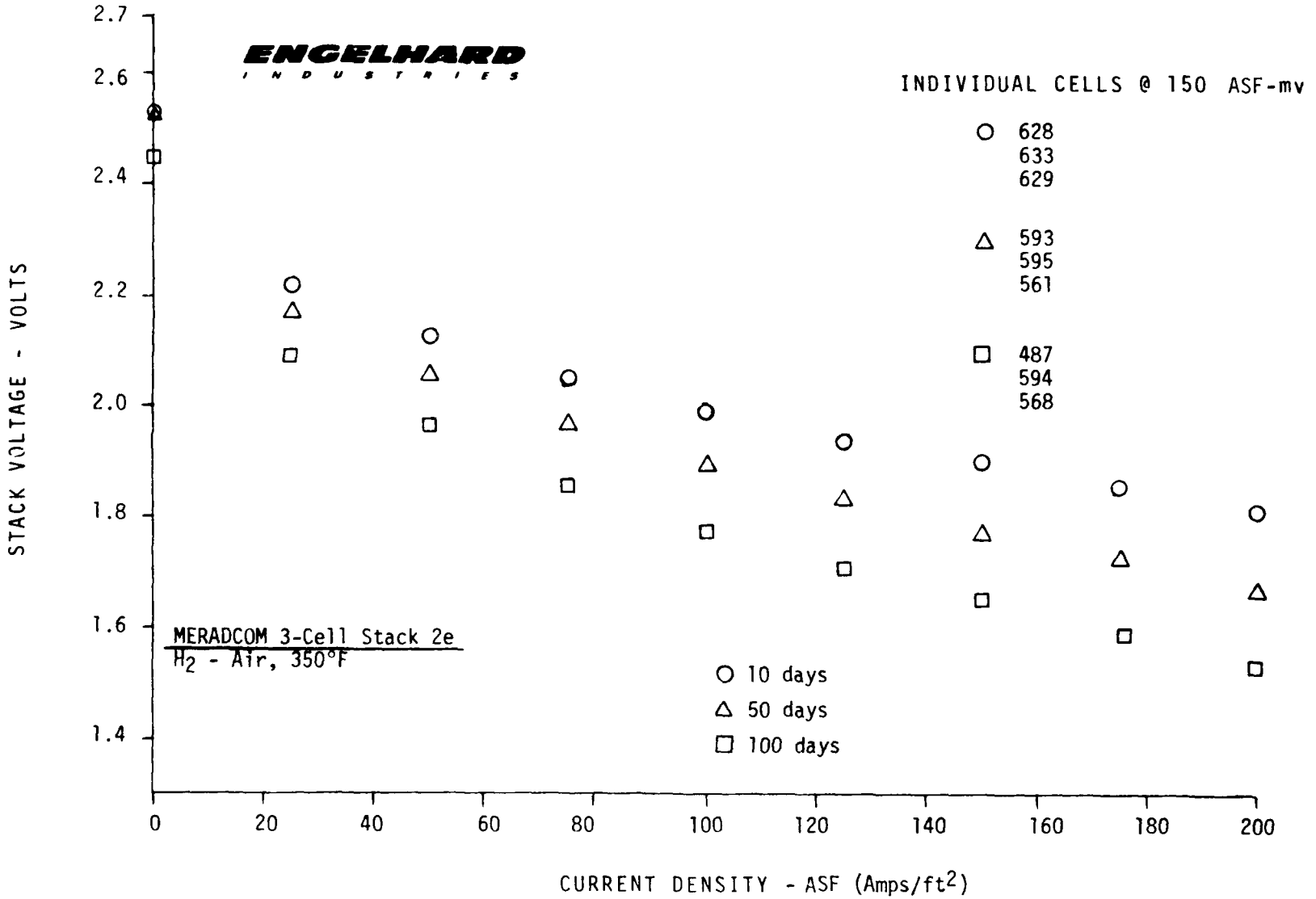
ENGELHARD
INDUSTRIES
INDIVIDUAL CELLS @ 150 ASF-mv
628
633
629
593
595
561
487
594
568
STACK VOLTAGE - VOLTS
2.7
2.6
2.4
2.2
2.0
1.8
1.6
1.4
MERADCOM 3-Cell Stack 2e
H2 - Air, 350°F
10 days
50 days
100 days
0
20
40
60
80
100
120
140
160
180
200
CURRENT DENSITY - ASF (Amps/ft2)

Figure 38

6.2.11 Stack 3e

The performance history of Stack 3e is shown in Figure 39. Individual cell voltages under load beginning with 60th day of operation are shown in Figure 40. Voltage-current relationships taken on the 10th, 50th, 83rd, and 100th days of operation are shown in Figure 41.

On the 61st day of operation, Stack 3e was switched to operation on the 65% H_2, 23% CO_2, 10% H_2O, 2% CO fuel mixture. During the 12 days of operation on this fuel (see Figure 40), erratic performance was observed in the lower two cells. The upper cell, however, remained stable in performance. The stack was returned to operation on 90% H_2, 10% H_2O and diagnostic tests were performed to determine whether the decline in performance of the lower cells was due to poor flow distribution or CO effects. The results of this testing are shown in Table 9.

The two fuel streams that did not contain CO did not show any definite trends in decline of individual cell performance. Operation on the two CO containing streams, however, showed declines similar to those observed earlier. In both cases, the bottom cell showed the greatest performance loss, followed by the center cell. The upper cell showed negligible or zero loss. These results indicate that the decline in performance resulted primarily from decreased tolerance to CO effects rather than from unequal flow distribution or hydrogen partial-pressure sensitivity.

Because CO tolerance can be a function of cell operating temperature, temperature profiles of the three cells were taken. Figures 42 through 44 in the appendix show in-plane temperature profiles of the cells when operating on pure hydrogen. Figures 45 through 47 in the appendix show the in-plane temperature profiles of the same cells operating on the 65% H_2, 23% CO_2, 10% H_2O, 2% CO mix. It should be noted that these measurements are not true "center-of-the-cell" measurements but measurements taken between the cell cathode and the adjacent, lower bipolar plate. Figure 48 in the appendix shows diagrammatically the location of the thermocouple traverses.

The six thermal profiles show that for both fuels, the temperature profiles of the top and center cells are very similar, differing by approximately 1°F. The lower cell temperature profiles are approximately 5°F below those of the upper two. To determine if the temperature profiles might have been influenced by unequal

ENGELHARD
INDUSTRIES

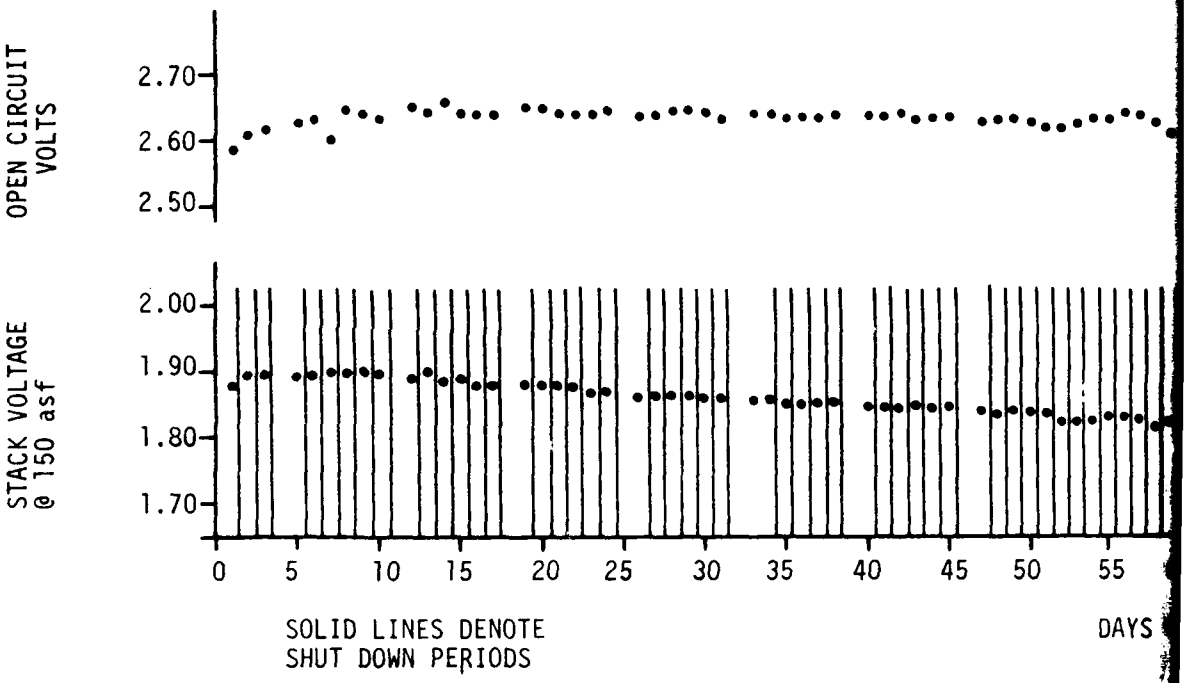

MERADCOM 3-CELL STACK 3e

H_2-AIR, 350°F

Figur

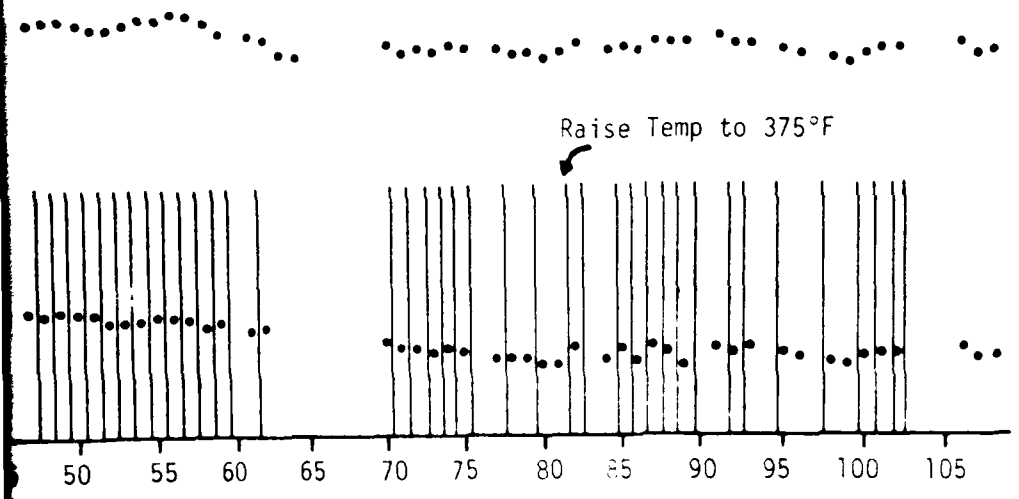
Raise Temp to 375°F
50
55
60
65
70
75
80
85
90
95
100
105
DAYS ON TEST

Figure 39

ENGELHARD
INDUSTRIES

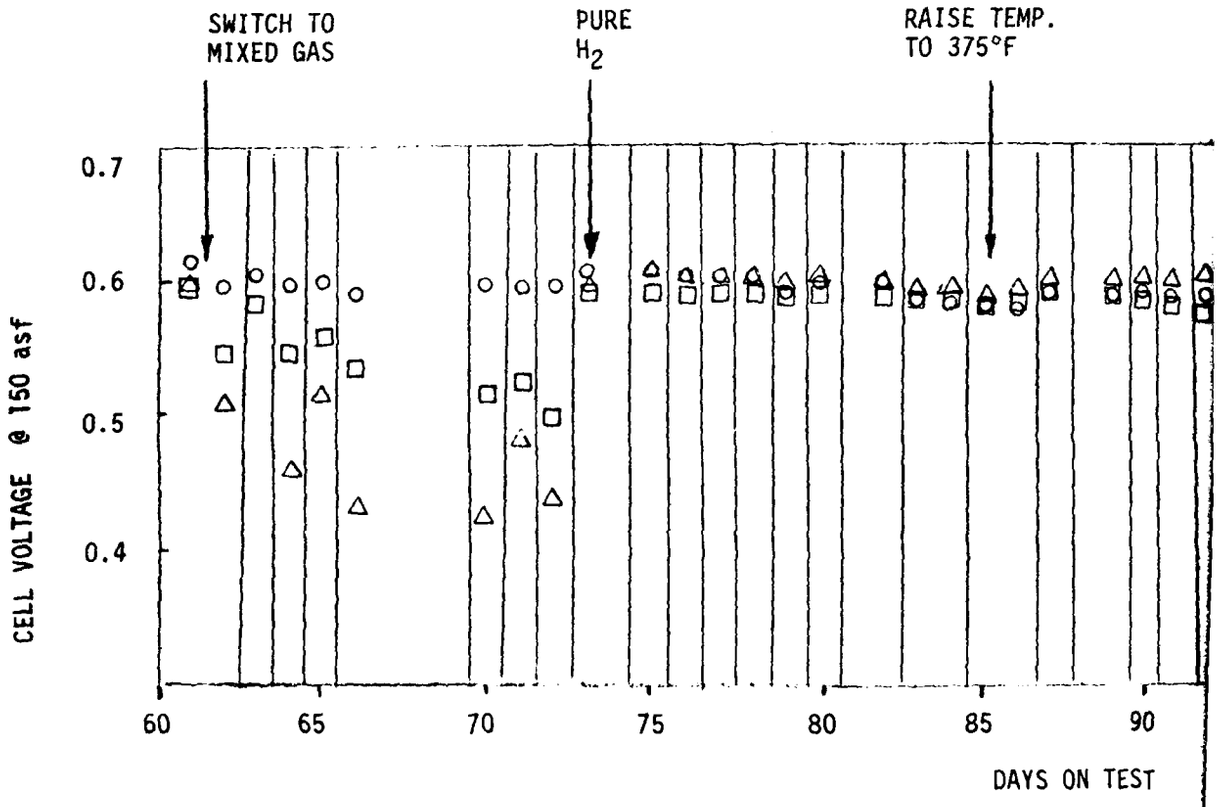

MERADCOM 3-CELL STACK 3e

Figure 10

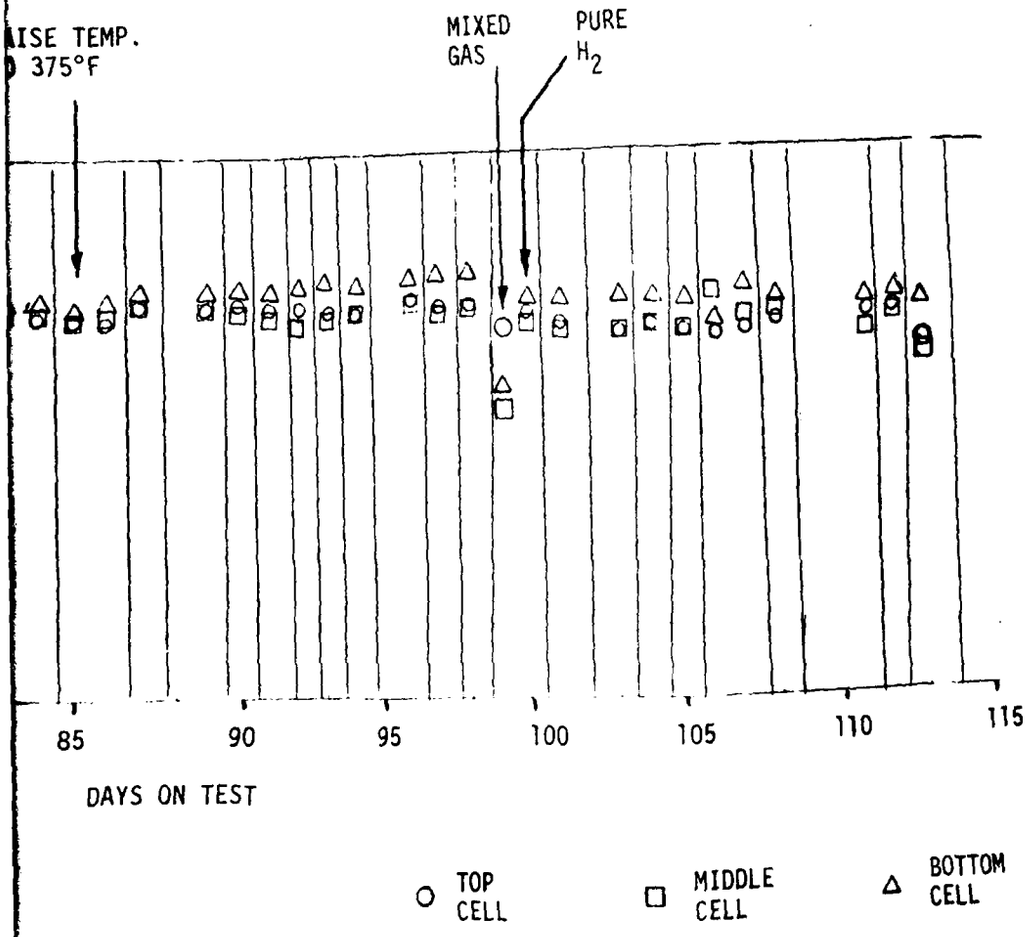
ISE TEMP.
375°F
MIXED GAS
PURE H_2
85
90
95
100
105
110
115
DAYS ON TEST
TOP CELL
MIDDLE CELL
BOTTOM CELL

Figure 10

ENGELHARD
INDUSTRIES

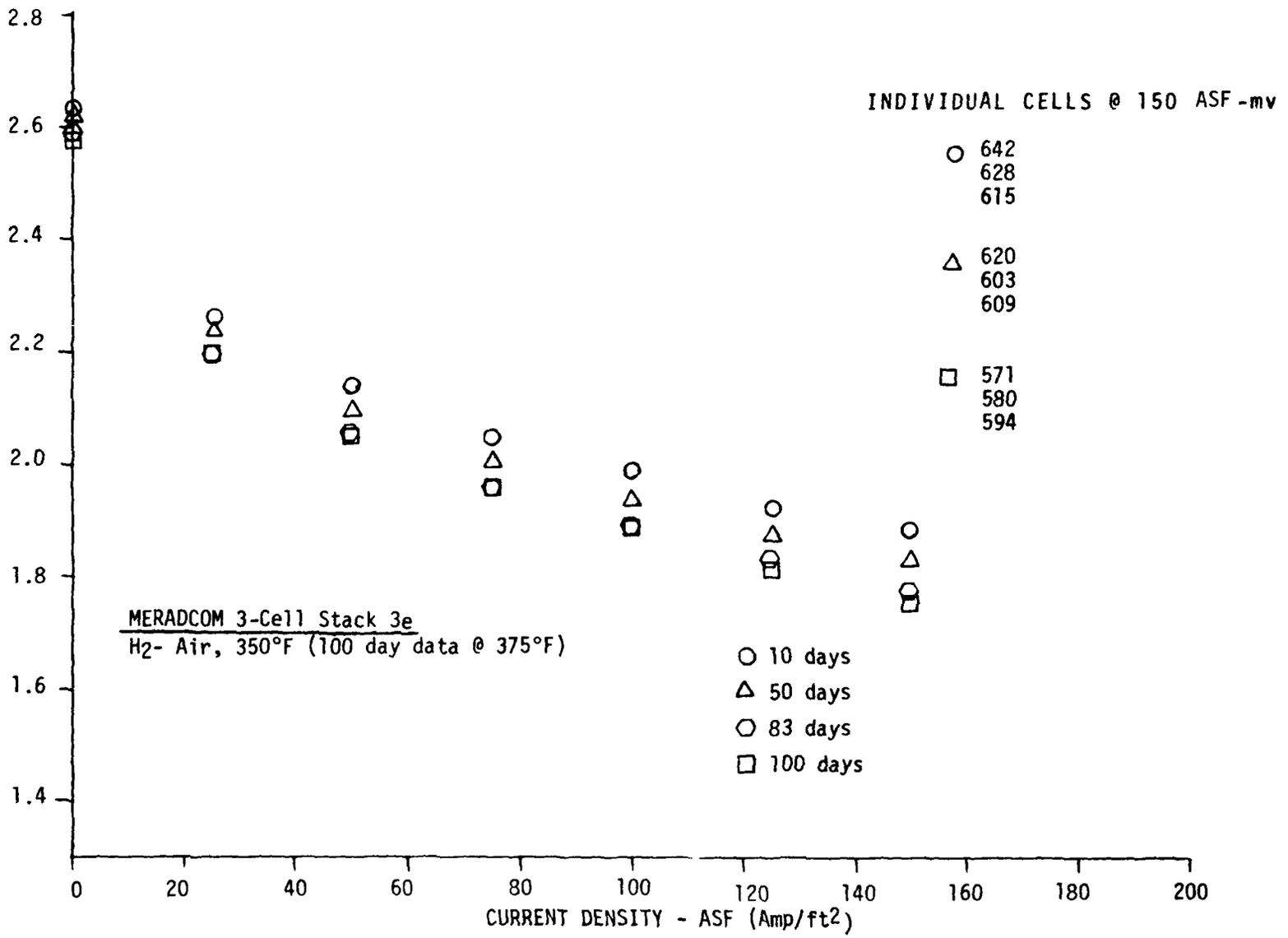

Figure 41

ENGELHARD

3-Cell Stack 3-e

Diagnostic Testing Summary

Hydrogen/≈ 150 ASF

Utilization -	70%	80%	90%	Δ mv
Top cell	610 mv	606	566	44
Middle cell	590	590	563	27
Bottom cell	596	595	578	18

65% H_2, 23% CO_2, 10% H_2O, 2% CO/≈125ASF

Utilization (approx.)	50%	55%	60%	Δ mv
Top cell	598 mv	598	598	0
Middle cell	513	508	501	12
Bottom cell	423	415	406	17

65% H_2, 25% N_2, 10% H_2O/≈125 ASF

Utilization (approx.)	70%	80%	90%	Δ mv
Top cell	584 mv	582	570	14
Middle cell	577	564	551	26
Bottom cell	570	571	552	18

88% H_2, 10% H_2O, 2% CO/≈125 ASF

Utilization (approx.)	55%	70%	75%	Δmv
Top cell	602 mv	596	591	11
Middle cell	560	546	536	24
Bottom cell	557	521	506	51

Table 9

operation of the end plate heating pads, the power consumption of each pad was checked. The upper and lower heating pads were found to be operating equally.

Temperature differences can contribute to CO tolerance effects. It is doubtful, however, that the small temperature differences observed were responsible for the reduced performance of the center and bottom cell.

6.3 2-KW Fuel Cell Stack Design

A design for a 2-KW, liquid cooled fuel cell stack was developed as part of this effort. The fuel cell stack design had the following characteristics:

No. of cell	62
Cell active area	6" x 9 3/4" (0.406 ft^2)
Overall cell dimension	7" x 10.688"
No. of cooling plates	8
Cooling plate frequency	every 8 cells
Bare stack dimension (excluding manifolds and bolting)	7" x 10.688 x 15.73 h
Overall stack dimensions	10" x 12 3/4" x 18 3/4" h
Bare stack weight	55.5 lbs.
Overall stack weight	78.1 lbs.

The test stacks operated during this program employed a heavy, laboratory type bolting system. The overall weights and volumes given above are based on a conceptual design utilizing honeycomb stiffened, aluminum end plates.

7.0 CONCLUSIONS

The initial 3-cell stack testing demonstrated conclusively that the primary performance losses associated with start-up/shut-down cycling were due to breaching of the electrolyte matrix. The testing of 3-cell Stacks 1, 2 & 3e showed that start-up/shut-down cycling losses would be eliminated or greatly reduced by the use of a matrix having improved acid transport characteristics combined with regular acid addition. Although the original cause of rapid cell decay associated with shut-down cycling appears to be eliminated, some long term decay in all three stacks was observed. This decay was greater than that observed in single-cells and stacks operated for similar periods of time but without shut-down cycling.

Figures 36, 38 and 41 show the voltage-current relationships of the three stacks taken after 10, 50 and 100 days of operation. Individual cell voltages at 150 ASF taken at these times are given in the figures. In all three stacks, over half the decay seen over the ninety day period was due to decay of one of the three cells. The center cell of Stack 1e was exceptionally stable showing only a 2 mV loss after 2400 hours of testing. In general, the changes in offset and slope of the V-A curves with time indicate that the decline in stack performance was due to both decreased catalyst performance and electrode flooding. It can be seen that between the 50 and 100 day lines of Stack 1e and between the 10 and 50 day lines of Stack 3e only a change in offset is present. This indicates that the performance declines observed during these periods were due primarily to catalyst activity losses. All other V-A curve "pairs" show change in offset and slope.

The inability of Stacks 1e and 3e to operate stably on CO-containing fuel streams after approximately 1400 hours of operation on pure hydrogen was traced to diminished anode catalyst activity, with poisons other the CO suspected of playing a role. The center cell of Stack 3e showed a nominal performance loss associated with operation on CO-containing fuel streams, indicating that the factors contributing to decreased CO tolerance did not affect all cells equally.

Initial cell stacks had high voltage losses associated with corrosion of the current collector/termination plate interface. These losses were reduced by copper plating the current collector plates and interposing a sheet of graphite foil between the current collector plates and termination plates.

A 2 kilowatt, liquid cooled, fuel cell stack was designed based on the components utilized in the three cell stack testing program. A conceptual design of a lightweight bolting system was prepared to permit an overall stack weight consistent with the requirements of portable field equipment.

8.0 RECOMMENDATIONS

1. Additional investigations should be performanced to determine the effects of carbon monoxide containing fuel streams on fuel cell stacks subjected to multiple start-up/shut-down cycling.

2. Methods of improving CO-tolerance of fuel cell anodes should be investigated. This would include higher-temperature operation and anode composition modifications.

3. If carbon monoxide effects are shown to be deleterious to long term fuel cell performance, methods of elimination (or partial elimination) of carbon monoxide from the fuel stream should be investigated.

4. The start-up/shut-down testing of Stacks 1e, 2e and 3e utilized electrodes of similar hydrophobicity. The effects of higher wet-proofing levels on start-up/shut-down tolerance should be investigated.

5. In Stacks 1e, 2e and 3e acid inventory was maintained by external, manual acid addition. Similar testing should be conducted on cell stacks incorporating internal acid storage.

6. The bipolar plates used in the three-cell stack testing phase of this program showed excellent corrosion resistance and dimensional stability under cell operating conditions. The fabrication costs, however, are presently too high for commercial use. Alternative bipolar plate construction and fabrication methods are presently being investigated. Such efforts should continue in order to attain cost-effective bipolar plate structures.

APPENDIX

THERMAL PROFILE TESTING

ENGELHARD INDUSTRIES

MERADCOM 3-CELL STACK 3e

TOP CELL TEMPERATURE PROFILE - 150 asf - 90% H_2, 10% H_2O

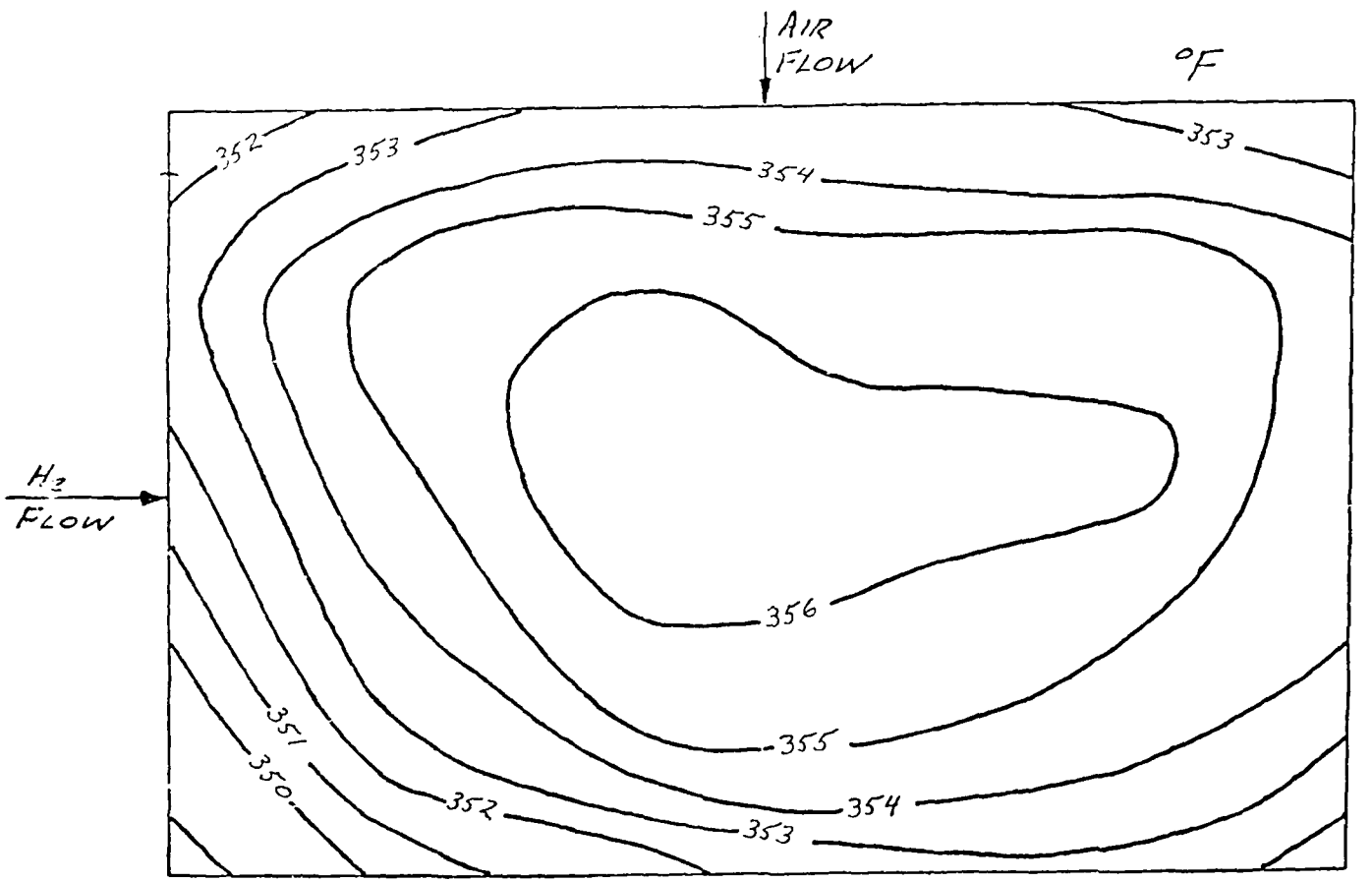

33⅓ % AIR UTILIZATION

10/17/79
PG

Figure 42

ENGELHARD
INDUSTRIES

MERADCOM 3-CELL STACK 3e

CENTER CELL TEMPERATURE PROFILE - 150 asf, 90% H_2 10% H_2O

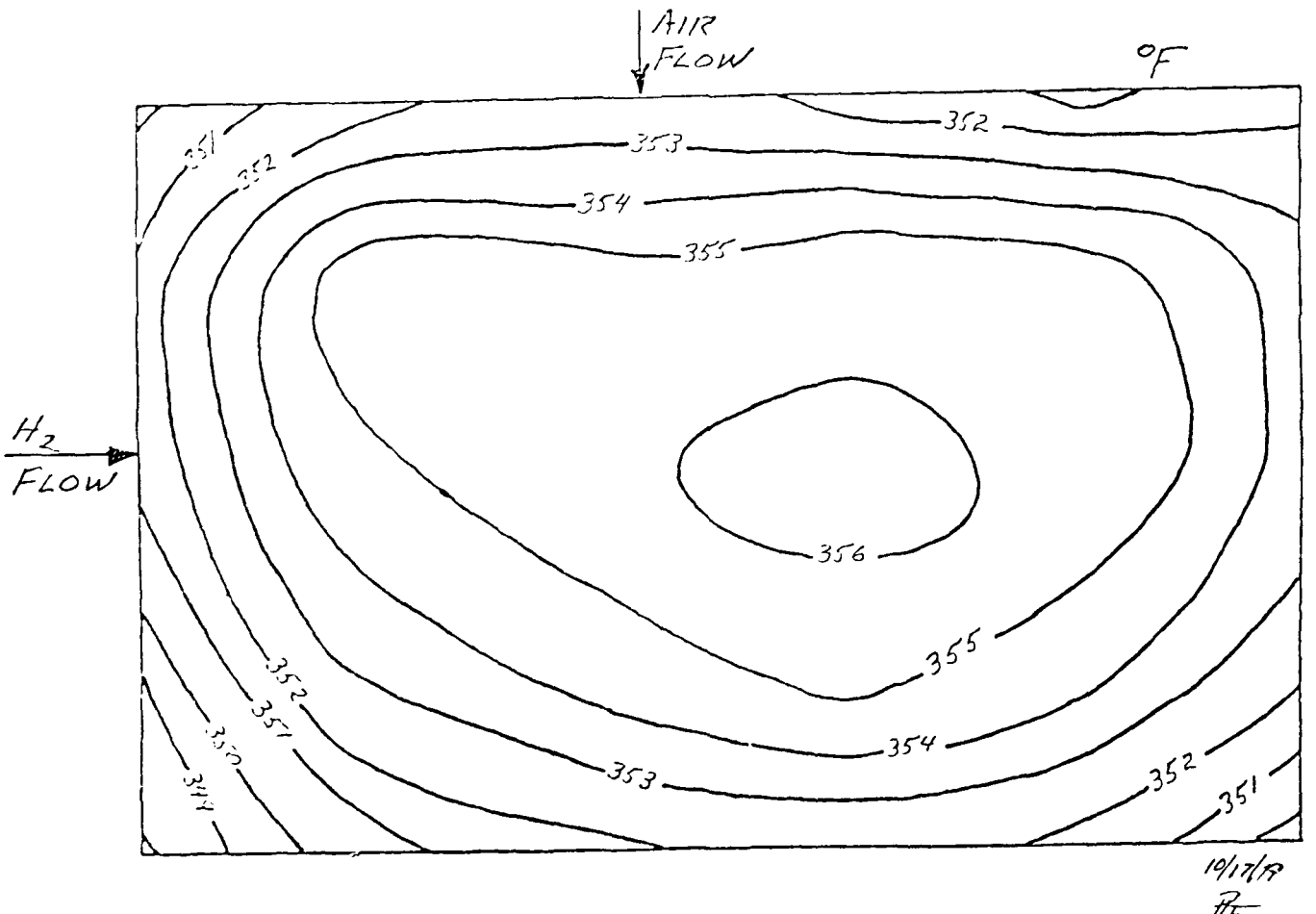

33 1/3 % AIR UTILIZATION

10/17/R

RF

Figure 43

ENGELHARD INDUSTRIES

MERADCOM 3-CELL STACK 3e

BOTTOM CELL TEMPERATURE PROFILE - 150 asf - 90% H_2, 10% H_2O

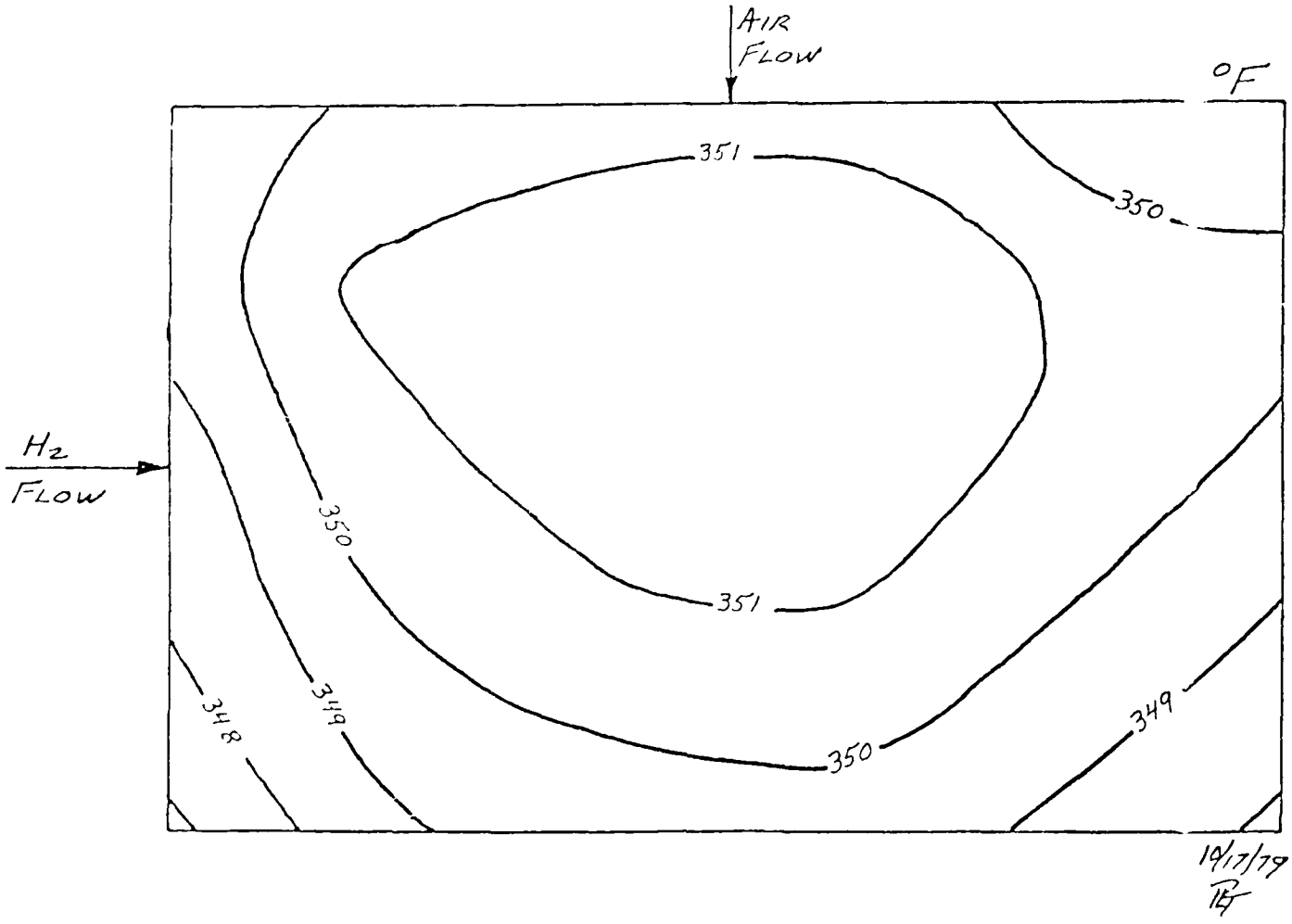

Figure 44

AD-A090 143 ENGELHARD MINERALS AND CHEMICALS CORP EDISON N J ENG--ETC F/G 10/2
PHOSPHORIC ACID FUEL CELL DEVELOPMENT,(U)
SEP 80 A KAUFMAN, P L TERRY DAAK70-77-C-0206

UNCLASSIFIED NL

2 of 2
AD
A090143

END
DATE FILMED
11 80
DTIC

ENGELHARD INDUSTRIES

MERADCOM 3-CELL STACK 3e

TOP CELL TEMPERATURE PROFILE - 125 asf - 65% H_2, 23% CO_2, 10% H_2O, 2% CO

≈ 50% UTILIZATION

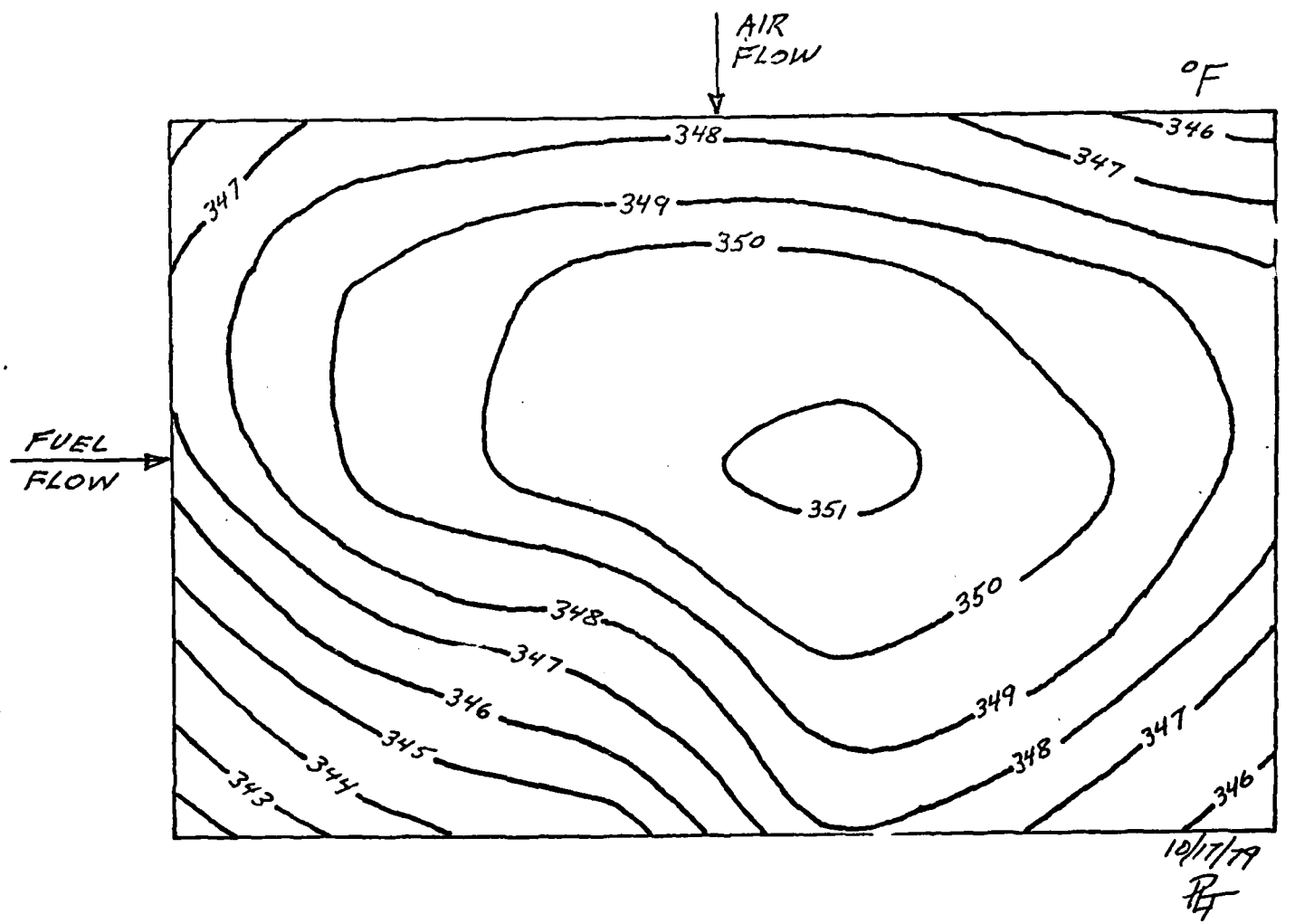

Figure 45

ENGELHARD INDUSTRIES

MERADCOM 3-CELL STACK 3e

CENTER CELL TEMPERATURE PROFILE - 125 asf - 65% H_2, 23% CO_2, 10% H_2O, 2% CO

≈ 50% UTILIZATION

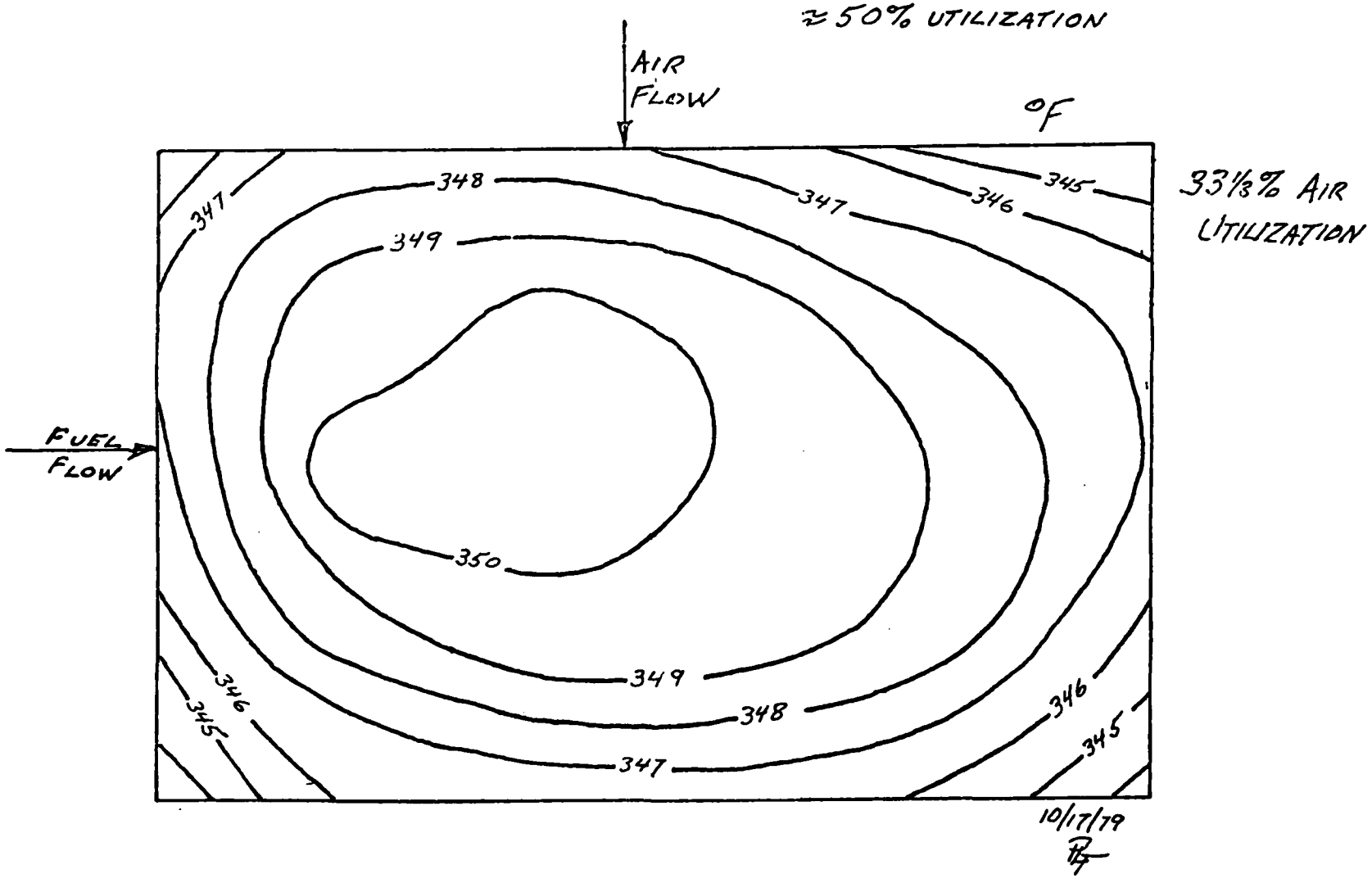

Figure 46

ENGELHARD INDUSTRIES

MERADCOM 3-CELL STACK 3e

BOTTOM CELL TEMPERATURE PROFILE - 125 asf - 65% H_2, 23% CO_2, 10% H_2O, 2% CO
≈ 50% UTILIZATION

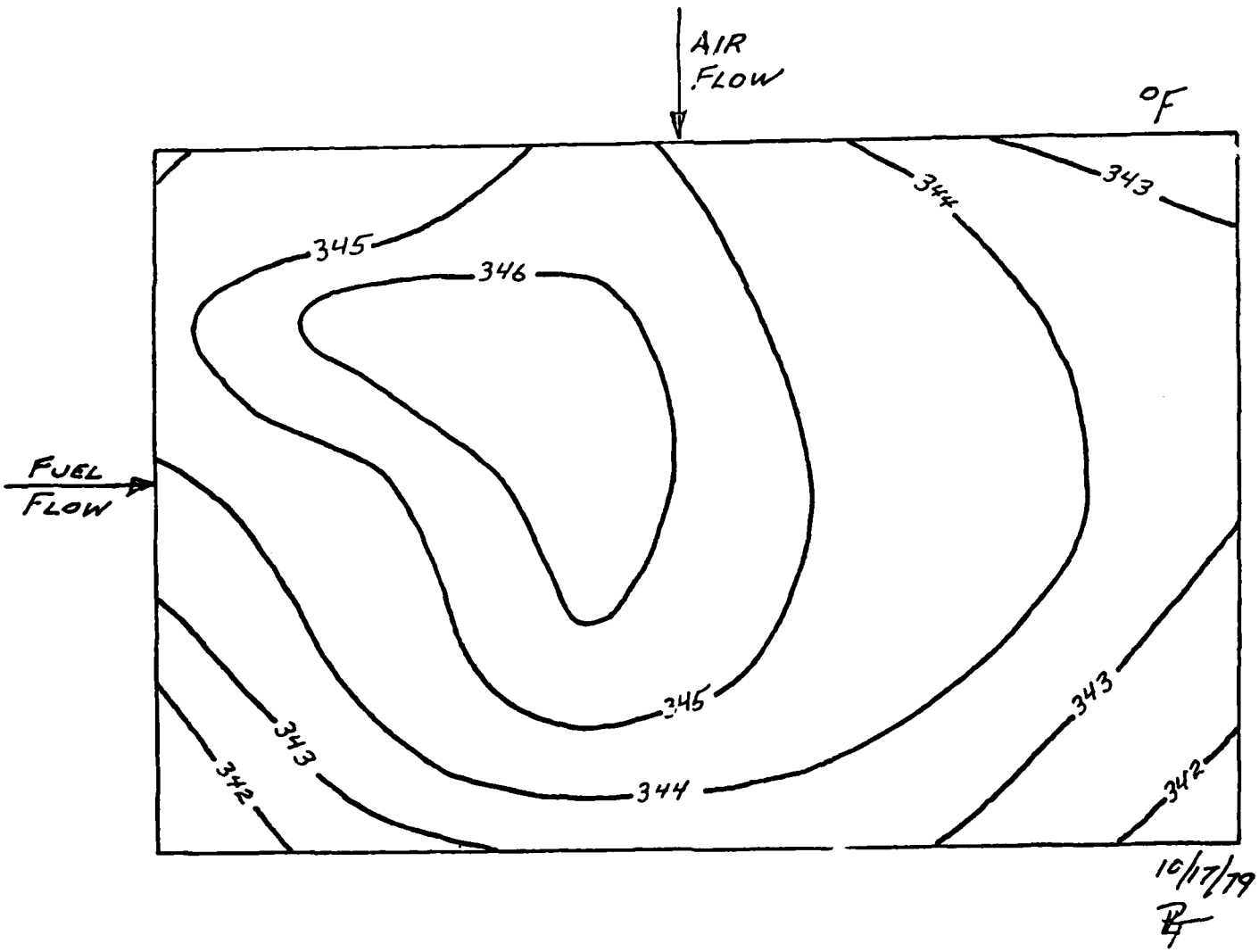

Figure 47

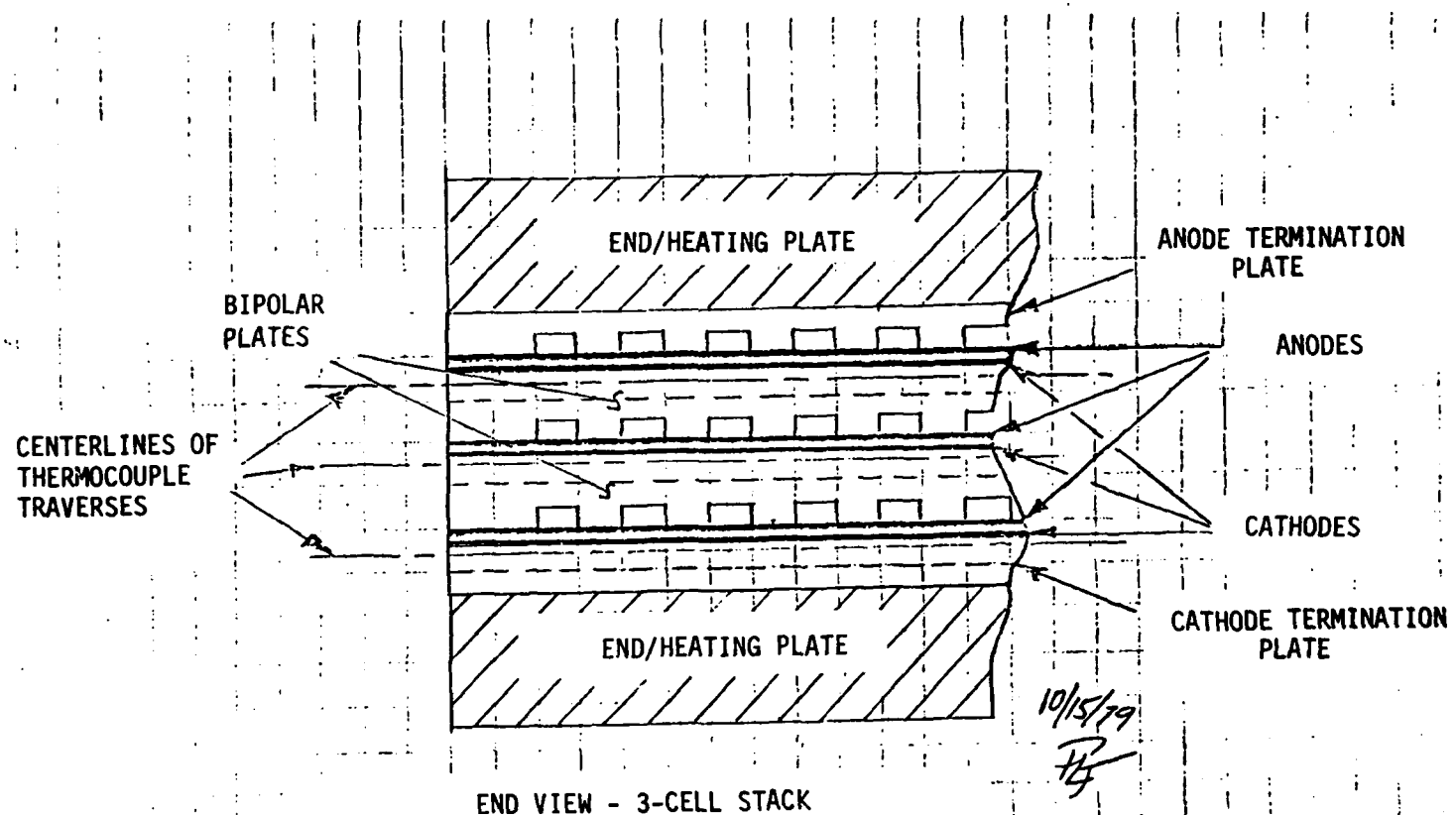
END/HEATING PLATE
ANODE TERMINATION PLATE
BIPOLAR PLATES
ANODES
CENTERLINES OF THERMOCOUPLE TRAVERSES
CATHODES
CATHODE TERMINATION PLATE
END/HEATING PLATE
10/15/79
END VIEW - 3-CELL STACK

Figure 48

DISTRIBUTION LIST

Commander (12)
Defense Documentation Center
Cameron Station, Bldg. 5
ATTN: TISIA
Alexandria, VA 22314

Chief (1)
Research Development & Acquisition
Office, Deputy Chief of Staff
Department of the Army
Washington, DC 20310

Office of the Under Deputy Secretary (1)
of Defense (Research & Advanced Technology)
ATTN: ASST DIR, Electronics & Physical
Sciences
Washington, DC 20301

Director, Technical Information (1)
Advanced Research Projects Agency
1400 Wilson Blvd
Arlington, VA 22209

Commander (1)
US Army Materiel Development
and Readiness Command
ATTN: DRCDE-D
5001 Eisenhower Avenue
Alexandria, VA 22333

Commander (1)
US Army Tank-Automotive R&D Command
Technical Library, DRDTA-UL
Warren, MI 48090

Commander (1)
US Army Electronics R&D Command
ATTN: DELET-PB
Fort Monmouth, NJ 07703

Commander (1)
US Army Transportation Research &
Engineering Command
ATTN: Research Directorate
Fort Eustis, VA 23604

Technical Documents Center (2)
US Army Mobility Equipment R&D Command
ATTN: DRDME-WC
Fort Belvoir, VA 22060

Chief (1)
Naval Ships Engineering Center
Department of the Navy
ATTN: Code 6157D, Mr. Albert Himy
Washington, DC 20362

Director, Power Branch (1)
Office of Naval Research
ATTN: 473
800 Quincy Street
Arlington, VA 22217

Department of the Navy (1)
Office of Naval Research
Ballston Tower #1
800 N. Quincy Street Code: 472, Rm 624
Arlington, VA 22217

Commander (1)
Naval Ordnance Test Station
ATTN: Technical Library
China Lake, CA 93555

Commander (1)
Naval Electronics Laboratory Center
ATTN: Research Library
San Diego, CA 92152

Director (1)
US Naval Research Laboratory
ATTN: Code 2027
Washington, DC 20390

Commander (1)
Aerospace Power Division
ATTN: AFAPL/PO (Mr. J.D. Reams)
Wright-Patterson Air Force Base
Dayton, OH 45443

DISTRIBUTION LIST

Commander (1)
Department of the Air Force (AFSC)
Rome Air Development Center
ATTN: TUGG (Mr. F.J. Mollura, 3068)
Griffiss AFB, NY 13441

Power Information Center (1)
Franklin Research Center
20th and Race Streets
Philadelphia, PA 19130

Director (1)
George Marshall Space Flight Center
ATTN: Mr. J.L. Miller (M-ASTR-E)
Huntsville, AL 38809

Director (1)
Lewis Research Center
National Aeronautics & Space Administration
ATTN: Mr. H.J. Schwartz (M.S. 309-1)
21000 Brookpark Road
Cleveland, OH 44135

Dr. Paul Nelson, Director (1)
Argonne National Laboratory
Bldg 205
9700 South Cass Avenue
Argonne, IL 60439

Mr. Norman Rosenberg (1)
US Department of Transportation
Transportation Systems Center
55 Broadway
Cambridge, MA 02142

US Department of Energy (1)
ATTN: Mr. Gary Voelker
Division of Fossil Fuel Utilization
Mail Station E-178, Germantown
Washington, DC 20545

Electrochimica Corporation (1)
2485 Charleston Road
ATTN: Technical Library
Mountain View, CA 94040

General Electric Company (1)
50 Fordham Road
ATTN: L.J. Nuttall
Bldg 1A
Wilmington, MA 01887

Power Systems Division (1)
United Technologies Corporation
ATTN: Al Meyer
PO Box 109
Governor's Highway
South Windsor, CT 06074

Union Carbide Corporation (1)
Parma Research Center
PO Box 6166
ATTN: Dr. R. Brodd
Parma, OH 44101

Energy Research Corporation (1)
ATTN: Dr. B.S. Baker
3 Great Pasture Road
Danbury, CT 06810

Dr. S.B. Brummer (1)
Director of Physical Research
EIC, Inc.
55 Chapel Street
Newton, MA 02158

Electric Power Research Institute (1)
ATTN: A.P. Fickett
P.O. Box 10412
Palo Alto, CA 94304

Universal Oil Products, Inc. (1)
Ten UOP Plaza
ATTN: Stephen N. Massie
Government Contract Administrator
Des Plains, IL 60016

Technology Center (1)
ESB Incorporated
19 W. College Avenue
ATTN: Dr. D.T. Ferrell, Jr.
Yardley, PA 19067

DISTRIBUTION LIST

Dr. Paul Stonehart (1)
Stonehart Associates, Inc.
34 Five Fields Road
Madison, CT 06443

Dr. R.T. Foley (1)
Chemistry Department
The American University
Washington, DC 20016

Hugh J. Barger, Jr. (1)
Box 2232
Davidson, NC 28036

Department of the Air Force (1)
Sacramento Air Logistics Center (AFLC)
ATTN: David C. Hall
2852 ABG/DEE
McClellan AFB, CA 95652

Defense Research Establishment (1)
ATTN: E. Criddle
Ottawa, Ontario, Canada, KIA024

US Army Engineer School (1)
Director of Combat Developments
ATTN: ATZA-CDM (MAJ Mundt)
Fort Belvoir, VA 22060

DOD Project Manager-Mobile Electric Power (1)
ATTN: DRCPM-MEP-TM (G. Burchette)
7500 Backlick Road
Springfield, VA 22150

Logistics Evaluation Agency (1)
ATTN: DALO-LEI (Jack Daveau)
New Cumberland Army Depot
New Cumberland, PA 17070

Dr. John O. Smith (1)
Chief, Engineering Analysis Branch
Control Systems Laboratory
Research Triangle Park, NC 27711

Office Deputy Chief of Staff (1)
Research, Development and Engineering
ATTN: DAMA-CSS (MAJ Hiemann)
Washington, DC 20301

Gas Research Institute (1)
ATTN: Mr. Vincent Fiore
10 West 35th Street
Chicago, IL 60616

Jet Propulsion Laboratory (1)
California Institute of Technology
ATTN: Dr. John Houseman
Fuel Conversion Group
4800 Oak Drive
Pasadena, CA 91103

Commander (1)
US Army Test & Evaluation Command
ATTN: DRSTE-IN (Mr. Huant)
Aberdeen Proving Ground, MD 21005

DELTA Electronic Control Corporation (1)
ATTN: Mr. Larry Suelzle
2801 S.E. Main Street
Irvine, CA 92714

Westinghouse R&D Center (1)
ATTN: Mr. D.Q. Hoover
1310 Beulah Road
Pittsburgh, PA 15235

Commander (2)
US Army Training & Doctrine Command
ATTN: ATCD-MC (MAJ Miller)
Fort Monroe, VA 23651

Commander (1)
Harry Diamond Laboratories
DELHD-RDD (Benderly)(Batteries)
Adelphi, MD 20783

DISTRIBUTION LIST

Commanding Officer (1)
David Taylor Naval Ship R&D Center
Annapolis Division
Anapolis, MD 21402

Commander (10)
US Army Mobility Equipment R&D Command
ATTN: DRDME-ECS (E. Starkovich)
Fort Belvoir, VA 22060

Department of the Navy
Office of Naval Research (1)
ATTN: Code 425
800 North Quincy Street
Arlington, VA 22217

Commander (1)
US Air Force Security Service
ATTN: DCS/Communications-Electronics (ESO)
San Antonio, TX 78241

Commander (1)
Marine Corps Development & Education Center
ATTN: M&L Division (M. Horstkamp)
Quantico, VA 22134

Commanding Officer (1)
US Army Signal Warfare Lab
ATTN: DELSW-CC, Mr. Crabbe
Arlington Hall Station, VA 22212

Institute of Gas Technology (1)
3434 South State Street
ATTN: Dr. KF. Blurton
Chicago, IL 60616

Institute of Defense Analysis (1)
400 Army-Navy Drive
Arlington, VA 22202

Director (1)
National Aeronautics & Space Administration
ATTN: Code RPP (Mr. A. Dan Schnyer)
Washington, DC 20546

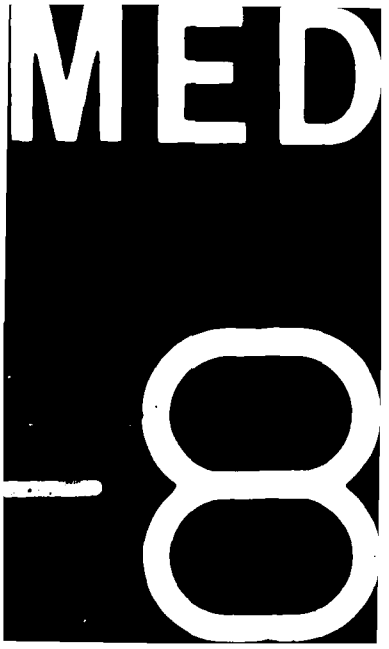
MED
8